2012

Combustion and emissions characteristics of a compression-ignition engine using ammonia-DME mixtures

Christopher Wolfgang Gross
Iowa State University

Combustion and emissions characteristics of a compression-ignition engine using ammonia-DME mixtures

by

Christopher W. Gross

A thesis submitted to the graduate faculty

in partial fulfillment of the requirements for the degree of

MASTER OF SCIENCE

Major: Mechanical Engineering

Program of Study Committee:
Song-Charng Kong, Major Professor
Terrence Meyer
Stuart Birrell

Iowa State University
Ames, Iowa
2012

Table of Contents

List of Figures

List of Tables

Acknowledgements

I especially want to thank Dr. Song-Charng Kong for being my major professor and allowing me to participate in this interesting study. He has provided me with much insight and guidance throughout the last two years in order to increase knowledge and finally gain this degree.

I would like to acknowledge Iowa Energy Center for financial support in order to conduct this study, especially Mr. Norman Olson, as well as Thomas Stach from the Robert Bosch LLC for his support. I also want to thank Dr. Terrence Meyer and Dr. Stuart Birrell for being on my committee.

I want to thank Matthias Veltman, Jorden Tiarks, Cuong van Huyng, and Praveen Kumar for providing support and advice or just a helpful hand whenever I needed it. I want to thank Jim Dautremont and Larry Couture for providing their large experience and knowledge for whatever question I was asking or whenever I needed their help.

Abstract

In this study operating characteristics of a compression-ignition engine using mixtures of ammonia and dimethyl ether (DME) are investigated. Ammonia can be regarded as a carbon-free fuel that can help mitigate greenhouse gas emissions. Ammonia is one of the world's most synthesized chemicals and its infrastructure is well established. Recent technological advances also show that ammonia can be produced from renewable resources, making it an attractive energy carrier.

In the present study, a high-pressure mixing system is developed to blending liquid ammonia with DME that serves to initiate combustion. The engine uses a modified injection system without fuel return to prevent fuel mixture from vaporizing in the return line. Results using different mixture quantities of ammonia and DME show that ammonia causes longer ignition delays and limits the engine load conditions due to its high autoignition temperature and low flame speed. The inclusion of ammonia in the fuel mixture also decreases combustion temperature, resulting in higher CO and HC emissions. NO_x emissions increase due to the formation of fuel NOx when ammonia is used. However, improvements for the same operating conditions were made by increasing the injection pressure using 40%NH_3–60%DME. Exhaust ammonia emissions is on the order of hundreds of ppm under the conditions tested. Soot emissions are extremely low for all cases. Double injection schemes using 20%NH_3–80%DME are also employed and found not to extend engine performance. Its effects on the exhaust emissions vary with operating conditions.

Chapter 1 Introduction

1.1 Motivation

As a major consumer of fossil fuels, internal combustion engines inevitably produce emissions of carbon dioxide (CO_2), an important greenhouse gas. While carbon monoxide (CO), unburned hydrocarbons (HC), nitrogen oxides (NO_x), and particulate matter (PM) are regulated by the government, there are no direct regulations on CO_2 emissions. One can argue that CO_2 emissions are indirectly regulated by the brake specific fuel consumption (BSFC). Nonetheless, methods to mitigate CO_2 emissions are urgently needed. The use of alternative fuels, such as biorenewable or non-carbon-based fuels can be viewed as a means to reducing the life-cycle carbon emissions. The deployment of new technologies, such as electric hybrid vehicles, plug-in electric vehicles, and fuel cell vehicles, also has the potential to help increase fuel efficiency and thus reduce carbon emissions.

Among the above approaches, the use of hydrogen (H_2) as a carbon-free fuel has been discussed extensively, and hydrogen-fueled internal combustion engines and fuel cells have been researched, which developed large public interest. However, there are challenges in using hydrogen for transportation due to infrastructural issues such as production, storage, and handling. Although it has received much less attention, ammonia (NH_3) combustion with air does not produce CO_2 emissions either. Furthermore, ammonia is plentiful and its production, storage, handling, and distribution facilities are available worldwide. It can be easily liquefied

and stored under moderate pressure and shows a much higher energy density than hydrogen.

Ammonia can be an attractive energy carrier due also to its versatile production methods. It can be produced by electrolysis, solid-state synthesis, and solar thermochemical synthesis from renewable sources (Avery, 1988) (Hejze et al., 2008). Ammonia can be seen as a hydrogen energy carrier. As an example, in many occasions wind turbines produce more electricity than demanded in the evening time when wind is the strongest but the demand is low. Excess electricity generated from wind turbines during off-peak hours can be used to produce ammonia, which in turn can be used in diesel generators to produce electricity when demands are high. Recent studies on solar thermochemical production of ammonia also show that a net efficiency ranging from 26 to 33% can be reached by combining the ammonia synthesis cycle with hydrogen production (Michalsky et al, 2011).

In a first approach, ammonia was used to power busses in Belgium already in 1942 due to an extreme shortage of diesel fuel during World War II (Koch, 1945). Later the U.S. military developed interest in ammonia combustion and theoretical and experimental studies were performed (Starkman et al., 1966). Ammonia combustion was realized successfully in spark-ignition engines while its combustion in compression-ignition engines was less successful (Pearsall et al., 1967), (Starkman et al, 1967) , (Bro et al., 1977). There are peculiar characteristics for using ammonia as an energy source. Besides the fact that it can be produced by electrolysis and solid-state synthesis from renewable sources, such as wind, solar and hydro power, it can be used as a hydrogen energy carrier. After the

aforementioned literature, there has not been significant ammonia engine research until recently due to the need to explore non-carbon fuel combustion in engines (Lui et al., 2003), (Grannell et al., 2008), (MacKenzie et al., 1996). It is shown in a diesel engine study that a maximum of 95% of energy replacement can be achieved when vapor ammonia is introduced into the intake manifold in combination with directly injected diesel fuel (Reiter et al., 2008). Rated power outputs can be exceeded by adding high quantities of ammonia. As more diesel fuel is replaced by ammonia in the above dual-fuel operation for the same power output, CO_2 emissions decrease monotonically. NO_x emissions show a low level until energy substitution by ammonia reaches 60% due to its lower combustion temperature (Reiter et al., 2008). As more ammonia is used, NO_x emissions increase due to fuel NO_x emissions.

With the focus on burning ammonia in engines, several considerations have to be made. These include the high ignition temperature, high latent heat, low energy content, fuel-bound nitrogen, and a low boiling point. The ignition temperature of 651 C and narrow ignition limits (16-25% by volume in air) require a very high compression ratio (approximately 30:1) for pure ammonia combustion in compression ignition engines. Furthermore, the fuel-bound nitrogen production during the combustion process increases the risk for high NO_x emissions. In addition, the power output for combustion in spark-ignition engines is about 20% lower than the operation on conventional gasoline with even increased specific fuel consumption (Koch, 1945). After all, combustion of ammonia in engines can be achieved with proper combustion strategies and also considerations towards its corrosive nature to materials such as copper, nickel, and plastics. It also has to be

mentioned that ammonia causes health effects in humans for concentration of 150 ppm up to 300 ppm, where it can be instantaneously life- and health-threatening.

Despite the above challenges and necessary considerations as well as limited literature on ammonia combustion in engines, the renewed interest in using ammonia as an alternative engine fuel to reduce greenhouse gas emissions has led to the present research. Ammonia can be an appropriate fuel for spark-ignition engines due to its high resistance to auto ignition. However, it is of great interest to use ammonia for power generation because most of the generators are based on compression-ignition engines.

1.2 Objective

The objective of this project is to study the combustion and emissions characteristics of a compression-ignition engine that burns mixtures of ammonia and DME. The engine used is a Yanmar L70V single cylinder compression-ignition engine. In its original setup, fuel is supplied to the injector at very high pressure with excess fuel being discharged at ambient temperature, which will cause ammonia to vaporize if ammonia is used to replace diesel fuel directly. Therefore, the original fuel injectors were replaced with a new injection system to avoid the low pressure fuel return. Furthermore, a piston pump is used to further increase the pressure of the fuel mixture and store it in an accumulator to create a setup similar to a common rail. Due to the high vapor pressure of ammonia, a relatively low injection pressure of about 130 – 200 bar seems to be sufficient to achieve good atomization of the fuel

and therefore allow the use of an electronically-controlled injector with a maximum pressure rating of 200 bar.

The results of fuel consumption, engine performance, and exhaust emissions are presented based on experimental engine tests. Hereby it is differentiated between the combustion of 100% dimethyl ether (DME) as a baseline and the combustion of different fuel mixtures of DME and NH_3.

Dynamometer tests will be performed to measure the engine power, fuel consumption is calculated from the exhaust gas emissions, and a full set of engine performance data, including start of injection (SOI), injection pressure and mass of fuel injected, is collected throughout every test mode. The according set of test modes was defined following present standards. Exhaust emissions will be measured, including soot, nitrogen oxides (NO_x), carbon monoxides (CO), carbon dioxides (CO_2), unburned hydrocarbons (THC) and ammonia (NH_3).

Chapter 2 Literature Review

2.1 Physical Properties of Ammonia

Ammonia, or also anhydrous ammonia due to its absence of water, is a compound of one nitrogen atom and three hydrogen atoms with the formula NH_3. The particles are thereby distributed as followed (2-1) with a fully occupied nitrogen atom.

$$: \dot{\underset{\cdot}{N}} \cdot + 3\, H \cdot \rightarrow \quad H \\ : \underset{\cdot\cdot}{N} : H \\ H \qquad (2\text{-}1)$$

In a 3D perspective the nitrogen is at the peak of a trigonal pyramid above the hydrogen plane, which bond in an equilateral triangle. The angle in between two H-N-H axes is 107.8°.The ammonia molecule experiences a dipole moment of 1.42 D, due to a stronger electronegativity of the nitrogen in respective to the hydrogen as well as due to the unsymmetrical molecular arrangement. The dielectric constant of liquid ammonia is 16.03 at 25°C (Billaud et al., 1975) and therefore offers a considerable ability to dissolve many substances (Appl, 1999).

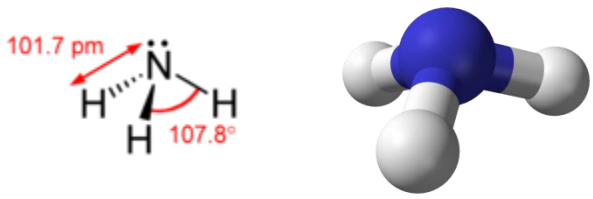

Figure 2.1 – Molecular structure of anhydrous ammonia

Ammonia can be liquefied at ambient temperature (300 K) and a pressure of about 10 bar. The density hereby is around 600 kg/m^3, which contains approximately 105 kg/m^3 of hydrogen. This is a higher hydrogen content by mass volume than liquefied hydrogen itself (71 kg/m^3) and therefore simplifies the storage onboard a vehicle or at a refueling station in low pressure steel tanks.

Due to its very high vapor pressure, ammonia is expected to vaporize much faster than conventional diesel fuel if injected as a liquid into the hot combustion air close to the end of the compression stroke. Therefore it can be beneficial for the application in compression-ignition engines. A proper atomization at lower injection pressure can also be assumed.

As listed in Table 2-1 the heat of vaporization as a function of temperature reduces by about 13% when the temperature of ammonia is increased from 15°C to 50°C. In addition, the heat of vaporization exceeds that of conventional diesel fuels by about three times (375 kJ/kg).

Table 2-1 – Properties of saturated ammonia liquid and vapor (Appl, 1999)

Temperature (ºC)	Pressure (kPa)	Specific Volume		Heat of vaporization (kJ/kg)
		Liquid (L/kg)	Vapor (L/kg)	
-40	71.72	1.4490	1551.60	1388.1
-35	93.14	1.4620	1215.40	1373.1
-30	119.49	1.4754	962.90	1358.9
-25	151.54	1.4892	770.95	1343.8
-20	190.16	1.5035	623.31	1328.3
-15	236.24	1.5184	508.49	1312.4
-10	290.77	1.5337	418.26	1296.0
-5	354.77	1.5496	346.68	1279.1
0	429.35	1.5660	289.39	1261.7
5	515.65	1.5831	243.16	1243.8
10	614.86	1.6009	205.55	1225.2
15	728.24	1.6194	174.74	1206.1
20	857.08	1.6387	149.31	1186.3
25	1002.70	1.6590	128.16	1165.8
30	1166.60	1.6801	110.54	1144.5
35	1350.00	1.7023	95.699	1122.4
40	1554.60	1.7257	83.150	1099.5
45	1781.70	1.7505	72.484	1075.6
50	2033.00	1.7766	63.373	1050.6

Additional properties that are of interest are listed in the following table.

Table 2-2 – Physical properties of ammonia (Appl, 1999)

Property	Value	Unit
Atomic Weight M	17.0312	g/mol
Molecular Volume (at 0 ºC and 101.3 kPa)	22.08	L/mol
Gas constant R	0.48818	kPa m^3/(kg K)
Liquid density (at 0 ºC and 101.3 kPa)	0.6386	g/cm^3
Gas density (at 0 ºC and 101.3 kPa)	0.7714	g/L
Liquid density (at -33.43 ºC and 101.3 kPa)	0.682	g/cm^3
Gas density (at -33.43 ºC and 101.3 kPa)	0.888	g/L
Critical Pressure	11.28	MPa
Critical Temperature	132.4	ºC
Critical Density	0.235	g/cm^3
Critical Volume	4.225	cm^3 /g
Meting Point (Triple Point)	-77.71	ºC
Vapor Pressure (Triple Point)	6.077	kPa
Boiling Point (at 101.3 kPa)	-33.43	ºC
Heat of Vaporization (at 101.3 kPa)	1370	kJ/kg
Standard Enthalpy of Formation (gas at 25 ºC)	-46.22	kJ/mol
Standard Entropy (gas at 25 ºC, 101.3 kPa)	192.731	J/(mol K)
Net Heating Value	18.577	kJ/g
Gross Heating Value	22.543	kJ/g
Ignition Temperature (acc. to DIN 51794)	651	ºC
Explosive Limits		
NH_3-O_2-Mixture (at 20 ºC, 101.3 kPa)	15 - 79	vol % NH_3
NH_3-Air-Mixture (at 0 ºC, 101.3 kPa)	16 - 27	vol % NH_3
NH_3-Air-Mixture (at 100 ºC, 101.3 kPa)	15.5 - 28	vol % NH_3

2.2 Usage of Ammonia

There are two common ways of producing ammonia. One is as a byproduct of decomposition, the other method for commercially producing ammonia is the Haber-Bosch process. This involves combining elemental nitrogen with hydrogen which most often is obtained from decomposed methane found in natural gas. In order for the gases to combine chemically they need to be heated to 500°C, pressurized to approximately 150-200 bar and passed over an iron catalyst (Modak, 2002). The exothermic reaction is as follows:

$$N_2 + 3H_2 \longrightarrow 2NH_3 \qquad (2\text{-}2)$$

$$\Delta H_{298K} = -45.7 \frac{kJ}{mol} \qquad (2\text{-}3)$$

Ammonia synthesis consists of two different processes: the hydrogen and nitrogen production process and the ammonia synthesis process. Hydrogen production from natural gas reforming, coal gasification, water electrolysis, or steam-iron reaction thereby consumes the major part of energy during the overall ammonia production.

2.3 Ammonia as a Fuel

2.3.1 Feasibility as a Fuel

As mentioned before ammonia was considered as an alternative to conventional fuels as early as World War II (Koch, 1945) and in the 1960's (Starkman et al., 1966), (Pearsall et al., 1967), (Gray et al., 1966), but since then not much research has been done. However, besides being a carbon-free fuel, ammonia has many desirable characteristics. The low vapor pressure allows the storage of liquid ammonia at 10 bar at ambient temperature or cooled to -33°C at ambient pressures. In addition, it has a high octane rating of approximately 120 and an autoignition temperature of 651°C, thus it is highly resistant to autoignition. Due to its high autoignition temperature a cetane rating is not available for ammonia. This is important, especially for this research project, since it doesn't allow the utilization of ammonia in a conventional CI engine without appropriate modifications. This can either be increasing the compression ratio to up to 30:1 or heating the intake air to approximately 60 - 90°C. Both will increase the gas temperature in the combustion chamber. Table 2-3 shows a number of characteristics of various fuels.

Table 2-3 - Properties of various internal combustion fuels (National Institute of Standards and Technology, 2009)

Fuel	Liquid H_2	Gaseous H_2	Natural Gas	Ammonia	Propane	Gasoline	Methanol
Formula	H_2	H_2	CH_4	NH_3	C_3H_8	C_8H_{18}	CH_3OH
Storage Method	Cryogenic Liquid	Compressed Gas	Compressed Gas	Liquid	Liquid	Liquid	Liquid
Approximate AKI* Octane Rating	RON >130 MON very low	RON >130 MON very low	107	110	103	87-93	113
Storage Temp [°C]	-253	25	25	25	25	25	25
Storage Pressure [kPa]	102	24,821	24,821	1030	1020	101.3	101.3
Fuel Density [kg/m^3]	71.1	17.5	187.2	602.8	492.6	698.3	786.3
Heat Storage							
LHV [MJ/kg]	120.1	120.1	38.1	18.8	45.8	42.5	19.7
[MJ/L]	8.5	2.1	7.1	11.3	22.6	29.7	15.5
Fuel Requirement to Match Energy of 10 Gallons of Gasoline [MJ]	1123.3	1123.3	1123.3	1123.3	1123.3	1123.3	1123.3
Fuel Volume [L]	131.5	534.4	157.5	99.2	49.8	37.9	72.5
Fuel Weight [kg]	9.4	9.4	29.5	59.8	24.5	26.4	57.0

*Anti-Knock Index, (RON+MON)/2

For the distribution of ammonia as a fuel, the same infrastructure similar to propane can be used to transport and store ammonia as long as all brass, copper, and rubber based materials are replaced with mild steel and Teflon counterparts. Ammonia is also safer to handle when compared to hydrogen. Hydrogen can produce an easy flashback with a very high burning velocity and low minimum ignition energy. Furthermore, hydrogen must be stored at high pressures (180 – 650 bar) at ambient temperatures, or has to be chilled to -250°C for liquid storage (MacKenzie and Avery, 1996). Both of these storage systems are more costly than

tanks needed to store ammonia because of the need for heavier construction or lower storage temperatures.

2.3.2 Combustion Characteristics

The explosive or flammability limits of ammonia are narrow (15-28% by volume in air at 0°C and 101.3 kPa) and the ignition temperature of 651°C is high compared to gasoline (370°C) and diesel (254°C). Therefore, ammonia is classified as a non-flammable but toxic gas by many agencies. The complete, stoichiometric combustion of ammonia in ambient air has an air-fuel-mass ratio ($A_{s,\ NH3}$) of 6.1and thus is significantly lower than those of conventional fuels. Equation 2-4 shows the stoichiometric reaction for ammonia with air.

$$\boldsymbol{NH_3 + 0.75(O_2 + 3.76N_2) \rightarrow 1.5H_2O + 3.32N_2} \qquad (2\text{-}4)$$

With the lower oxygen demand of ammonia combustion, the energy per unit mass of stoichiometric combustible mixture is similar to those of most engine fuels and can make up for the much lower net heating value (Table 2-3). The utilization of ammonia seems to be beneficial for a direct injection system, since thereby the cylinder gets filled with the maximum amount of air possible, thus neglecting the low energy content per unit volume of stoichiometric mixture of ammonia-air due to a low density of ammonia vapor. The non-stoichiometric reaction equation is given below. It is used to calculate the equivalence ratio for the lean and rich ignition limits.

$$\boldsymbol{NH_3 + \frac{a_s}{\phi}(O_2 + 3.76N_2) \rightarrow n_2H_2O + n_4N_2 + n_5O_2 + n_8NH_3} \qquad (2\text{-}5)$$

Since the rate of combustion in a CI-engine is limited by the rate at which air and fuel mix inside the combustion chamber, the narrow flammability limits and the equivalence ratio are of great importance in this research project. CI engines rely on an ignitable local equivalence ratio to start combustion and to maintain combustion with satisfactory mass transfer rates.

Table 2-4 – Limits for the Equivalence Ratio

	Ammonia Concentration (vol. %)	**Equivalence ratio**	**Energy Content of Mixture (MJ/kg)**
Lean Ignition Limit	15.5	0.65	1.83
Rich Ignition Limit	28.0	1.39	3.5

Table 2-5 – Limits of Flammability in Air (%-volume) (Majewski & Khair, 2006)

Fuel	**Stoichiometric (vol. %)**	**Lean Limit (vol. %)**	**Rich Limit (vol. %)**
Methane	9.47	5.0	15.0
Ethane	5.64	2.9	13.0
Propane	4.02	2.0	9.5
Isooctane	1.65	0.95	6.0
Carbon Monoxide	29.50	12.5	74.0
Acetylene	7.72	2.5	80.0
Hydrogen	29.50	4.0	75.0
Methanol	12.24	6.7	36.0
Ammonia	21.8	15.5	28.0

Additional important characteristics are the following.

- **Laminar Flame Speed**

  Ammonia has the lowest laminar flame speed (Table 2-6) among the most conventional fuels, indicating a slow combustion process. Thus, the reaction rates are low which is typically not desired for an internal combustion engine application. Ammonia is expected to limit the engine operation at high speed/high load conditions.

Table 2-6 – Laminar flame speed of ammonia compared to other fuels (Majewski & Khair, 2006)

Fuel	Autoignition Temperature in Air (°C)	Laminar Flame Speed (cm/s)
Ammonia	651	15
Propane	470	39
n-Hexane	233	39
Isooctane	418	35
Carbon Monoxide	609	39
Acetylene	305	141
Methane	537	34
Hydrogen	400	265
Methanol	385	48

- **Adiabatic flame temperature**

  According to Table 2-7, the adiabatic flame temperature of ammonia is not much lower than the temperature of the selected fuels. Therefore, it is feasible for the combustion in an internal combustion engine with a product temperature high enough to extract work during expansion.

Table 2-7 – Adiabatic Flame Temperature (K) of selected fuels (Majewski & Khair, 2006) and ammonia (air @ 1atm; T_0=298K)

Fuel	Equivalence Ratio		
	0.8 [K]	1.0 [K]	1.2 [K]
Ammonia	1826	1990	1910
Propane	2045	2270	2210
Cetane	2040	2265	2195
Octane	2050	2275	2215
#2 Fuel Oil	2085	2305	2260
Ethane	2040	2265	2200
Methane	2020	2250	2175
Ethanol	1935	2155	2045
Methanol	1755	1975	1810

- **Ignition Delay**

The ignition delay and the adiabatic flame temperature of mixtures of ammonia and methane as well as diesel as a secondary fuel have been investigated (Reiter et al., 2008). In the study it is found that, as ammonia concentration increases the mixture is more unlikely to auto ignite due to the high auto ignition temperature of ammonia. As a result, it is reported that, with the ammonia ratio in the fuel mixture being increased, the ignition delay increases, while the flame temperature is reduced. As a follow up, ignition delay and adiabatic flame temperature of mixtures of ammonia and DME have been studied in a Chemical Kinetic model as a part of this research project. The mechanism combined for the modeling are:

- DME.24 (Kaiser, E.w., Wallinton, T.J., Hurley, M.D., Platz, J., Curran, H.J., Pitz, W.J., and Westbrook, C.K.)
- NH_3 (Miller, J.S. and Bowman, C.T.)

5 different cases (20%/40%/60%/80%/100%) of the amount of ammonia present in the mixture at 3 different pressures have been investigated. The pressures were determined according to the maximum cylinder pressure recorded during 100% DME test runs. It is found that the ignition delay increases significantly with the amount of ammonia present in the fuel mixture. However it can be compensated by increasing the pressure.

- **Heat of vaporization**

Among conventional fuels ammonia is the least favorable for its application especially in a direct injection engine due to its very high heat of vaporization combined with a significantly low lower heating value (Table 2-8). About 72 kJ of energy is used to vaporize the amount of fuel containing 1 MJ of chemical energy and the cylinder temperature is reduced considerably because of the fast vaporizing ammonia. These low temperatures can cause misfire and prevent the engine from operation, since the compressed air in the cylinder cannot provide enough energy to initiate and maintain combustion. As a result the emission rates are above any regulation limits.

Table 2-8 – Heat of vaporization of selected fuels

Fuel	Heat of Vaporization (kJ/kg)	Heat of Vaporization (kJ/MJ_f)
Conventional Gasoline	380	8.94
Conventional Diesel	375	8.33
Methanol	1185	58.95
Ethanol	920	34.07
Dimethyl Ether	467	16.44
Ammonia	1370	72.87

2.3.3 Mixtures of Ammonia and Secondary Fuels

As mentioned before, ammonia is very favorable to mix with other hydrocarbon fuels. Equation (2-6) gives the incomplete combustion reaction for mixtures of ammonia with a secondary fuel.

$$n_1 NH_3 + (1-n_1) C_\alpha H_\beta O_\gamma N_\delta + \frac{\boldsymbol{a_s}}{\boldsymbol{\phi}} (O_2 + 3.76 N_2) \rightarrow$$

$$n_2 H_2O + n_3 CO_2 + n_4 N_2 + n_5 O_2 + n_6 NO_x + n_7 CO + n_8 NH_3 + n_9 C_\alpha H_\beta O_\delta N_\delta \quad (2\text{-}6)$$

Based on this, a study (Veltman, 2011) investigated the suitability of different fuels for the application in a compression ignition engine. It was found that the stoichiometric air-fuel ratio of the mixtures changes drastically with an increase in the quantity of ammonia, while the energy content per unit mass of stoichiometric mixture only drops slightly with a higher ammonia content.

As another result it can be seen that a concentration of about 60 wt.% ammonia when used with DME and about 70 wt.% when used with biodiesel or diesel are required to reduce to CO_2 emissions by 50% compared to the utilization of non-blended diesel fuel. With an increasing reduction of CO_2 the ammonia content increases as well, however with lower %-w concentration of ammonia in case of the DME, which ultimately lead to the usage of DME as a secondary fuel for this research project.

2.4 Ammonia as a Compression-Ignition Engine Fuel

Literature about the utilization of ammonia in compression ignition engines is very rare, because most research activities have been focused on utilizing ammonia in spark ignition engines due its high octane rating and in order to avoid ignition problems because of the high autoignition temperature.

However, in a first step Gray et al. (1966) conducted material tests away from the engine to then move on to the investigation of ammonia combustion as a part of the so-called “Energy Depot Concept,” which called for deployment of small nuclear reactors to synthesize ammonia from water and atmospheric nitrogen via electrolysis and a Haber-Bosch ammonia synthesis loop in forward deployed locations (Gray et al., 1966) . As a result of these tests cast iron samples experienced a slight weight gain and discoloration and so did the aluminum samples, which lacked the discoloration. Furthermore, the copper lead bearing surfaces showed the greatest visual change with tarnish-like oxidation and weight loss due to pitted-type corrosion. However, the weight loss occurred to not even the same extend than for

hydrocarbon fuels and showed the biggest weight loss in contrast to those within the first 40 hours. Neoprene and rubber also seemed to be highly effected by ammonia compared to all other materials examined (swelling, loss of shape, and even disintegration). In the end, all materials except neoprene, rubber, copper, would be suitable for ammonia combustion use. In addition, oil samples were taken at every 40-hr interval and no changes were noted to the composition or properties of the REO-145 oil used so that at the completion of the 120-hr mark, the deterioration level of the oil was less than that of a gasoline engine.

The following major engine tests investigated the performance of a compression ignition engine by utilizing a Waukesha cooperative fuel research (CFR) compression ignition engine with a cetane combustion chamber. Thereby the ammonia was cooled to about 10 ºF below ambient to avoid cavitation at the inlet of the mechanical fuel injection pump, which had been modified to increase pump capacity and to compensate for a higher fuel flow rate requirement. The engine was operated at a speed of 900 rpm and an intake air temperature of 150 ºF and jacket temperature of 210 ºF, respectively. However, ammonia did not ignite and the engine stalled at an initial compression ratio of 30:1. Engine operation was possible under an increased compression ratio of 35:1 and raised jacket and intake air temperatures of 300 ºF. Injection timing ranged from 90 to 70 CAD before top-dead-center (BTDC) and ammonia flow rates of 2-5 lbs/hr. After all, ignition delay increased slightly with increased engine speed.

According to Gray et al. (1966) the ammonia-air-mixture in the cylinder is likely to be close to homogeneous at all times due to the early injection timing and

focused on improving combustion by means of pilot injections, fuel additives and introduction of combustion promoting gases to the intake air and glow plugs. Gray et al. (1966) was able to successfully operate the engine using pilot injections using a diesel fuel with a cetane number of 53. Compression ratio could be lowered again to 30:1 as could the intake air temperature (150 ºF) and the jacket temperature (210 ºF).Thereby, the best combustion was observed at ammonia injection event no later than 40 CAD before the end of the diesel injection. The maximum IMEP of approx. 100 psi was achieved with diesel pilot injections at 12 CAD BTDC, and ammonia injected 80 CAD BTDC. Diesel flow rate at this condition was 0.96 lbs/h with an ammonia flow rate of approx. 2.5 lbs/h. In addition it was observed that the compression ratio could be lowered even more with an increasing cetane number of the diesel fuels.

As a final approach Gray et al. (1966) experimented with the utilization of glow and spark plugs to initiate combustion if only ammonia is used. The results hereby show that regular spark and glow plugs couldn’t initiate combustion, while a high temperature glow plug placed so that the injected ammonia crosses the glow plug can successfully ignite the ammonia-air-mixture in the cylinder. Even though combustion could be maintained with a compression ratio of 23:1, 210 ºF jacket temperature and 150 ºF air inlet temperature utilizing the high temperature glow plug it was reported that combustion was very sensitive to plug placement and ammonia flow rate. Therefore Gray et al. (1966) turned to bench experiments utilizing a constant volume pressure vessel.

Others also investigated utilization of ammonia in a direct injection diesel engine (Bro et al., 1977) (Reiter et al., 2008). Hereby ammonia vapor was introduced to the intake air and ignited by means of a small diesel pilot injection. With an increasing amount of ammonia being present during combustion, the ignition delay increased significantly and substantial amounts of unburned ammonia were observed in the exhaust gas in both researches. Bro et al. (1977) even concluded that ammonia is the least suitable alternative fuel for compression ignitions engines due to its high concentration in the exhaust, slow combustion and long ignition delay.

Pearsall and Garabedian (1967) used another approach to show the practicability of ammonia as a fuel. After investigating the utilization of ammonia in compression ignition engines when premixed with the intake air and ignited by means of a short diesel pilot injection, they converted the CI engine into a spark ignition engine with no secondary fuel. The engine had a compression ratio of 30:1, but was still proved unsuccessful in terms of direct injection of liquid ammonia. A drop in the peak pressures of about 250 psi led to the conclusion that the vaporization of the ammonia cooled the chamber too much for the fuel to ignite. After extensive tests, compression ignition could be achieved at engine speeds below 1200 rpm if the ammonia was premixed with the intake air. Converting the engine into a spark ignition engine included the installation of a magneto, the replacement of the injector for a spark plug and the removing of the injection pump. Running with three different compression ratios, an increase of the peak pressures were observed as well as a drop of the BSFC. The authors ultimately concluded that an engine

utilizing ammonia as the main fuel should be of the spark ignition type with a high energy ignition source.

Starkman et al. (1967) used a compression ignition engine with ammonia; however a spark plug was used to ignite the fuel mixture.

2.5 Summary

Besides being carbon-free, ammonia has several desirable attributes. It has a high energy density, it is relatively easy to store, and it is one of the world's most synthesized chemicals. However, its ignition temperature is relatively high at 651°C, and it must be combusted in concentrations of 15-28% by volume in air.

In earlier studies, it was shown that ammonia could provide sustainable combustion when used as a primary fuel or in conjunction with a pilot fuel or spark source in either a spark-ignition or a compression-ignition engine, both with its own ideal operation parameters. It has been proven that spark ignition combustion is possible but with approximately 70% energy output. In order to combust ammonia in a CI engine, the CR must be very high (approximately 30:1), or there must be a pilot ignition source available to provide sufficient ignition energy. In order to use ammonia in a CI engine, our research group has conducted research in inducting vapor ammonia into the intake port and using diesel fuel to initiate combustion (Reiter et al., 2008). It was demonstrated that this approach was feasible but exhaust ammonia is too high (on the order of thousands of ppm). This thesis work is designed to take another approach to realize ammonia combustion in CI engines, namely injecting liquid mixtures of ammonia and DME directly into the cylinder with

DME as the ignition source. It is hoped that by using direct injection when both valves are closed, ammonia will not escape the combustion chamber, thus reducing exhaust ammonia emissions.

Chapter 3 Experimental Setup

3.1 Engine

The engine used for this study is a Yanmar L70V single-cylinder, direct-injection diesel engine. It was specifically chosen for this project because of the following favorable characteristics. For one its small size can improve the safety within the laboratory as well as the maintenance costs by having a small amount of fuel stored on site and low fuel flow rates. Also, the high compression ratio stands for higher temperatures at top dead center of the compression stroke and is therefore projected to improve the combustion of ammonia. The technical data is shown in Table 3-1.

Table 3-1 - Engine geometry and operating conditions

Engine Model	Yanmar L70V
Engine Type	Air Cooled, Four Stroke, Compression Ignition
Combustion Type	Direct Injection
Cylinder Arrangement	Vertical
Type of Aspiration	Natural Aspiration
Bore x Stroke (mm)	78 x 67
Compression Ratio	20:1
Total Displacement (cm^3)	320
Valves per Cylinder (Int./Exh.)	(1/1)
Rated Speed (rpm)	3600
Rated Power (kW)	4.3
Brake Specific Fuel	268
Balancing System	Single, Counter-Rotating, Balancer Shaft
Type of Injection System *	Electronic Fuel Injection
Injection Pump *	Air operated high pressure piston pump
Injector Nozzle *	BOSCH high pressure gasoline direct injection

While the base engine uses a single plunger pump and mechanical fuel injector to pressurize and the fuel into the combustion chamber, the setup for this

research project has been changed. The injection system was replaced by an electronically controlled injection system in order to utilize ammonia and to have a better control of the injection event.

The injector used for the project is a Bosch fuel injector that is usually used in direct-injection gasoline engines. To accommodate the unit into the cylinder head, a few modifications were made. Besides the changes to the unit itself, which was modified to accept a 5/16 in Swagelok compression ring fitting in order to withstand the injection pressure as well as the utilization of different o-ring material, the cylinder head had to be adapted to the new set up. The new electric injection valve, an 180W glow plug, a cylinder pressure sensor, and thermocouples to measure cylinder head temperature and intake air temperature were included into the cylinder head.

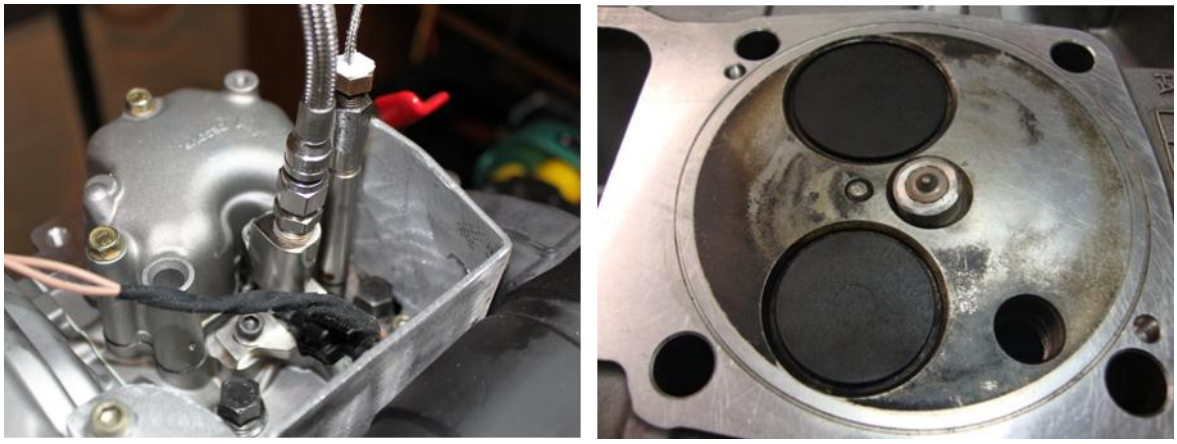

Figure 3.1 – Cylinder head unit with injector, glow plug and pressure transducer

For proper installation the injector was fitted into a stainless steel sleeve that was fabricated according to the manufacturer's specification. Both are inserted into the cylinder head and are held in place by a clamp and a bolt at the same place where the original fuel injector was mounted. Finally a copper washer prevents the leakage from the combustion chamber at the bottom of the sleeve. The injector itself produces a 70-degree spray cone, where the centerline of the spray is tilted 15 degrees off the centerline of the injector. The mounting of the injector is off center from the center of the cylinder head and tilted another 20 degrees towards the exhaust valve. This creates an overall spray axis angle of 5 degrees from the cylinder axis, since the spray tilt and the mounting tilt are arranged to compensate each other.

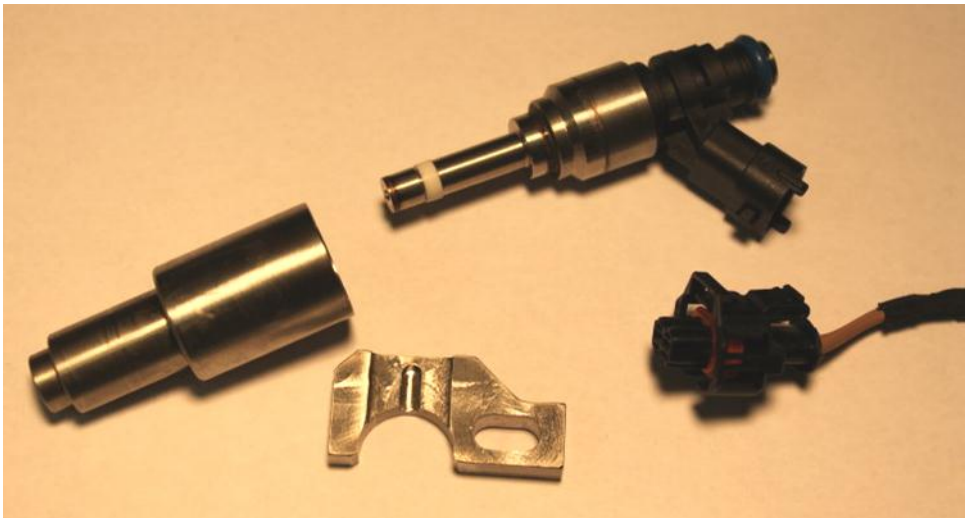

Figure 3.2 – Bosch GDI fuel injector with sleeve, clamp and wiring couple

Even though the injector is installed as close as possible into the combustion chamber, there is still a recess from the surface of the cylinder head. From the experimental results to be discussed later, it may be possible that the liquid spray impinges on the surface of the wall of the recess space, thus resulting unburned fuel. In addition, it has to be mentioned that the narrow spray pattern may limit the air utilization and mixing.

3.2 Fuel System

As mentioned earlier, the stock fuel injection system is replaced by an electronically controlled fuel system in order to overcome material incompatibilities as well as other issues associated with its specific application for this project. With the utilization of the electronic injector, flexible injection timing and multiple injections can be realized. Furthermore, the low pressure fuel return from the stock system was avoided, which would cause the pressurized liquid fuel mixture to return to its gaseous state immediately. The GDI prototype has a maximum pressure capability of 200 bar, which is significantly lower than conventional diesel fuel injection systems, that operate at 1500 bar for proper atomization of the fuel to reduce particulate emissions. Although the injection pressure capability is too low to run the engine on regular diesel fuel, it is expected that an injection pressure of 150 – 200 bar is sufficient to provide a fuel atomization good enough to operate the engine on dimethyl ether and ammonia. Vaporization will progress quickly during the injection process due to their considerably higher vapor pressures.

During the engine test, the fuel mixture is drawn from the mixture tank, equipped with a visual access to investigate possible separation, by an air-operated high-pressure piston pump. The pump pressurizes the fuel to the desired injection pressure of 150 to 200 bar. For security reasons one solenoid valve is installed between the tank and the pump and the air supply and the pump respectively and connected to the emergency circuit. This prevents leakage of the fuel in case the injector gets damage due to high injection pressures. The fuel injection pressure is regulated by precisely varying the inlet pressure of air to the high pressure piston pump. During injection, fuel runs through a common rail to eliminate pressure waves from the pump and in a final section all the way to the fuel injector the fuel is heated by a heating sheet controlled by a temperature controller. A Compact-Rio real-time controller monitors crankshaft position, cam shaft position, throttle position, and rail pressure to insure accurate injection timing and injection duration. With the pump flow rate being higher than the fuel consumption rate of the engine the pump also typically stalls during the compression stroke, remains stalled until sufficient fuel is consumed and then performs an intake stroke. Fuel is drawn from the mixture tank and the pump outlet pressure is constant till all the fuel in the rail is consumed by the engine. This caused problems for an installation of a flow meter upstream the piston pump. Due to the stalling of the pump the fuel flow rate is highly intermittent and cannot be measured correctly. Furthermore the pressure downstream of the pump is too high and no mass flow meter can be found, that would provide a safe operation. As a result the fuel consumption is being calculated out of the measured exhaust gas emissions and the combustion air consumption.

3.3 Fuel Supply

Due to the high resistance of ammonia to auto ignition a secondary fuel is needed to initiate combustion. Veltman et al. (2011) has investigated 3 different fuels as possible secondary fuels. The energy content of the stoichiometric air-fuel mixture versus the concentration of ammonia in the mixture as well as the production of carbon dioxide per energy content of the fuel was taken into consideration. As a result, the utilization of DME is recommended due to higher reductions on CO_2 emissions compared to a mixture of ammonia and diesel or bio-diesel with the same ammonia concentration.

In order to create mixtures of liquid ammonia and DME at desirable concentrations, a fuel preparation system was developed. The preparation system is located in a fume hood with continuous ventilation and allows precisely measuring and correcting the required fuel mix concentrations. First, liquid ammonia and DME flow from their storage tanks into the respective holding tanks by bleeding vapor to store the two prior to mixing and to even them out in pressure. Once liquid is drawn from the holding tanks filling is stopped. Mixing is performed under 150 psia that is generated by adding gaseous nitrogen to the tanks. This creates a differential pressure of 50 psia to the fuel mixture tank (100 psia). The mixing system, consisting of a flow meter and automated needle valves that are regulated using a National Instruments C-Rio real time controller, controls the mass flow rate of each fuel into the mixture tank. In addition check valves prevent reversed flow into the holding tanks. The real time controller monitors mass flow rate and density of both liquids and simultaneously updates the set point of the valves to ultimately generate

the desired ammonia and DME concentration. After the mixing process the valves will get closed and the pressure in the mixing tank is increased to 150 psia, also by adding gaseous nitrogen.

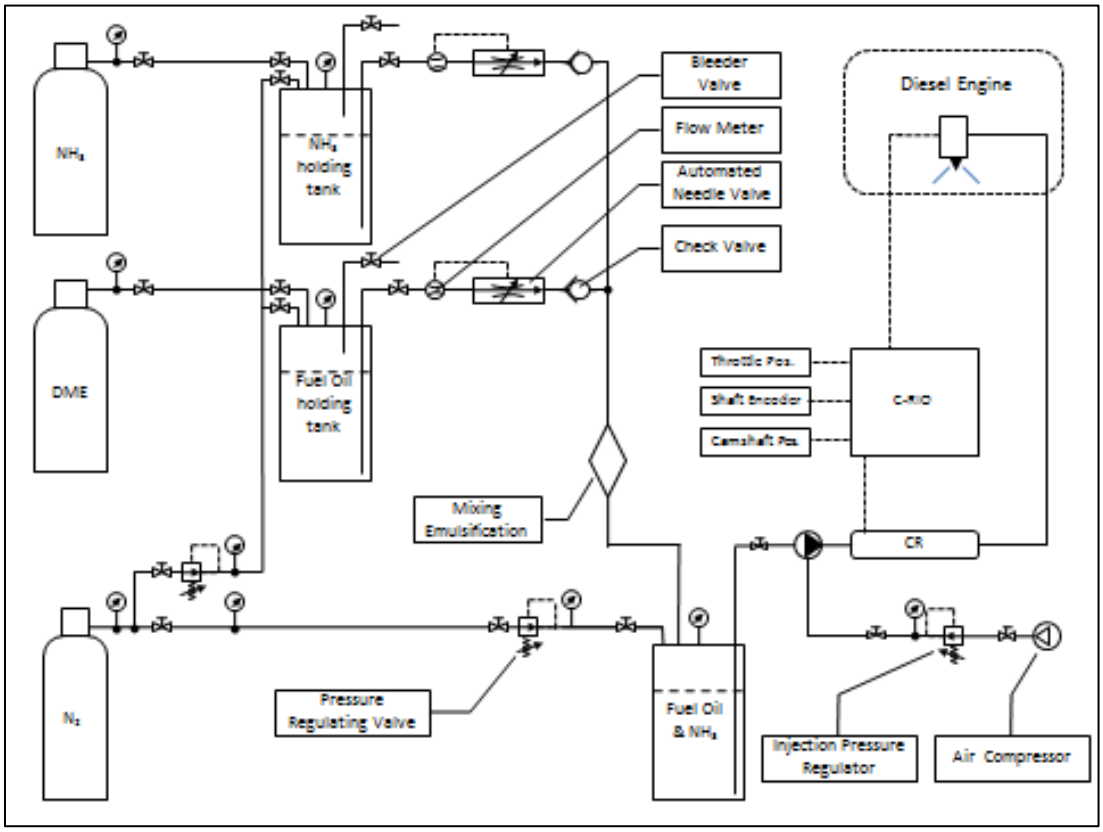

Figure 3.3 – Fuel flow diagram

3.4 Test Stand

The engine test stand consists of a heavy-duty steal frame that engine and dynamometer are mounted to. A Klam K10C electromagnetic retarder is used to load the engine. Engine and retarder are coupled directly utilizing a vibration damping flexible tire shaft coupling. Engine torque is measured utilizing a Copper

Instruments load cell with a nominal capacity of 100 lb. and an Action iQ Q448 bridge signal conditioner. The load cell is located 12 in from the center of the engine's output shaft and is attached to the retarder utilizing a torque arm.

A surge air tank with an approximate volume of 10 gal is mounted below the engine. Intake air is drawn from the room and consumption is measured utilizing a Meriam laminar flow element with a nominal capacity of 50 cfm and a Honeywell differential pressure transducer. The surge tank and intake air manifold are insulated with fiber glass and ethylene propylene diene monomer foam respectively. A computer controlled single tubular heating element with a nominal power output of 1.1 kW is installed along the centerline of the surge tank and can be used to heat the intake air up to 90°C. All temperatures are measured utilizing type K thermocouples. Crankshaft position and engine speed are determined utilizing a BEI Industries optical shaft encoder; mounted to the flywheel. The shaft encoder has a resolution of 1440 pulses/rev and also provides a single pulse reference signal at top dead center.

3.5 Engine Control Unit

National Instruments Compact-Rio system and LabView programming language have been implemented to control the engine operation. The C-Rio system offers easy configuration and the installed microprocessor is powerful enough to process complex control orders such as the determination of the injection strategy, the observation of sensor inputs, communication with the host computer and storage

of the recorded data on a USB-stick. Meanwhile the field gate point array (FPGA) on its back plate performs all the time critical operations. A total of 7 inputs (Camshaft Position, Crankshaft Position, Throttle Position, Wheel Speed, Fuel Pressure, Engine Temperature, Intake Air Temperature) and 2 outputs (Fuel Injector and Emergency Stop) are obtained by the C-Rio system, which is connected with the host computer through a local area network (LAN) cable for data logging, software reprogramming and communication.

In order to open the electronic fuel injector a coil within the injector generates a magnetic field. Hereby a boost voltage to lift the needle, which is much higher than the current to keep the injector open, is applied according to common practice with automotive injectors. The boost voltage makes sure that the current and the magnetic field is built up fast. The voltage requested by Bosch for a fast response is 60 V in order to quickly gain a coil current of 10 A, while the supply voltage and coil current have to be stepped down to 12 V and 2.5 A to prevent overheating of the coil. The power stage required to fulfill those specifications was designed and built by Veltman (2012). It includes a circuit to control the amount of current applied as well as a secondary logic to apply the boost voltage of 60 V for the first 0.5 ms of the injection. The power stage itself receives a 5 V signal, where the frequency of it is a function of the engine speed and the duty cycle is a function of the throttle position. Tests performed by Veltman et al. showed that the operation on a 12 V supply allows the injector to open within 0.75 ms, while the boost voltage of 60 V rises the coil in about 0.25 ms. This time reduction of 0.5 ms or about 11 CAD at the engine

rated speed of 3600 RPM becomes crucial for high speed operation and multi injections schemes especially. It would cause the injection events to overlap and never close, hence produce one long instead of two distinguished injection events.

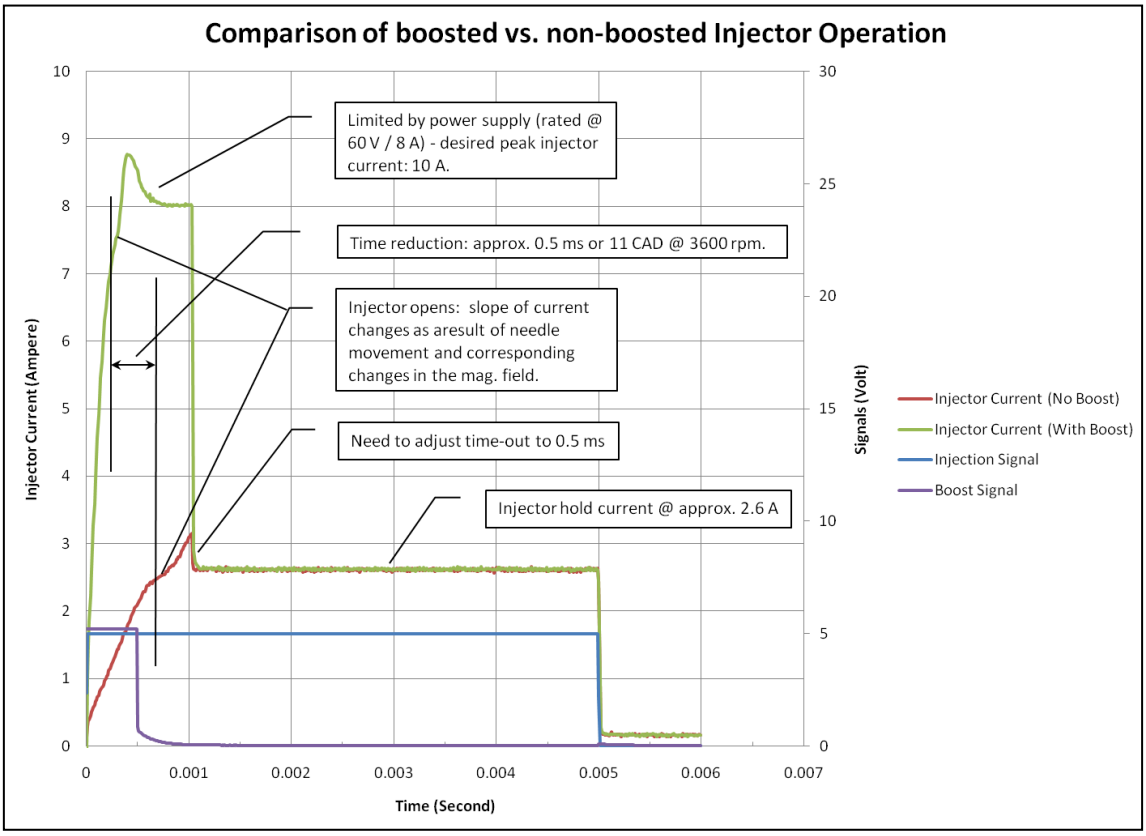

Figure 3.4 – Injector current versus coil using custom power stage (Veltman, 2011)

In addition, the fuel flow rate is determined by a simple injection bench. With the power stage being operated at a fixed frequency of 30 Hz in order to simulate the 3600 RPM, Diesel fuel was supplied to the injector at 15 MPa by the high pressure piston pump. The test included a total of 10,000 injection events and the fuel was collected in a tank placed on a scale. Results showed that the mass per

injection approaches zero for an injection duration of 0.25 ms. Therefore the injector response was estimated to be 0.24 ms through interpolation which then also determined to advance the electronic signal to the coil by 0.24 ms to ensure that the injection event and hence the fuel entrance to the combustion chamber take place exactly when desired. For an injection duration of 0.4 ms and longer, the fuel flow rate was estimated to be 2.68 mg/ms.

The software configuration uses relatively simple calculations and references to determine the fuel mass to be injected, the injection timing and the numbers of injections (single or double).The system is divided into time critical tasks taken by the FPG platform and other monitoring tasks taken by a micro controller. This also decreases the computational load for both. When the engine is running (run-mode) all sensors and the user inputs are monitored and checked against predefined limits (governor setting and maxi. Temperature) as well as the injection timing and duration is determined based on current engine speed and throttle position.

If the user cuts of the fuel supply or other circumstances cause the engine speed to drop below 400 RPM the system transfers into idle state. Only in this state the software execution can be stopped. A total of threads are executed in parallel and organized by their priority and rate of execution to cover both time critical as well as less time critical tasks. In addition the interface offers control over the two safety solenoid valves, the glow plug cycle, an injector flush option and an emergency stop.

The controlling of the dynamometer is also managed through a LabView interface custom designed by GDJ Inc. to meet the requirements of our application. The interface provides the user with a remote like dynamometer control to increase

and decrease the load manually or automatically through an RPM controller. It also includes the ignition and starter buttons for the engine itself and displays all the important engine parameters.

3.6 Measurement of Exhaust Emissions

The gaseous emissions are measured using a combination of Horiba MEXA 7100DEGR and 1170NX emissions analyzers. The emissions data recorded include CO, CO_2, NOx, HC, O_2, and NH_3. Heated sampling lines are used. In particular, exhaust ammonia emissions are measured using a Horiba MEXA 1170NX analyzer that can measure ammonia and NOx emissions simultaneously. The above emissions analyzers have been widely used in industry for studying diesel exhaust emissions as well as the performance of selective catalytic reduction (SCR) systems utilizing urea injection. The smoke number is measured using an AVL 415S soot meter. The cylinder pressure is measured using a Kistler 6125B piezo-electric pressure transducer together with a Kistler 5010 charge amplifier. The cylinder pressure is measured every 0.1 crank angle degrees and averaged over 50 engine cycles. In addition the composition of the exhaust gas emissions, recorded at all times, allows together with the air flow rate the calculation of the fuel consumption.

Chapter 4 Results and Discussions

4.1 Test Procedure

To determine the engine performance and exhaust gas emissions, a set of baseline tests were carried out up front. The testing was performed in two steps: 1) evaluation of the engines maximum brake mean effective pressure (bmep) capability and 2) evaluation of the performance and emissions for 25 modes. The maximum bmep capability is based on the maximum engine power output of 4.67 kW, which was observed at an engine speed of 3480 rpm, while the maximum engine torque was seen at 3033 rpm. The 25 modes were determined as follows and include all 13 modes of the European Steady-State test cycle (ESC).

The modes, included by the ESC (marked modes 2 – 13 in Figure 3-1) range from medium to high engine speeds and loads plus one mode at idle. Modes 2 – 13 are conducted at three engine speeds (A, B, C) with 100 %; 75 %; 50 %; and 25 %; load factors.

The engine speeds are defined as follows:

1. The high speed n_{hi} is determined by calculating 70 % of the declared maximum net power. The highest engine speed where this power value occurs (i.e. above the rated speed) on the power curve is defined as n_{hi}.
2. The low speed n_{lo} is determined by calculating 50 % of the declared maximum net power. The lowest engine speed where this power value

occurs (i.e. below the rated speed) on the power curve is defined as n_{lo}.

3. The engine speeds A, B, and C to be used during the test are then calculated from the following formulas:

$$A = n_{lo} + 0.25(n_{hi} - n_{lo})$$

$$B = n_{lo} + 0.50(n_{hi} - n_{lo})$$

$$C = n_{lo} + 0.75(n_{hi} - n_{lo})$$

Twelve additional test modes were introduced by Veltman et al. (2011) in addition to the test modes defined by the ESC to better capture engine performance at low engine speeds as well as performance at peak torque and peak power. Modes 14 – 17 (peak power) and 22 – 25 (peak torque) were determined according to ISO 8178 and are based on 100%; 75%; 50%; and 25% load factors at the respective engine speed.

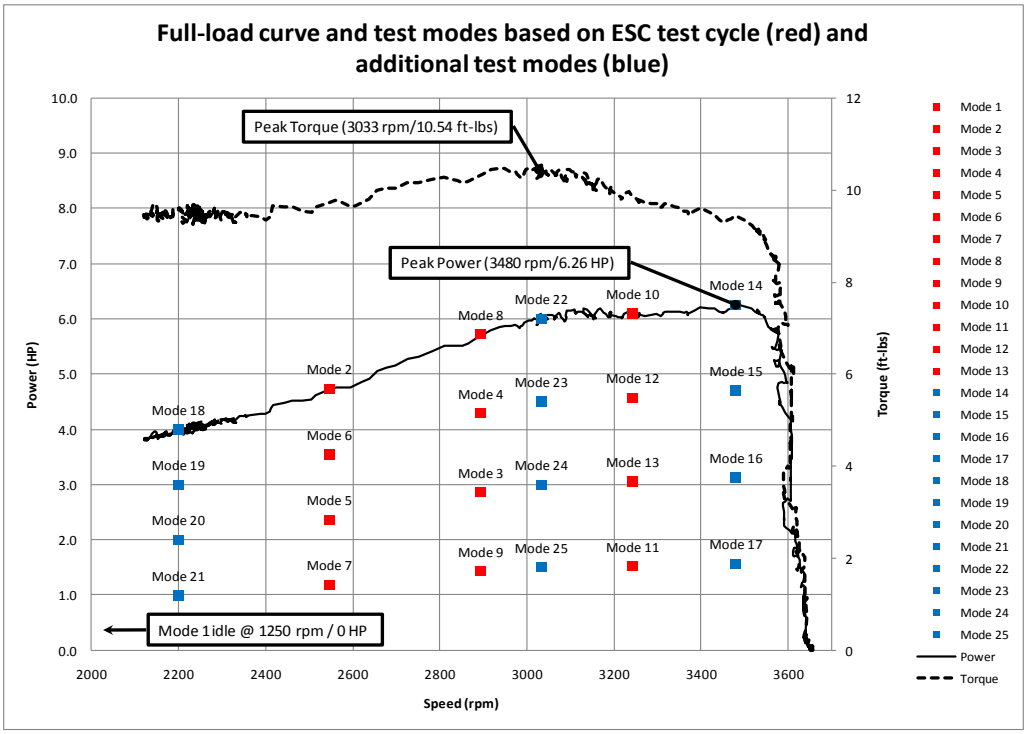

Figure 4.1 – Full-load curve for the unmodified engine and the 25 test modes

During the course of the project work using ammonia/DME with the new injection system, it is found that high load operations cannot be attained. Thus, the test conditions are chosen at low to medium loads at various engine speeds, as listed in Table 2. In addition Figure 4.2 shows the respective engine maps for the fuels tested. It is believed that the modes tested are representative of the appropriate speed conditions of the present engine.

Table 4-1 – Summary of test modes for fuel mixtures

Mode	Engine Speed (rpm)	Engine Power (kW)	Engine Torque (Nm)
5	2548	1.74	6.61
7	2548	0.87	3.31
9	2895	1.05	3.52
11	3243	1.12	3.34
20	2200	1.47	6.47
21	2200	0.74	3.24

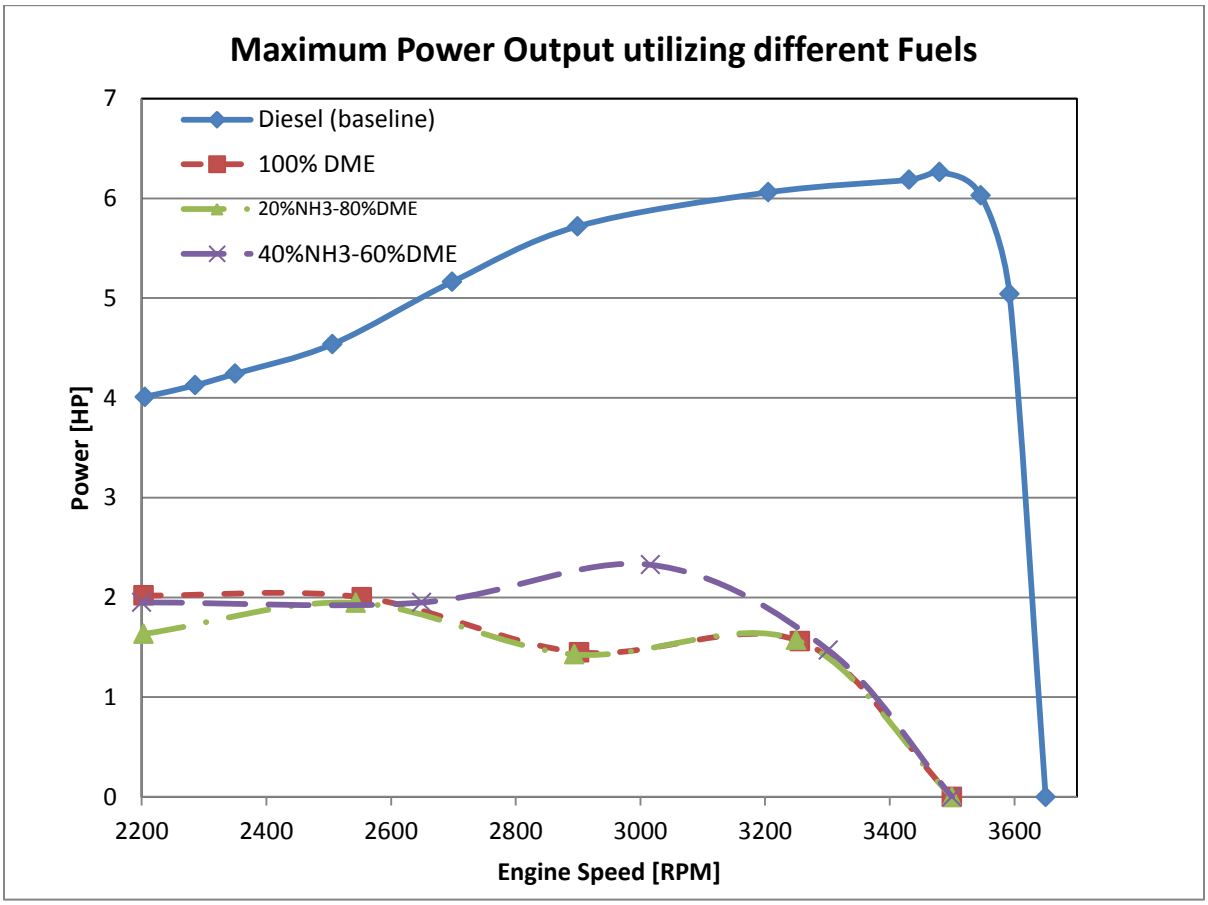

Figure 4.2 – Maximum power output using different fuels

For the subsequent testing, the engine was warmed up at medium load and medium speed and then operated at each mode for approximately 5 minutes to allow temperatures to reach steady state conditions prior to the data recording. The data of performance parameters and emissions was recorded over a period of 3 minutes and is presented in the final results as an average value. This provided acceptable results with a reasonable standard deviation.

4.2 Results using single injection

After the engine is modified to implement the new fuel injection system, tests are conducted using 100% DME and results are used to compare with those obtained using 20 wt.% ammonia – 80 wt.% DME mixtures and 40 wt.% ammonia – 60 wt.% DME mixtures. Note that results using the original engine using diesel fuel are not used for comparison since the entire injection system has been replaced.

It is observed that the operating range of the engine is limited when ammonia is used. Possible reasons are as follows. Ammonia has high latent heat but low lower heating value (18.6 MJ/kg for ammonia compared to 42 MJ/kg for diesel fuel). In order to achieve the same engine load, more ammonia is needed, which in turn cools down the in-cylinder air and slows down combustion. Combustion is further worsened due to the low flame temperature and low flame speed of ammonia. Additionally, the current peak injection pressure is 20 MPa, which is the rated pressure for the GDI injector used but is low in terms of diesel engine operation. While injection pressure was set to 150 bar using 100%DME and 20%NH_3–80%DME, it has to be increased to 180 bar in order to achieve combustion using 40%NH_3–60%DME. This therefore led to an improvement in fueling conditions and in-cylinder combustion and emissions as shown in the following sections. Another adjustment had to be made to the intake air temperature in order to compensate the cooling by the higher ammonia quantity in the fuel. The intake air was raised from 30 ˚C to 60 ˚C using 20%NH_3–80%DME and then again to 80 ˚C for the 40%NH_3–60%DME mixture.

Emissions are presented in reference to brake specific energy consumption (BSEC) in MJ/kWh. This parameter is introduced in place of brake specific fuel consumption (BSFC), which has the unit of g/kWh. The reason is that in this study different fuels with different heating values are used and it is less meaningful to monitor the total mass consumption rate of the fuel mixture. It is more instructive to present data with respect to energy consumption for this study. For comparison, when the engine produces 4.3 kW at 3,250 rpm using diesel fuel, the BSEC is 13.656 MJ/kWh, corresponding to a BSFC of 304.8 g/kWh.

For the mixtures of ammonia and DME, single injection schemes are tested according to the procedure and parameters mentioned above. The injection timing is swept from 5 crank angle degrees before top dead-center (BTDC) to 45 BTDC. For the modes that are tested, a complete sweep of all the injection timings is not always possible due to unstable combustion. However, retarded injection timings seem to be more favorable. The injection timings listed in Table 3 are chosen such that stable operations can be attained. Other operating conditions tend to result in excessive CO emissions or very steep cylinder pressure rise rates. In particular, when engine load is increased, the above phenomena become more pronounced and the engine is not able to reach steady-state operation.

4.2.1 Pressure and Heat Release Rate Histories

Comparisons of cylinder pressure and heat release rate histories using 100%DME, 20%NH_3–80%DME and 40%NH_3–60%DME are shown for each of the modes tested. Results show that ammonia results in longer ignition delay due to its

high resistance to auto-ignition (autoignition temperature = 651°C). The presence of ammonia, however, does not significantly deteriorate the combustion despite its high latent heat of vaporization and the low flame speed. While for all the modes testes the in-cylinder pressure is slightly lower for 20%NH_3–80%DME and about 10 bar lower for the 40%NH_3–60%DME, the peaks of heat release rates increase with increasing ammonia content. In fact, it is observed that from low speed/load conditions (Mode 20 and 21) over medium speed/load conditions (Mode 5, 7, 9) to high speed conditions (Mode 11), the difference in peak pressure, especially between the 40%NH_3–60%DME and the other two cases, increases. The values overall for the cylinder pressure hereby slightly decreases with higher speeds, ranging from slightly less than 50 bar using 40%NH_3–60%DME (Mode 5) to almost 75 bar using 20%NH_3–80%DME (Mode 20) .

With respect to the different load and speed conditions, heat release rates show increasing ignition delays mainly for the ammonia-DME fuel mixtures. The ignition delays for 100%DME, 20%NH_3–80%DME, and 40%NH_3–60%DME are 10-15 CAD, 10-20 CAD and 15-30 CAD, respectively. Their difference in value for the three cases fluctuates throughout the cases, but always shows higher numbers for the fuels containing ammonia. Again, the biggest similarities, with respect to ignition delay as well as for peak values, are found for low speed conditions (Mode 20). This mode also has the highest value of heat release rate with almost 30 J/deg using 40%NH_3–60%DME. The lowest value is around 7.5 J/deg using 100%DME (Mode 5, 7, 9).

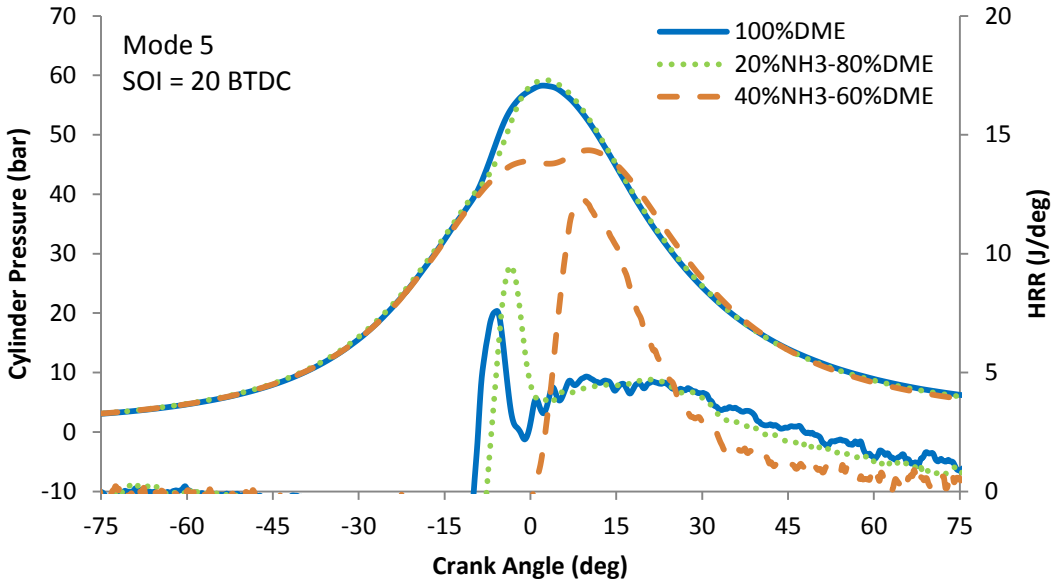

Figure 4.3 – Cylinder pressure and heat release rate for Mode 5 using single injection

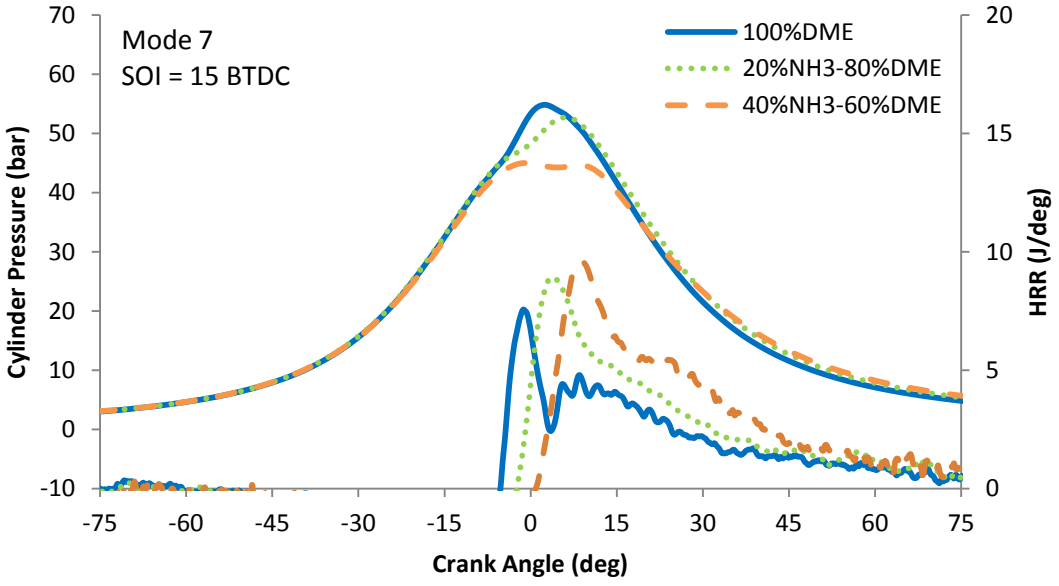

Figure 4.4 – Cylinder pressure and heat release rate for Mode 7 using single injection

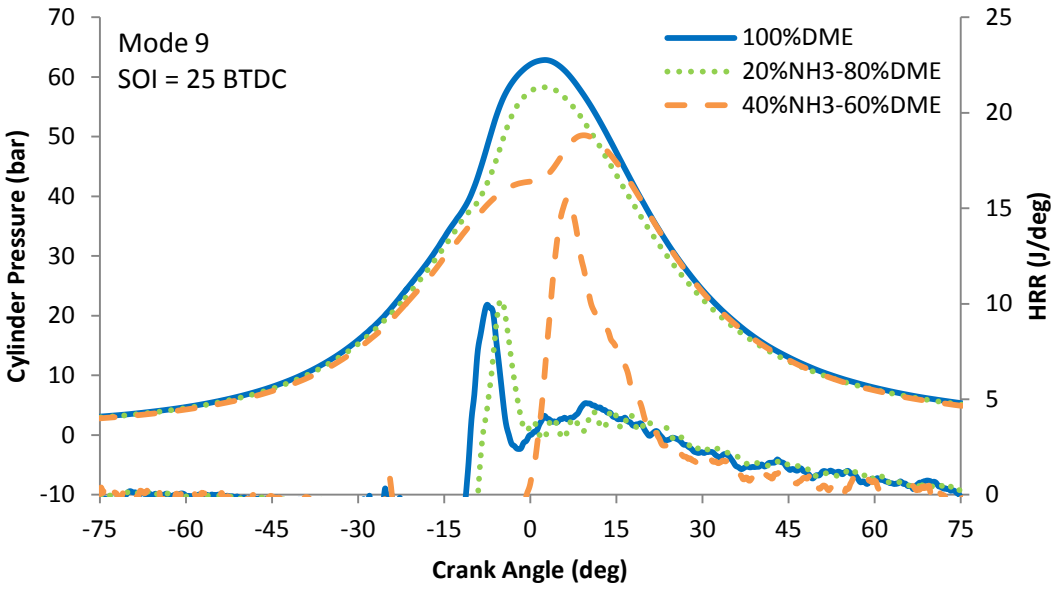

Figure 4.5 – Cylinder pressure and heat release rate for Mode 9 using single injection

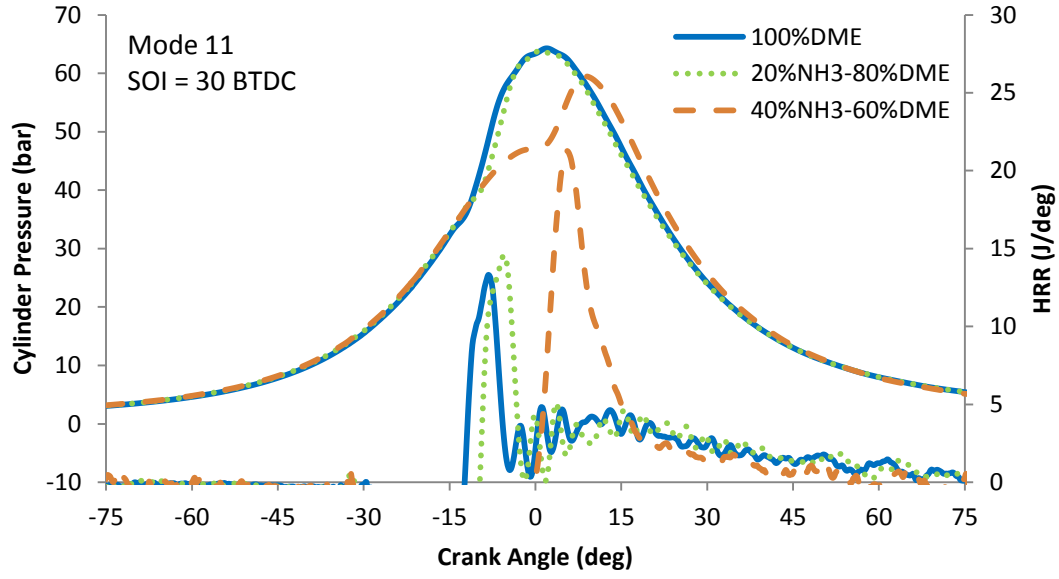

Figure 4.6 – Cylinder pressure and heat release rate for Mode 11 using single injection

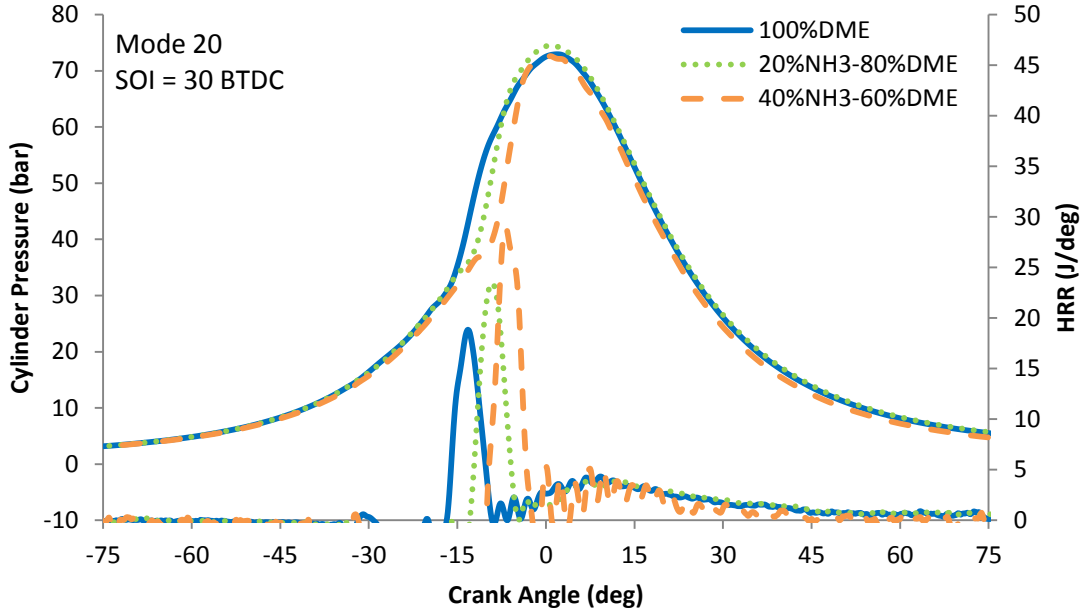

Figure 4.7 – Cylinder pressure and heat release rate for Mode 20 using single injection

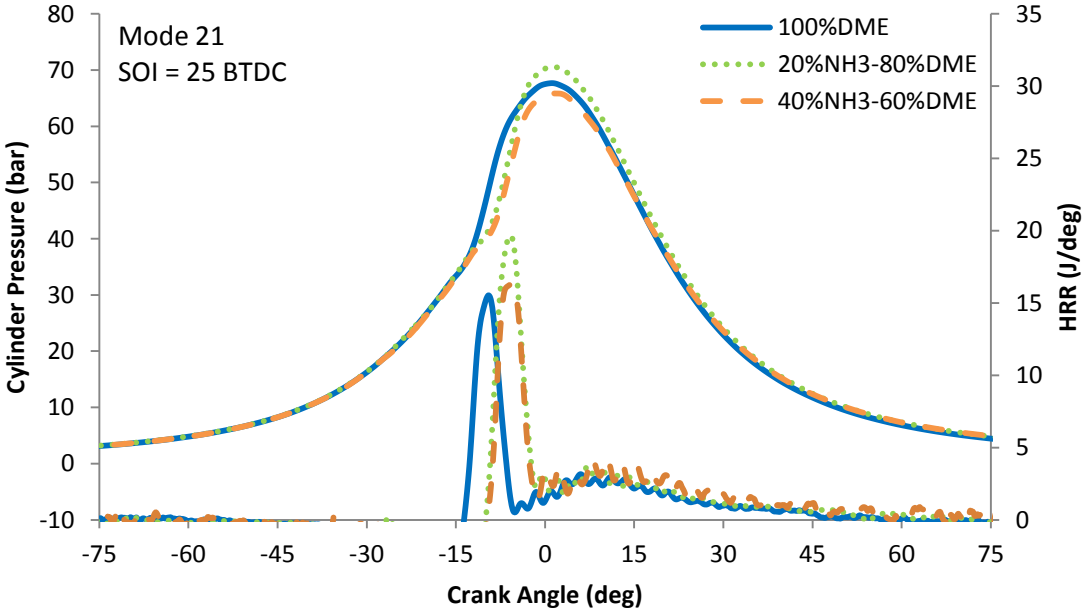

Figure 4.8 – Cylinder pressure and heat release rate for Mode 21 using single injection

4.2.2 NO_x and NH_3 Emissions

NOx emissions increase considerably when ammonia is involved in the combustion process, as shown in Fig. 4.9 to 4.11. In fact, NOx emissions are relatively low in terms of concentration (ppm) but the values are high when reported in terms of brake specific emissions. The red line thereby represents the EPA emissions regulations for NOx (7.5 g/kWh) for small output engines. The level of NOx emissions is around 15 g/kWh using 20%NH_3–80%DME mixtures at high fueling conditions, almost double the emissions using 100%DME. It is believed that the increase in NOx emissions is due to fuel NOx since the combustion temperature is lower when ammonia is involved, as evidenced from the lower cylinder pressure in the figures for the pressure histories. It is known that ammonia can serve as a reduction agent to reduce NOx to nitrogen and oxygen, as used in the modern SCR systems. However, under the present engine conditions, the fuel bound nitrogen in ammonia appears to be the major source of NOx emissions in the exhaust. Using 40%NH_3–60%DME mixtures, the NOx emissions in terms of concentration stay the same, but due to lower fueling conditions the emissions drop back down to levels using 100%DME. In fact, while levels of NOx emissions are about the same, the values for BSEC are half of those for 100%DME for some cases. This is mainly caused by increased injection pressure.

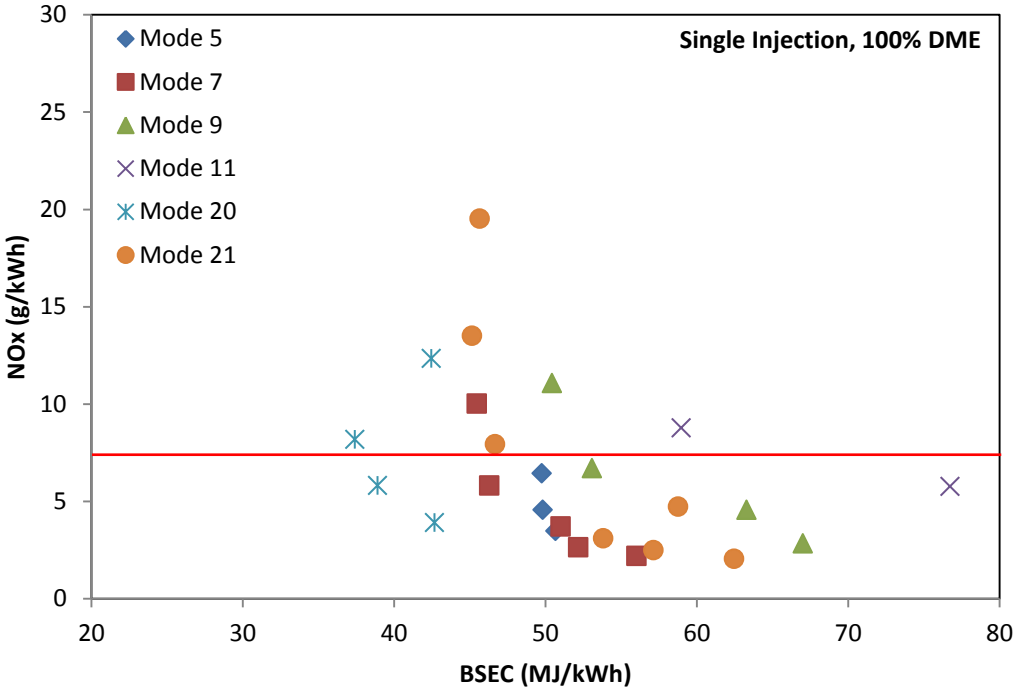

Figure 4.9 – NO_x emissions vs. BSEC of 100%DME using single injection

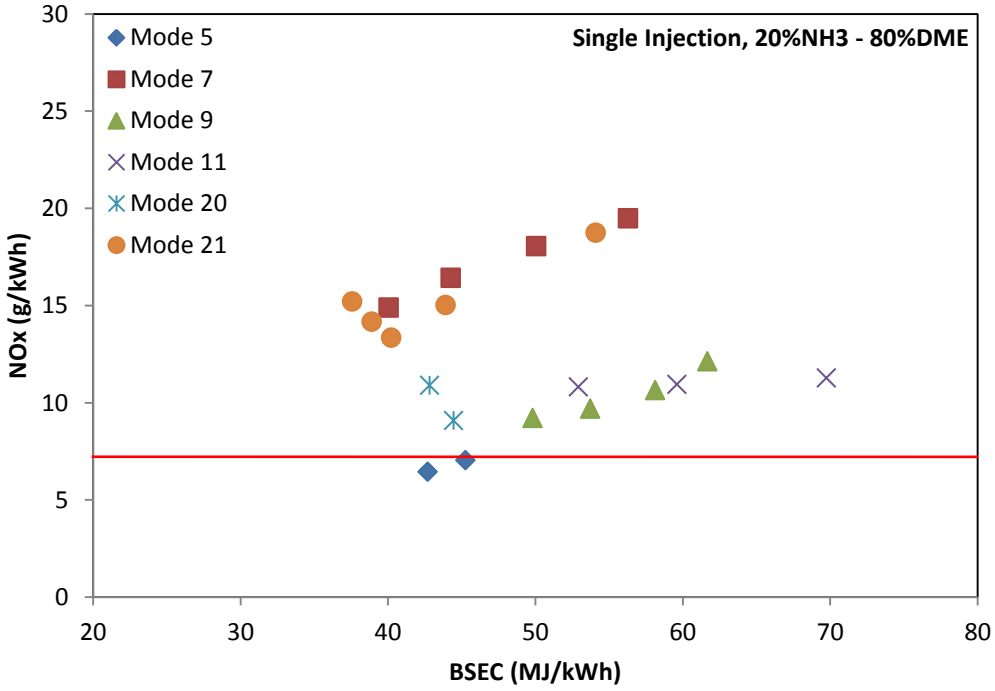

Figure 4.10 – NO_x emissions vs. BSEC of 20%NH_3- 80%DME using single injection

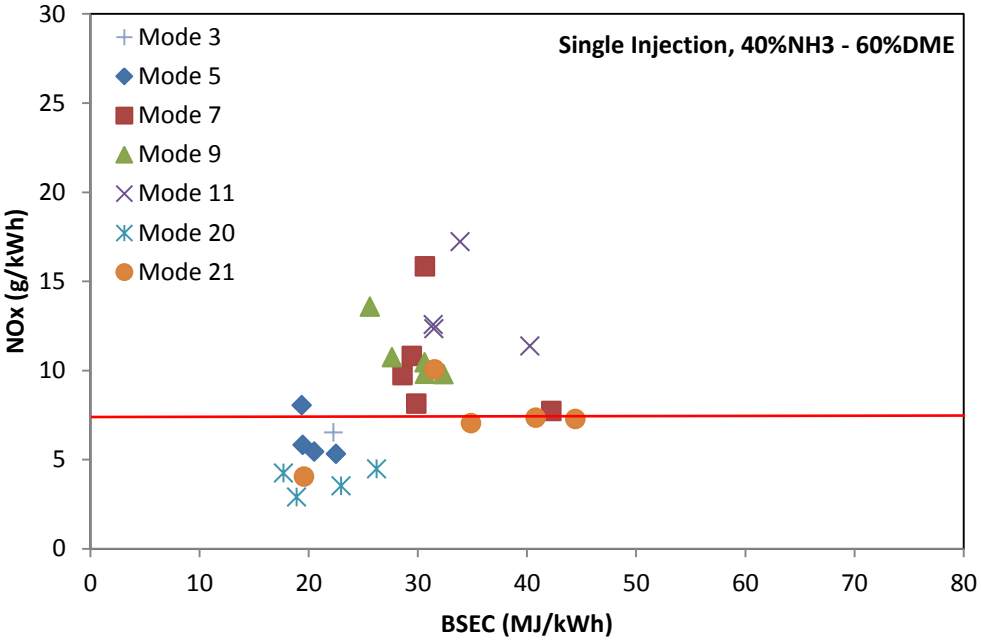

Figure 4.11 – NO_x emissions vs. BSEC of 40%NH_3- 60%DME using single injection

Ammonia emissions are shown in Figures 4.12 to 4.15. One of the concerns of using ammonia for combustion is the exhaust ammonia emissions, which can be harmful with unpleasant odor. Exhaust ammonia emissions are shown in both ppm and g/kWh. The emissions level of ammonia for the 20%NH_3–80%DME mixture is around 100 ppm for low speed/load conditions (Mode 20 and 21), around 400 ppm for medium speed/load conditions (Mode 5, 7, 9), and around 700 ppm for high speed conditions (Mode 11). As the ammonia quantity in the fuel is increased, emissions increase significantly. Using 40%NH_3–60%DME, ammonia emissions levels are around 400 ppm for low speed/load conditions (Mode 20 and 21), and vary from around 600 ppm to even up to 1400 ppm for both medium speed/load

conditions (Mode 3, 5, 7, 9) and high speed conditions (Mode 11). It should be noted that in a previous study using port injection of gaseous ammonia together with direct injection diesel fuel, the exhaust ammonia emissions are on the order of 1,000 to 2,500 ppm [12].

Values reported in terms of brake specific emissions, on the other hand, reflect the lower fueling condition and show similar levels for both conditions. Again, the lower brake specific energy consumption has to be pointed out.

The direct injection strategy employed in this study is shown to greatly reduce the exhaust ammonia emissions. For application in stationary power generation, exhaust ammonia can be diluted by air before released to atmosphere. It may also be possible that proper catalysts similar to those used in SCR systems can be used to convert exhaust ammonia and NO_x simultaneously, since ammonia is part of the de-NO_x process in present catalytic applications.

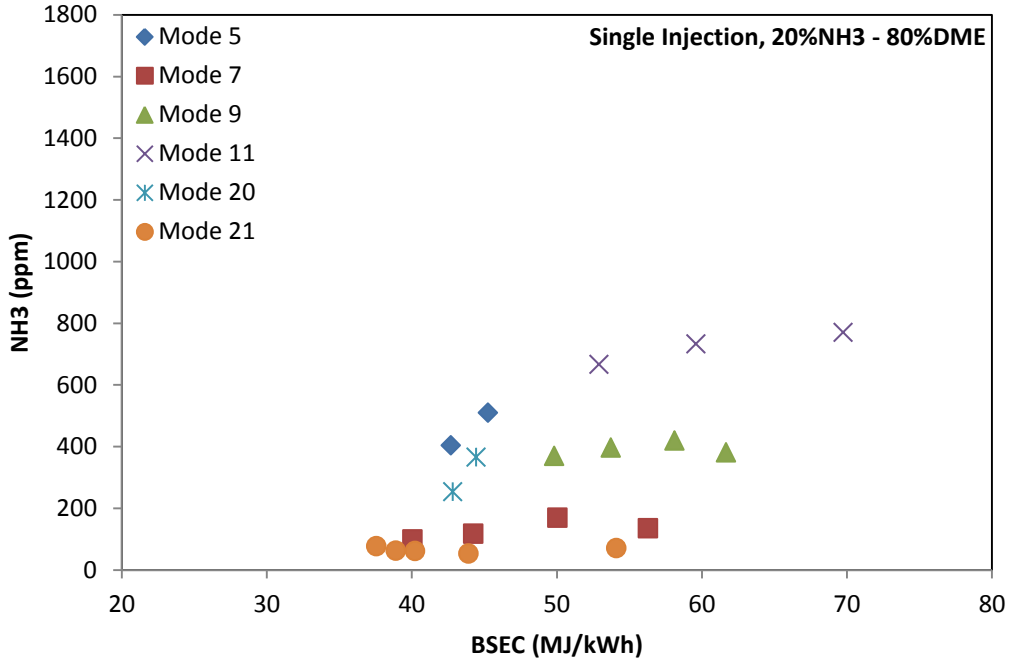

Figure 4.12 – NH_3 [ppm] emissions vs. BSEC of 20%NH_3- 80%DME using single injection

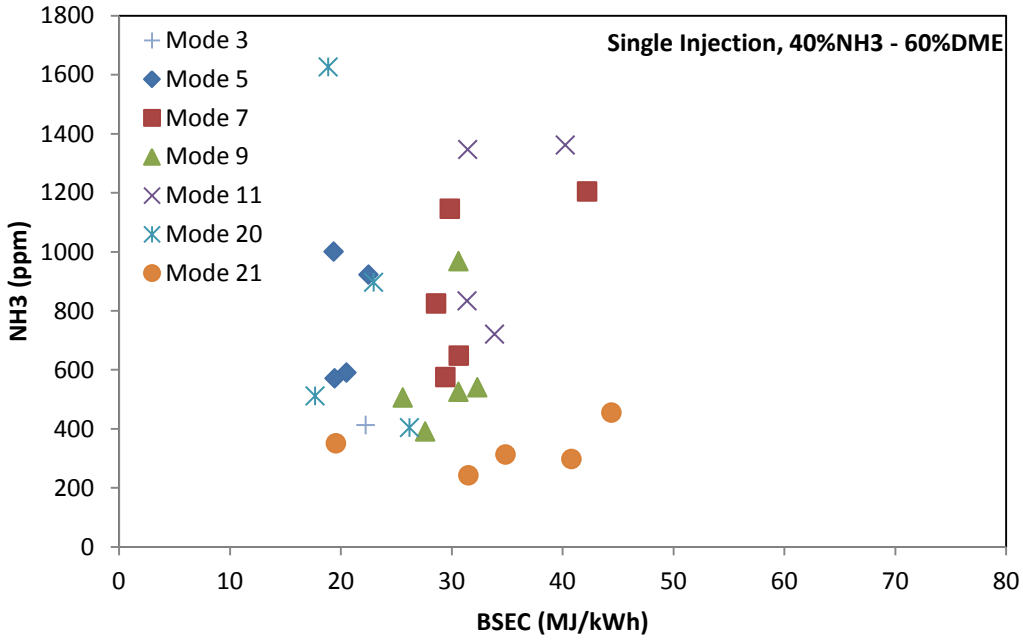

Figure 4.13 – NH_3 [ppm] emissions vs. BSEC of 40%NH_3- 60%DME using single injection

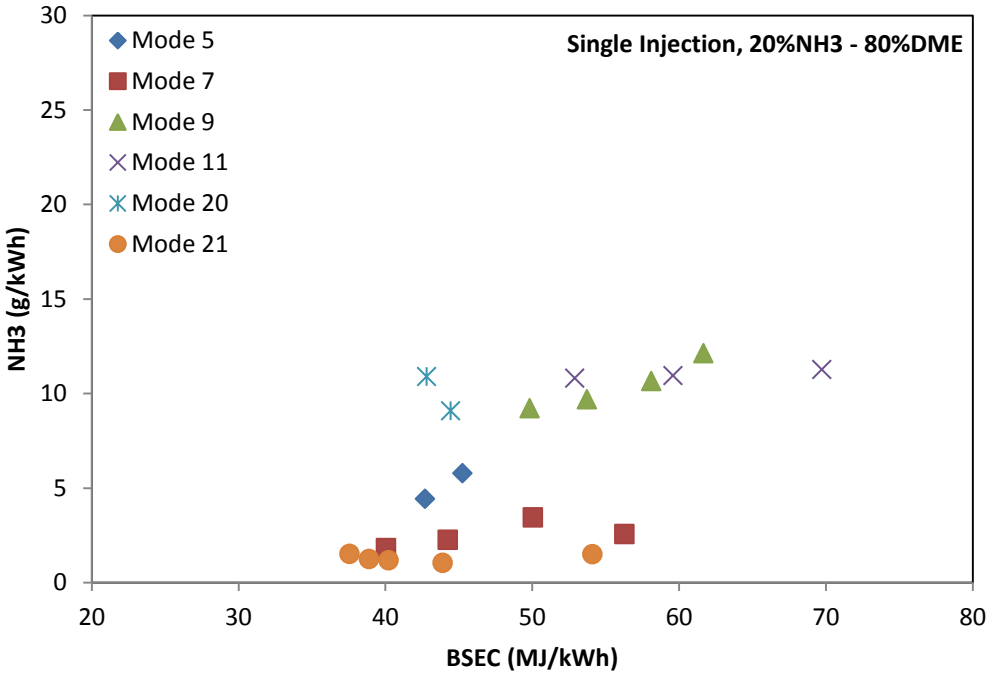

Figure 4.14 – NH_3 [g/kWh] emissions vs. BSEC of 20%NH_3- 80%DME using single injection

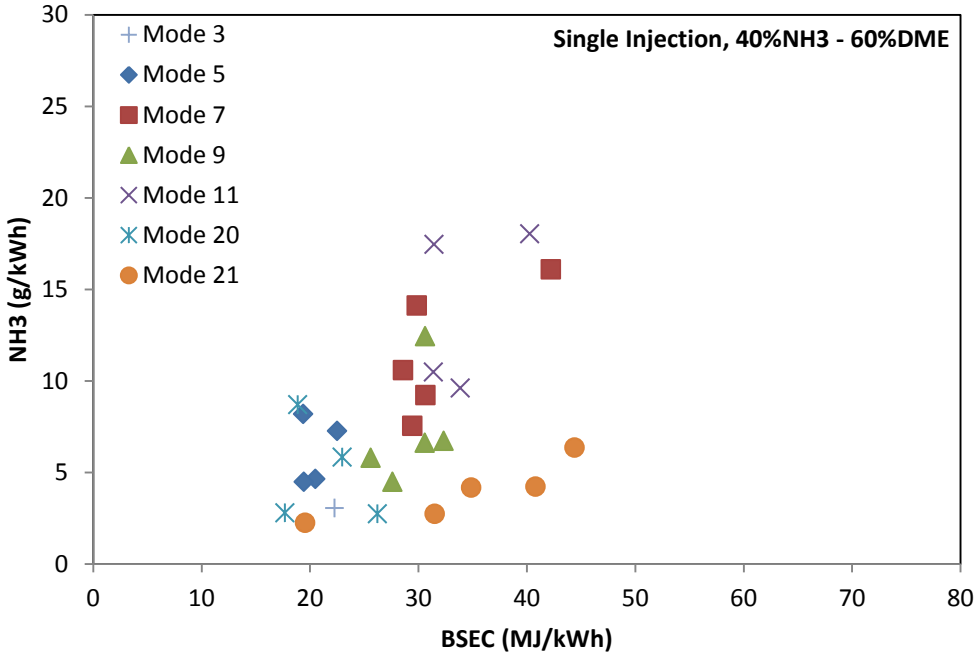

Figure 4.15 – NH_3 [g/kWh] emissions vs. BSEC of 40%NH_3- 60%DME using single injection

4.2.3 Soot Emissions

Soot emissions are shown in the following three figures for the different fuel compositions. It is found that soot emissions are at low levels under conditions studied with even lower emissions for higher ammonia contents. Soot emissions level is below 0.01 g/kWh using 20%NH_3–80%DME and even below 0.005 g/kWh using 40%NH_3–60%DME for the majority of conditions, in comparison with 0.02 g/kWh using 100% DME for most conditions. The low soot emissions level can be attributed to the following reasons. Typically soot emissions using DME is already very low. With ammonia in the fuel mixture, a higher quantity of carbons is replaced. Thus, in the fuel rich zone, fewer carbons are available to form soot.

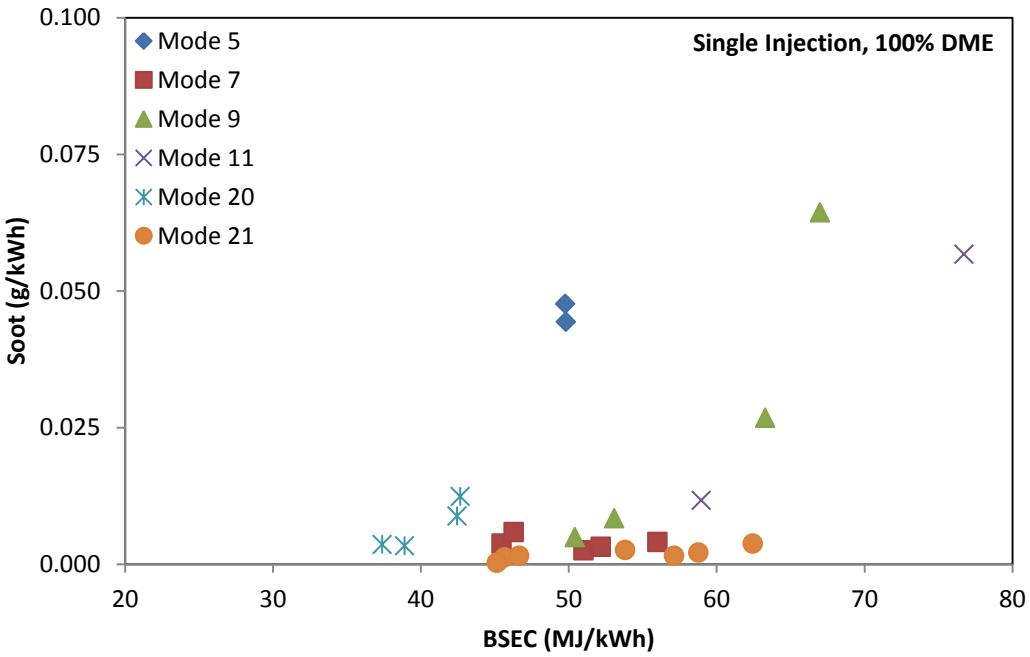

Figure 4.16 – Soot emissions vs. BSEC of 100%DME using single injection

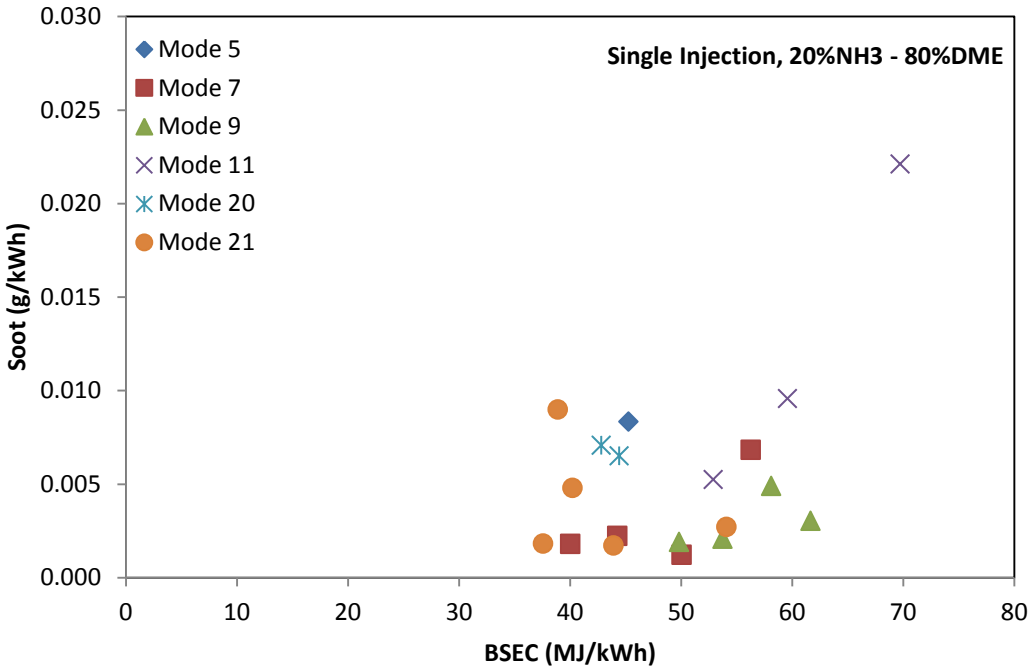

Figure 4.17 – Soot emissions vs. BSEC of 20%NH_3- 80%DME using single injection

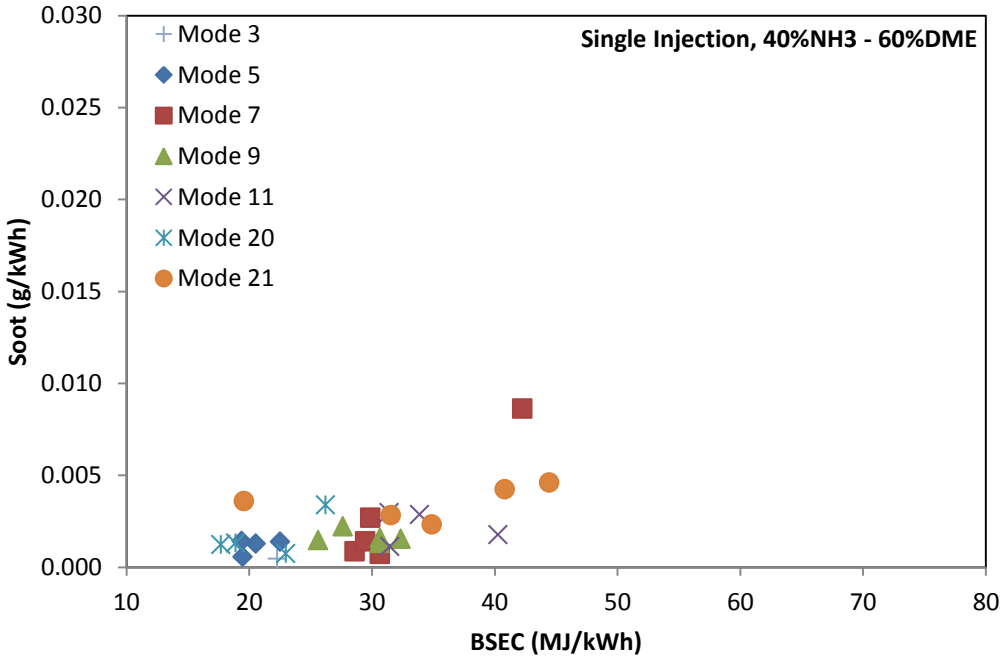

Figure 4.18 – Soot emissions vs. BSEC of 40%NH_3- 60%DME using single injection

4.2.4 Unburned Hydrocarbon and Carbon Monoxide Emissions

Figures 4.19 - 4.21 and Figures 4.22 - 4.23 show emissions of unburned hydrocarbons and carbon monoxide, respectively. The red line thereby represents the EPA emissions regulations for THC (6.6 g/kWh) and CO (0.4 g/kWh) for small output engines. The overall emissions levels using 20%NH_3–80%DME are similar to those using 100% DME, whereas the emission level for the 40%NH_3–60%DME is lower. In addition, values for the brake specific energy consumption are lower. It is noted that unburned hydrocarbon emissions deteriorate further and even get as low as 200 ppm for the more advanced injection timings using 40%NH_3–60%DME. The CO emissions are still relatively high under the present operating conditions. However, while CO emissions are ranging from 6,000 ppm to almost 10,000 ppm in raw data for the 100% and the 20%/80% cases, the CO emissions for the 40%/60% mixture drop significantly and average around 3000 ppm. It is thought that the low injection pressure (20 MPa) causes poor mixing and the lower combustion temperature due to the low content of ammonia further results in significant incomplete combustion. However, with higher quantities of ammonia replacing the carbon-based DME, NH_3 emissions become a sign for incomplete combustion while carbon emissions reaching lower levels.

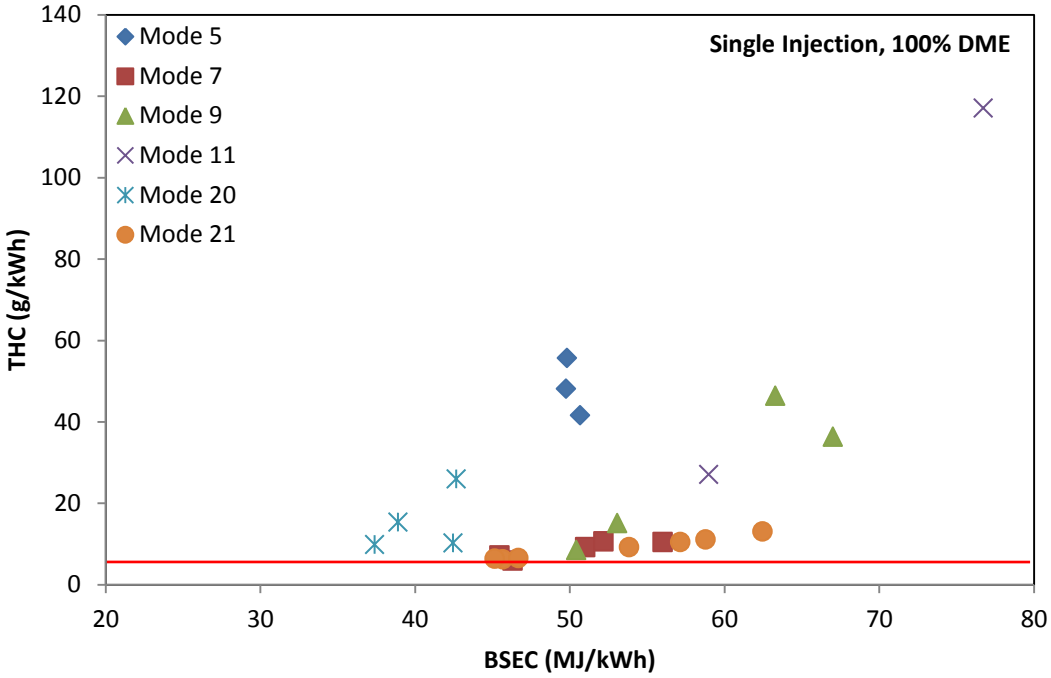

Figure 4.19 – HC emissions vs. BSEC of 100%DME using single injection

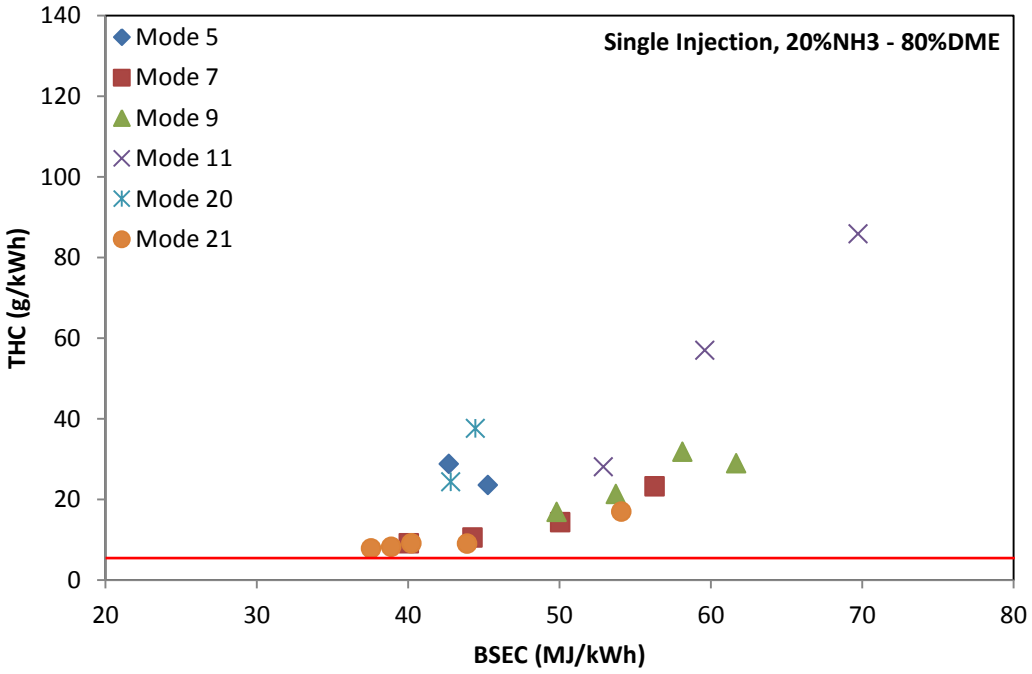

Figure 4.20 – HC emissions vs. BSEC of 20%NH_3- 80%DME using single injection

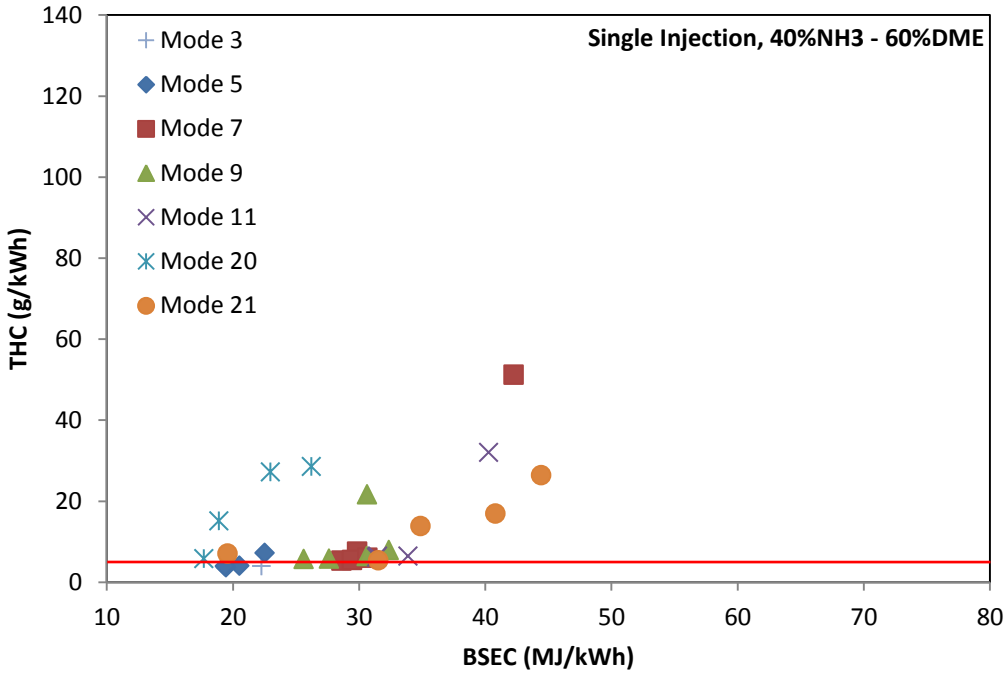

Figure 4.21 – HC emissions vs. BSEC of 40%NH_3- 60%DME using single injection

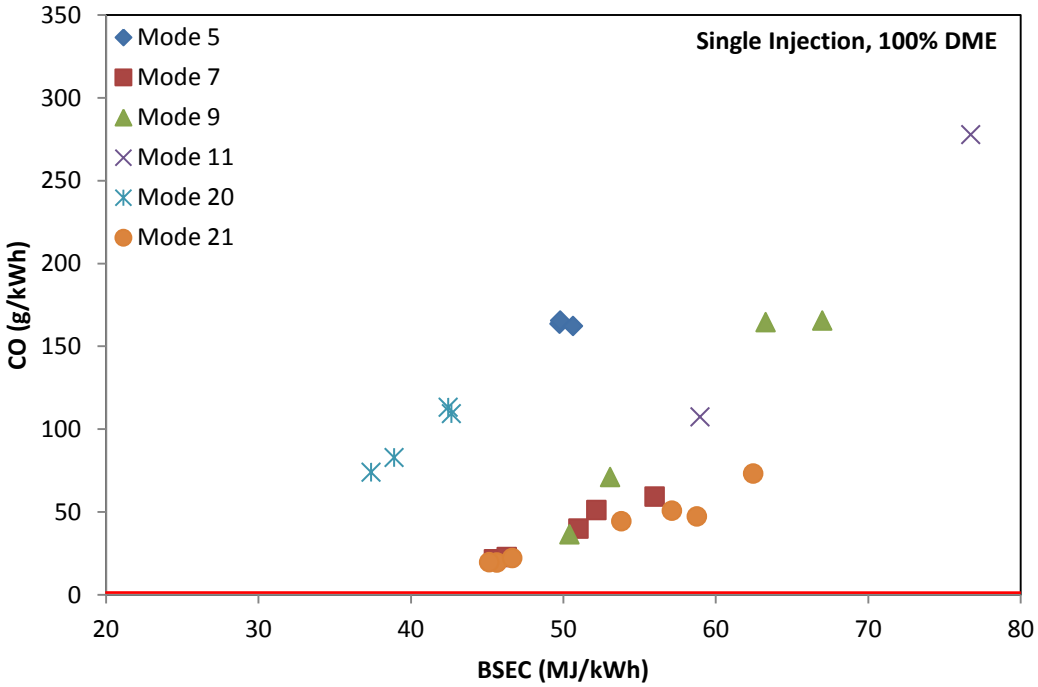

Figure 4.22 – CO emissions vs. BSEC of 100%DME using single injection

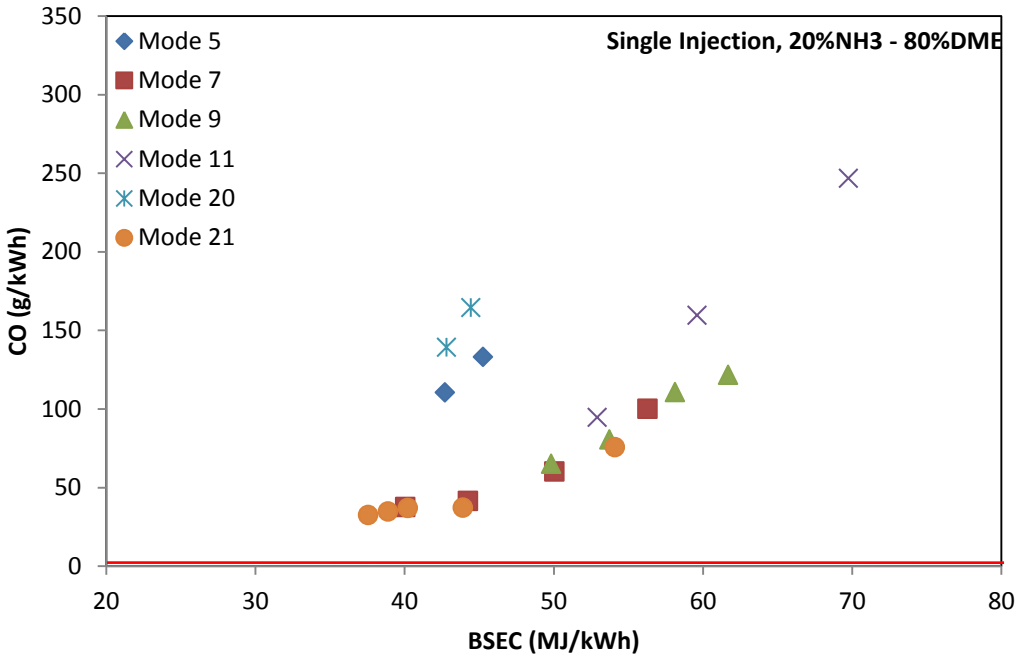

Figure 4.23 – CO emissions vs. BSEC of 20%NH_3- 80%DME using single injection

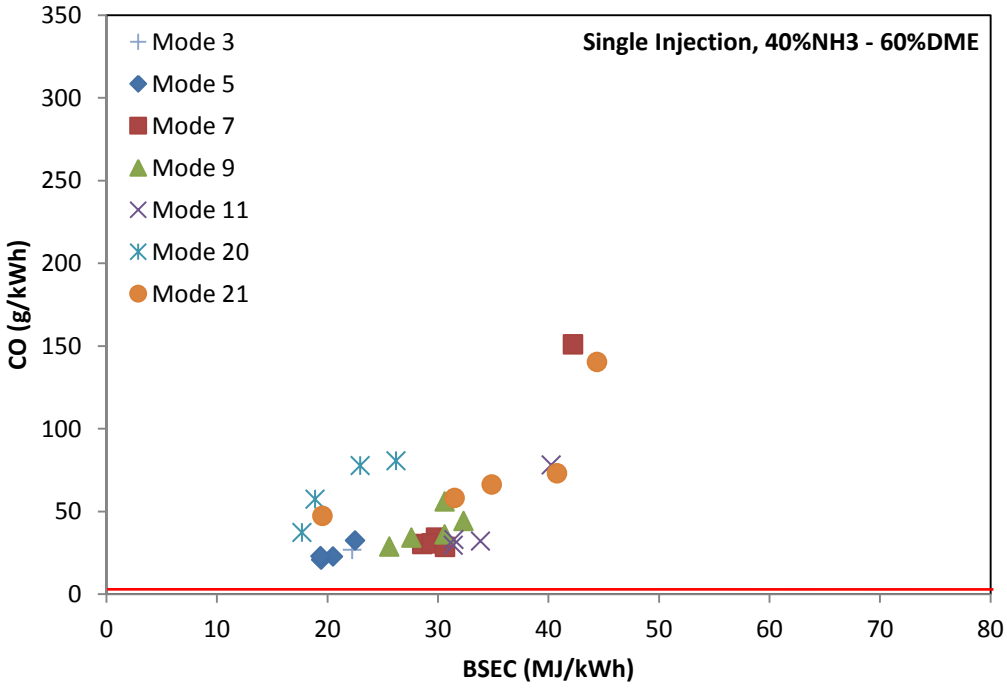

Figure 4.24 – CO emissions vs. BSEC of 40%NH_3- 60%DME using single injection

4.3 Results Using Double Injections

Double injections are used in an attempt to improve the air utilization, thus enhancing combustion quality and extending the operating range. It is anticipated that early pilot fuel has sufficient time for mixing to overcome the long ignition delay using ammonia. It is assumed that small quantities of pilot injections do not reduce the in-cylinder air temperature significantly during vaporization but pilot combustion can increase the in-cylinder temperature to enhance the combustion of main injections. Parametric study is conducted to determine the appropriate injection timings for pilot and main injections. It is observed that very early pilot injections cause the engine to knock. Thus, it is decided that the pilot injection timing ranges from 30 to 45 BTDC and the main injection timing is kept constant at 10 BTDC. Under these conditions pilot fuel is increased to 30% and 50% of the total fuel quantity. However, a complete sweep of all the injection timings is again not always possible due to unstable combustion.

4.3.1 Pressure and Heat Release Rate Histories

Figure 4.25 through Figure 4.28 show examples of cylinder pressure and heat release rate histories for the two pilot fuel quantities. For Mode 7 both quantities show almost identical pressure traces and only a slightly higher heat release rate history for 50% pilot. Mode 9, on the other hand, shows a difference in peak pressure of about 20 bar, where a lower value was recorded for the higher quantity pilot injection, and identical heat release rates. The pilot ignition occurs before the

injection of main fuel for Figure 4.25 as well as for Figure 4.26. Main fuel is injected during the peak of premixed burn.

Histories for Mode 21 are showing a higher peak pressure for 50% pilot injection as well as a heat release rate that is almost double the one for 30% pilot injection. Due to a very advanced pilot injection, main fuel is injected after the peak of pilot combustion. Premixed combustion ends before main fuel is injected. There is a gap of 5 - 10 CAD between the end of premixed burn and beginning of diffusion burn due to the long separation of pilot and main injections. It appears that such a long separation does not promote the combustion of main fuel since main fuel still has a considerably long ignition delay. It is found that it is preferable to inject pilot fuel later than 35 BTDC under the present setup.

Taking some of the observations into account, a trend can be observed for increasing engine speed. With an increase in engine speed, the lower pilot quantity slowly increases in terms of peak pressure and heat release rate.

For Mode 11 (Figure 4.27), data were collected for the 50% pilot injection, but with respect to the observed trend, it is expected the peak pressure and the heat release rate for the lower quantity to be even higher than the traces shown in the figure. Although it is not straightforward to distinguish between the combustion of pilot fuel and main fuel, it appears that pilot combustion does set up a high gas temperature to shorten the ignition delay of main fuel.

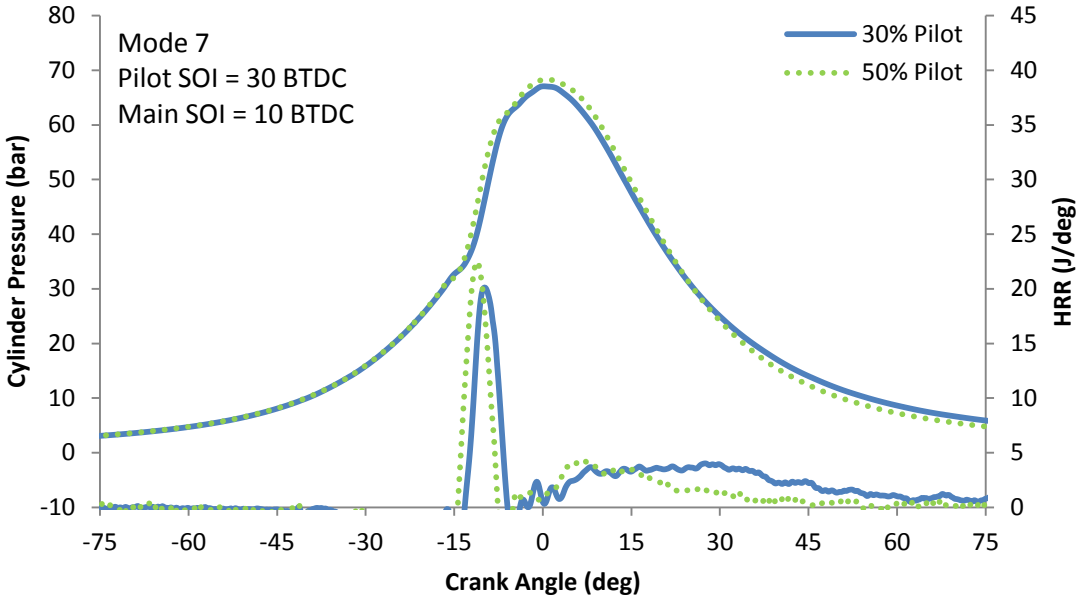

Figure 4.25 – Cylinder pressure and heat release rate for Mode 7 using double injections for 20%NH_3-80%DME

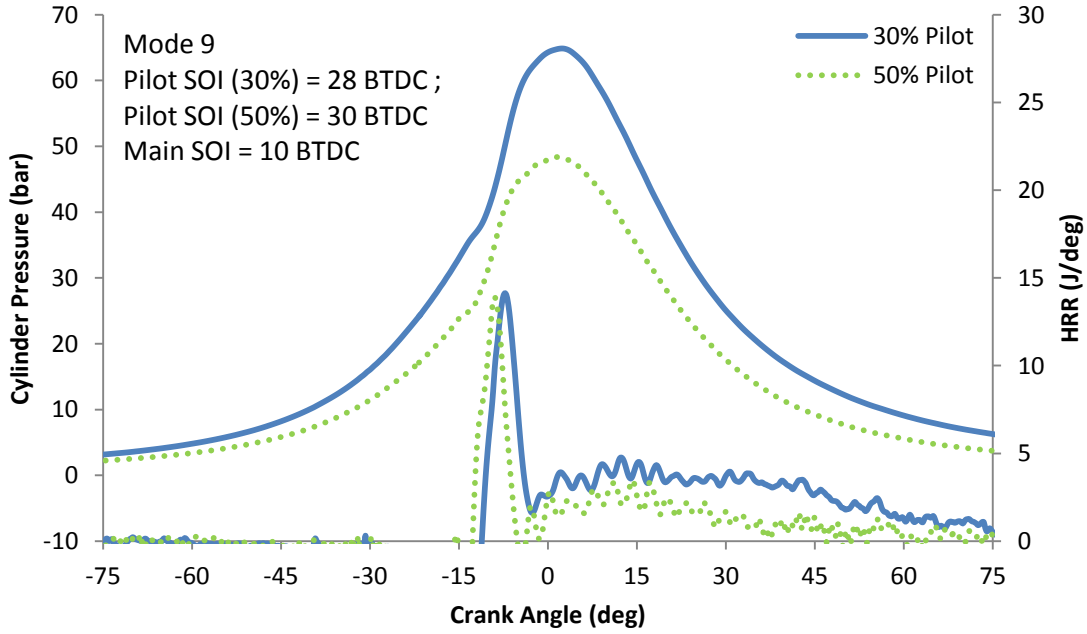

Figure 4.26 – Cylinder pressure and heat release rate for Mode 9 using double injections for 20%NH_3-80%DME

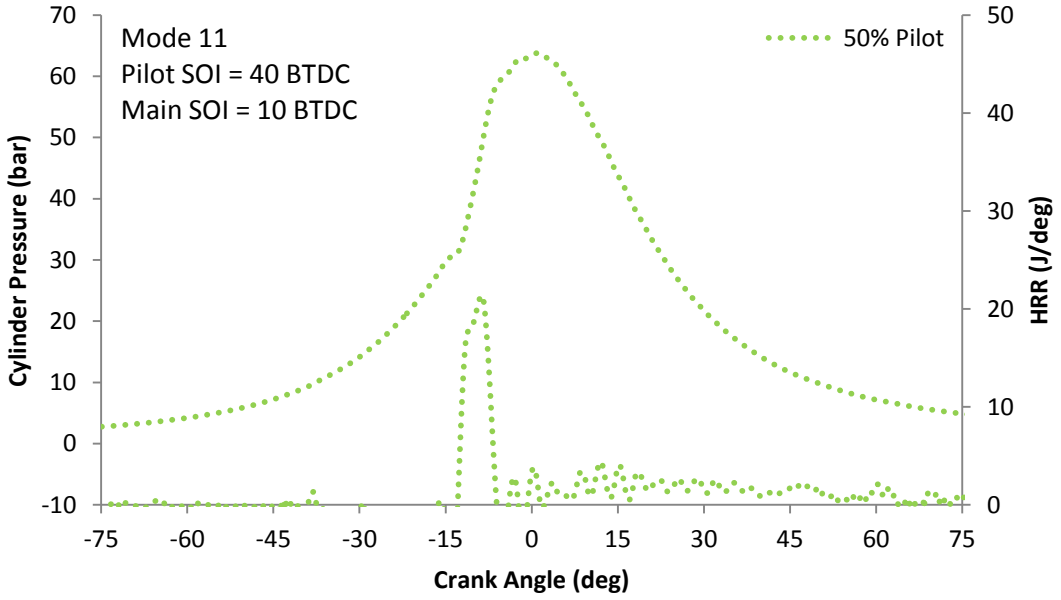

Figure 4.27 – Cylinder pressure and heat release rate for Mode 11 using double injections for 20%NH_3-80%DME

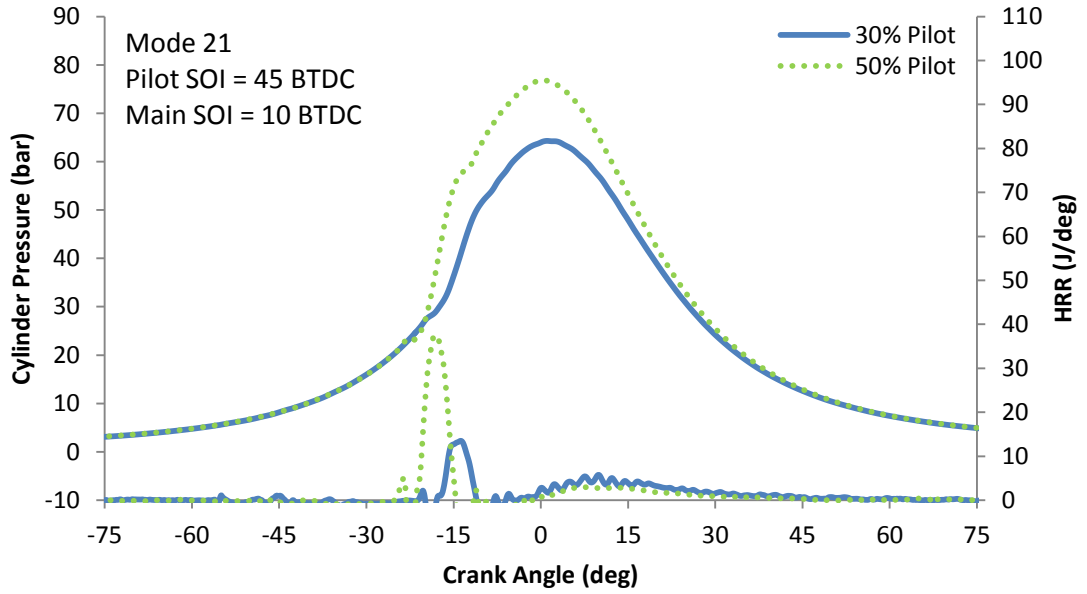

Figure 4.28 – Cylinder pressure and heat release rate for Mode 21 using double injections for 20%NH_3-80%DME

4.3.2 NO_x, NH_3 and Soot Emissions

The following figures show exhaust emissions of NOx, NH_3 and soot. Compared to single injection conditions, NOx emissions are higher in double injection cases due to the early combustion of pilot fuel that exposes in-cylinder gas at elevated temperature for a longer time. Within the two pilot quantities (Figure 4.29 and Figure 4.30), NO_x emissions are at the level ranging from about 7 g/kWh to right around 20 g/kWh (red line indicates EPA emission limit). However, double injections show higher values of BSEC, which make them less favorable than single injections.

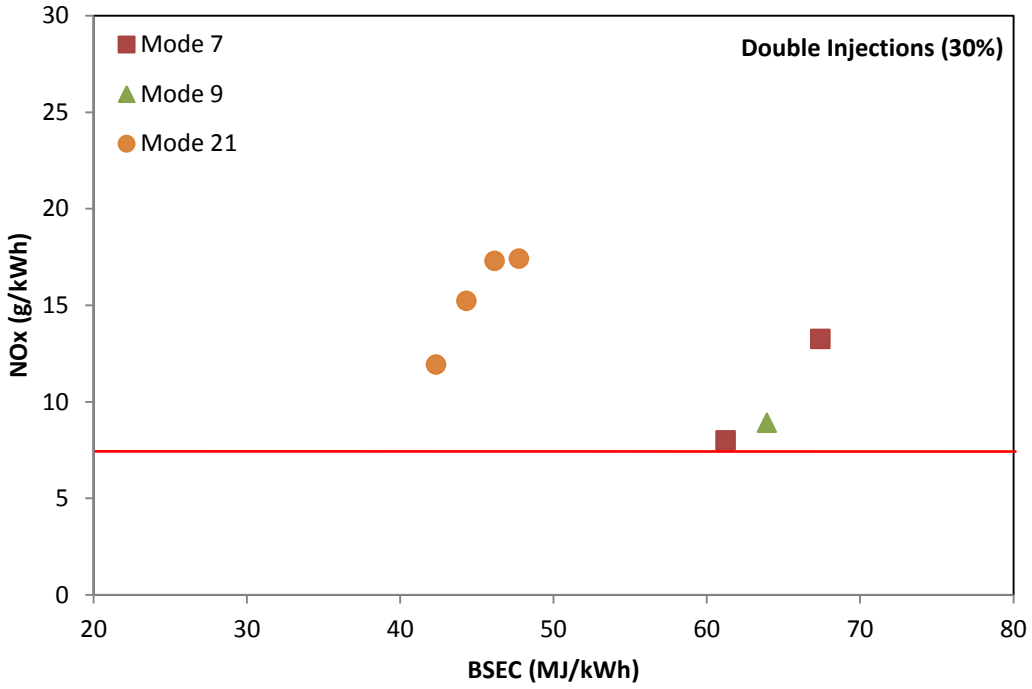

Figure 4.29 – NO_x emissions vs. BSEC using double injections

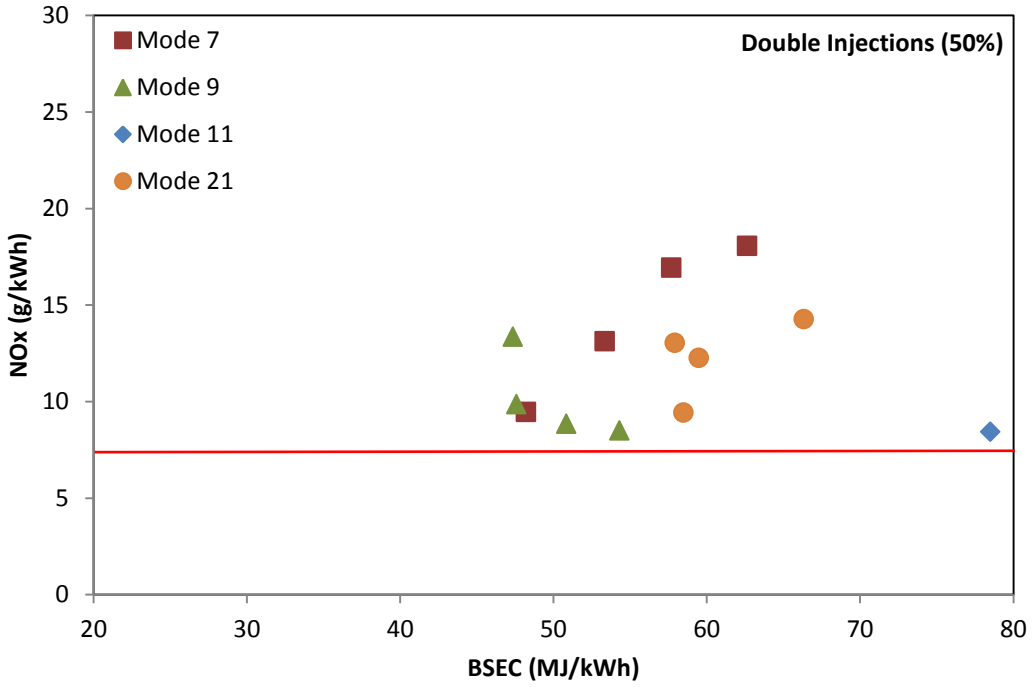

Figure 4.30 – NO_x emissions vs. BSEC using double injections

NH_3 emissions for the two pilot cases show hardly any difference in between each other. Emissions average approximately between 400 and 500 ppm, or approximately 8 g/kWh. It is also found that exhaust ammonia emissions are increased using double injection schemes compared to single injections. The reason is incomplete combustion since ammonia is a part of the fuel itself.

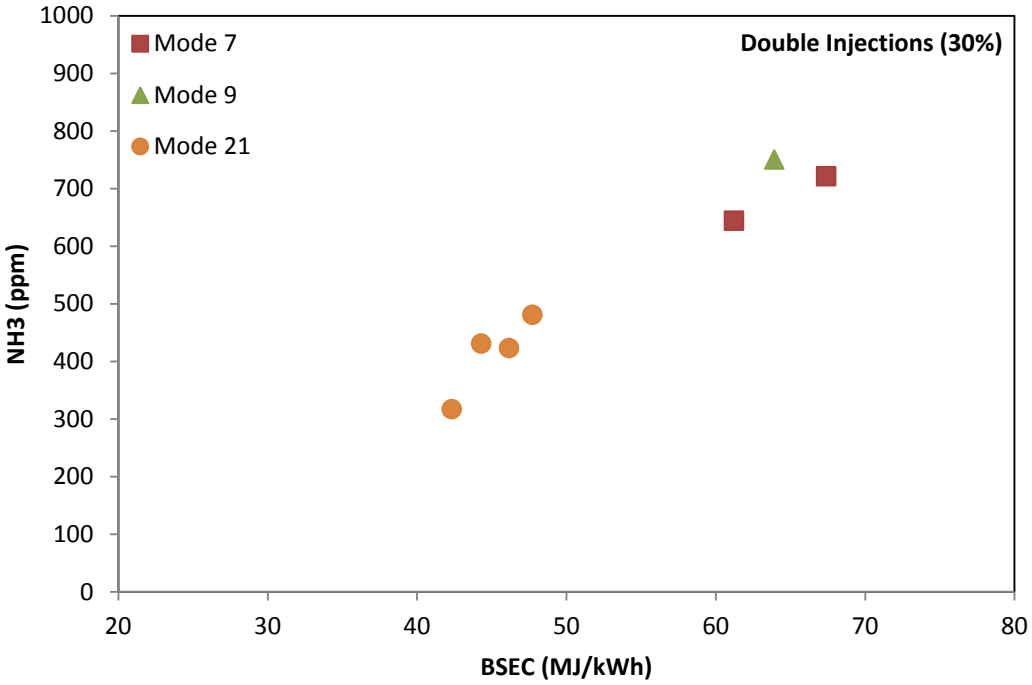

Figure 4.31 – NH_3 [ppm] emissions vs. BSEC using double injections

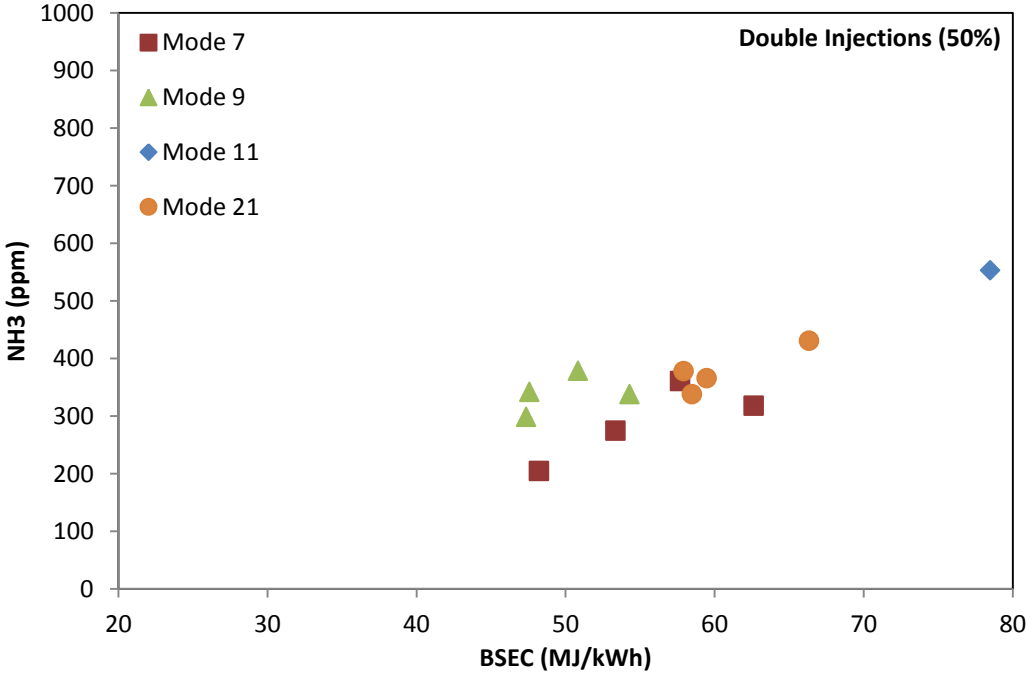

Figure 4.32 – NH_3 [ppm] emissions vs. BSEC using double injections

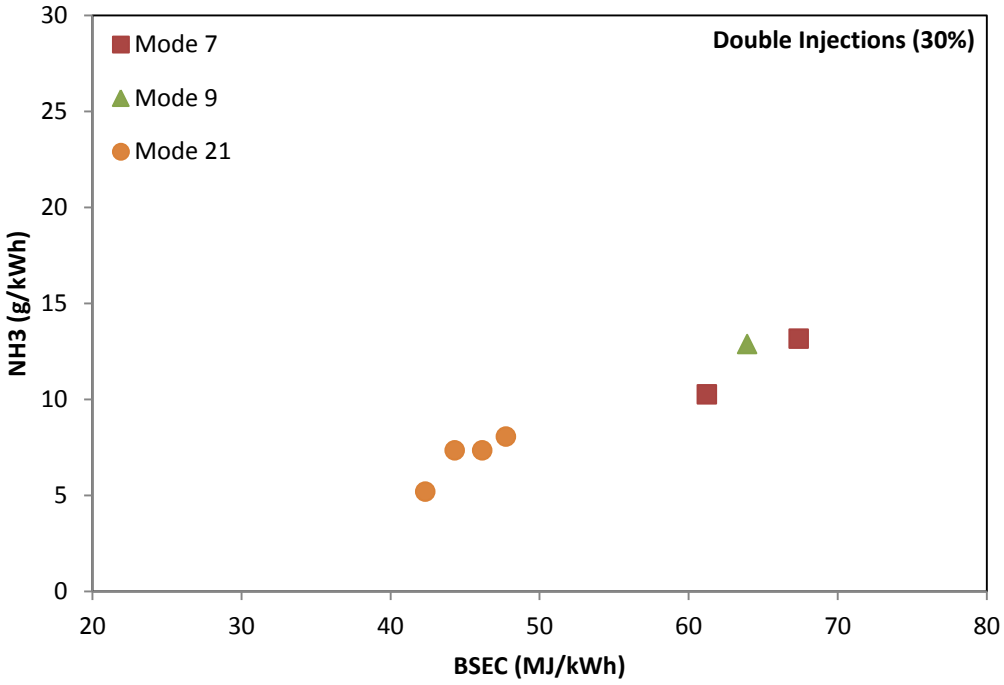

Figure 4.33 – NH_3 [g/kWh] emissions vs. BSEC using double injections

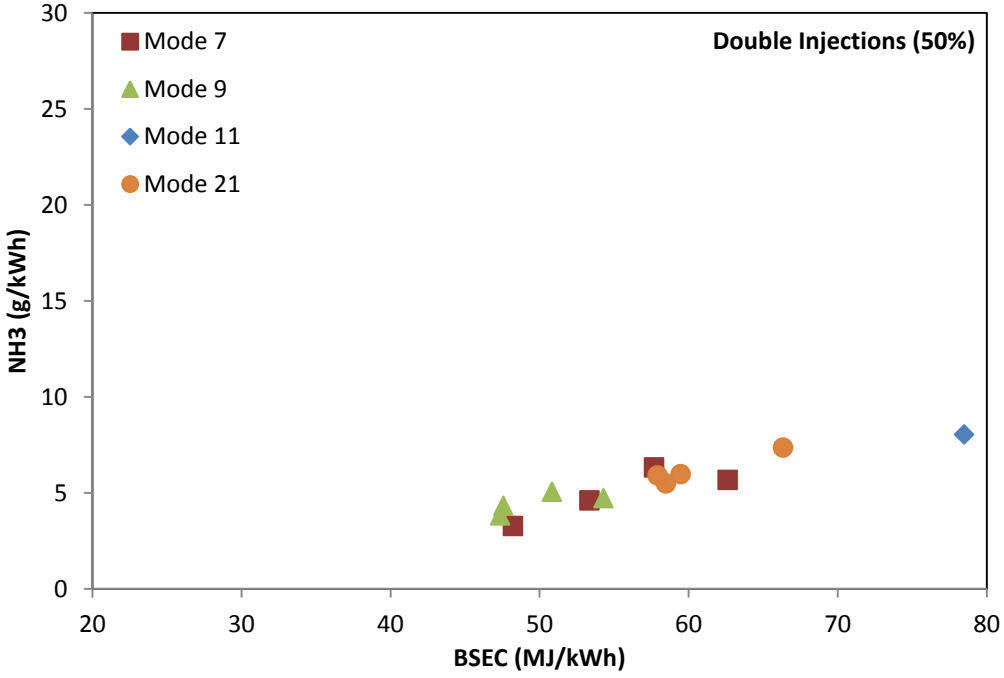

Figure 4.34 – NH_3 [g/kWh] emissions vs. BSEC using double injections

Soot emissions are comparable to those using single injections, both cases of pilot injections result in very low levels of soot emissions that don't even exceed level of 0.01 g/kWh. In several conditions, soot emissions are again too low to be measured using the present smoke meter.

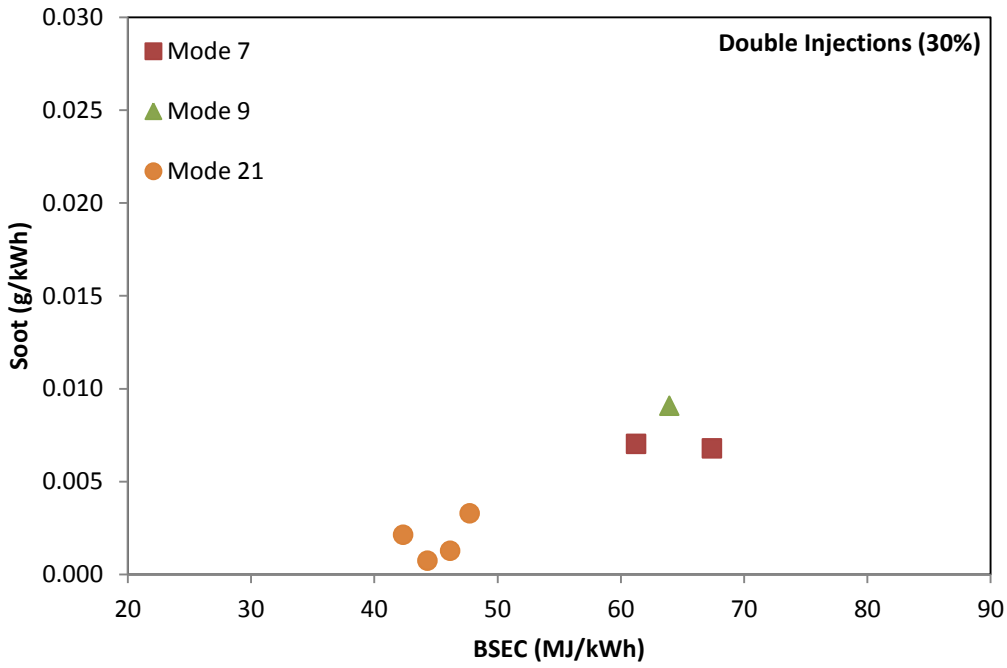

Figure 4.35 – Soot emissions vs. BSEC using double injections

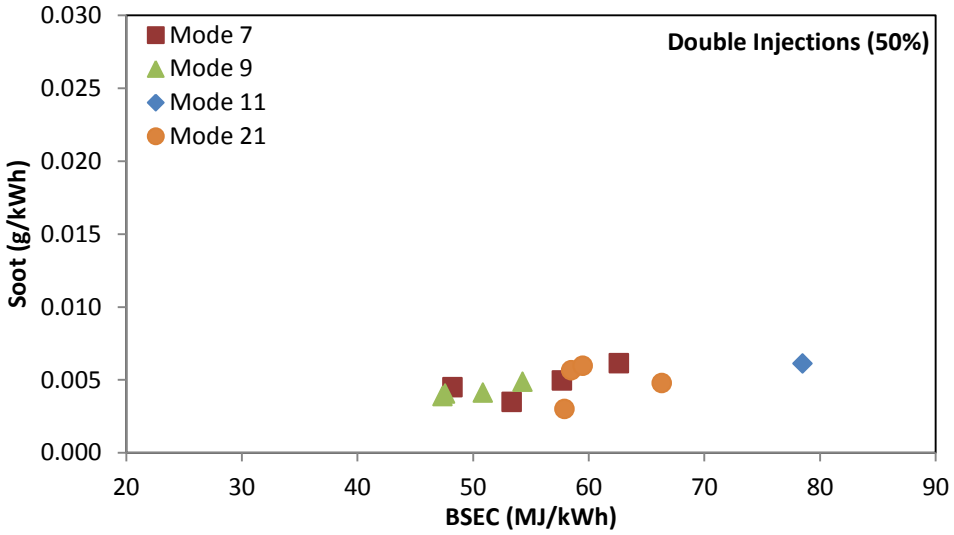

Figure 4.36 – Soot emissions vs. BSEC using double injections

4.3.3 Unburned Hydrocarbon and Carbon Monoxide Emissions

Results indicate that double injection schemes are not able to reduce exhaust HC and CO emissions, as shown in Figs. 4.37 to 4.40. The red lines again indicate the EPA emissions limits for both compounds. The emissions levels are similar for Mode 21 (low speed/load) using single and double injections and are still at an unacceptable level. When engine speed increases, HC and CO emissions increase significantly. The reason is thought due to the late injection of main fuel (i.e., 10 BTDC) as compared to most of the single injection cases. Furthermore, due to the reduced quantity, main fuel has less momentum to penetrate into the combustion chamber, resulting in poor air utilization and incomplete combustion. Also with respect to the increased NH_3 emissions, the portion of NH_3 decomposing to H_2 and H increases, which in then is detected via increased unburned hydrocarbon emissions.

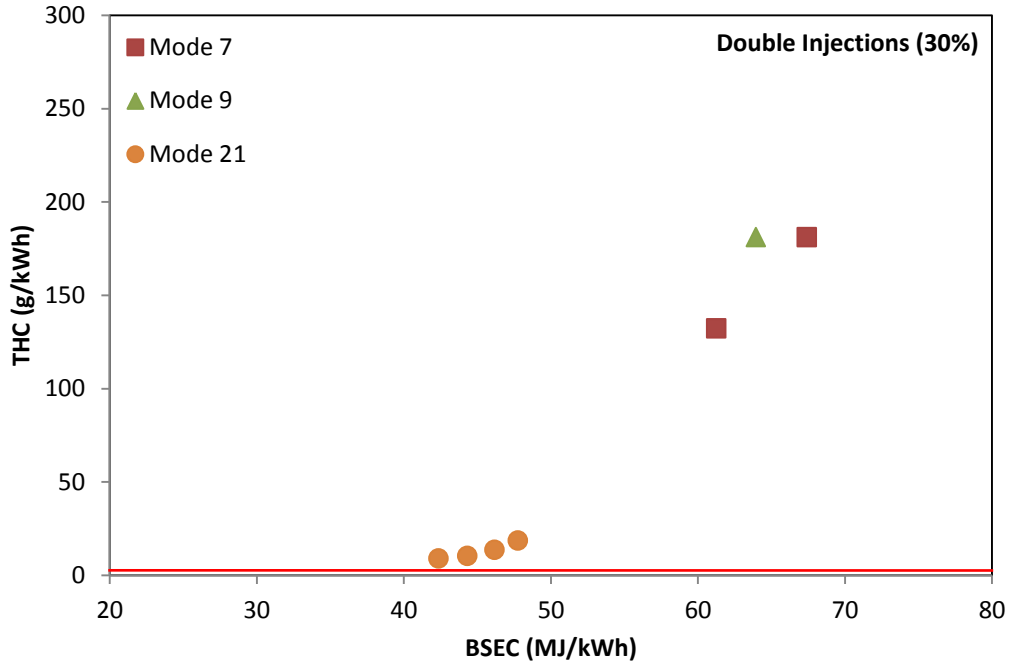

Figure 4.37 – HC emissions vs. BSEC using double injections

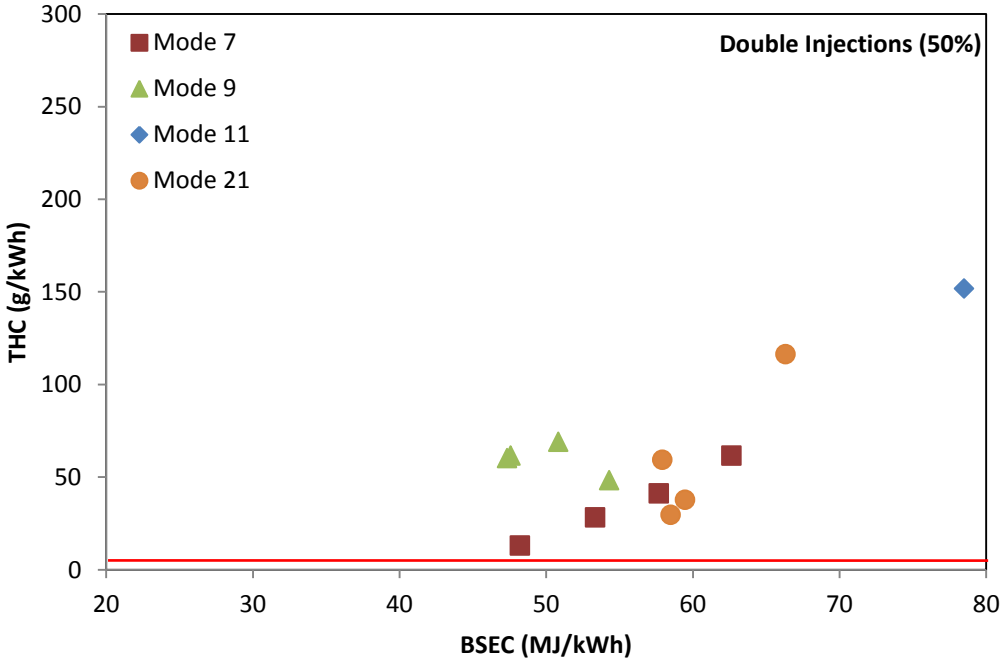

Figure 4.38 – HC emissions vs. BSEC using double injections

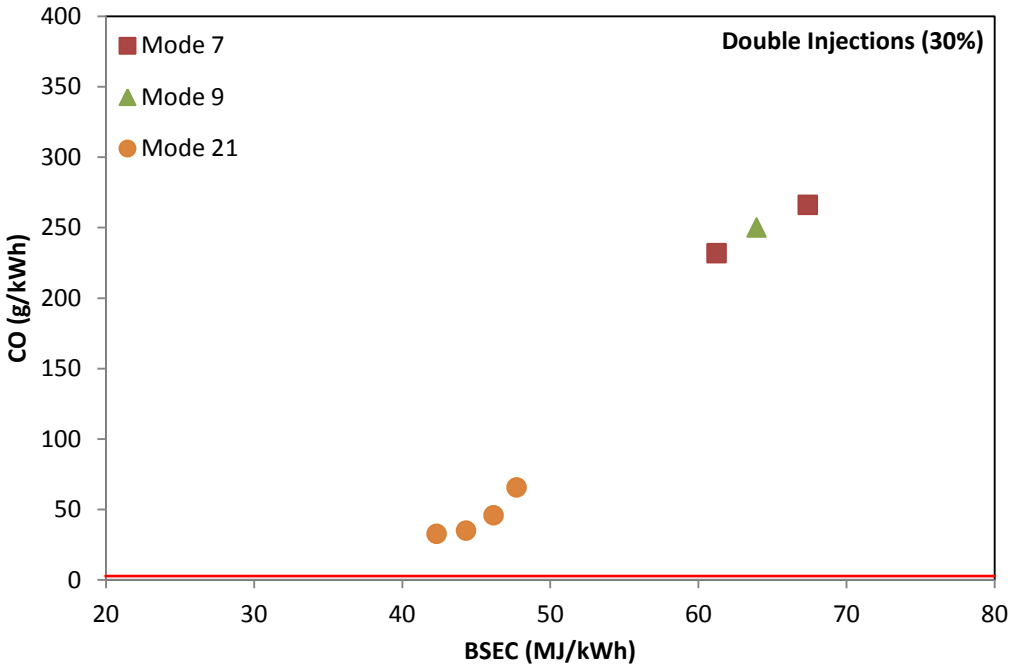

Figure 4.39 – CO emissions vs. BSEC using double injections

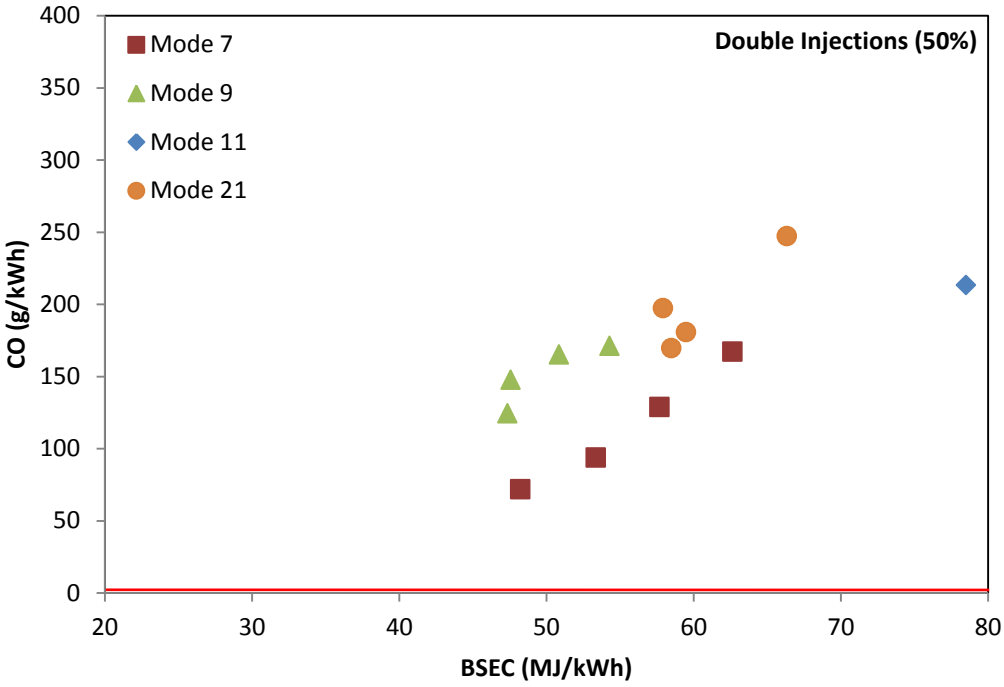

Figure 4.40 – CO emissions vs. BSEC using double injections

During this study, it is found that the double injection strategy is not able to extend the operating range of the present engine. The reason may be due to the significant incomplete combustion that inhibits the complete release of fuel energy to achieve stable engine operations. As a result the approach of generating two injection events has only been tested for 20%NH_3–80%DME mixtures.

Chapter 5 Summary and Recommendations

Combustion of ammonia/DME mixture in a compression-ignition engine is investigated. The engine uses a modified injection system that does not allow fuel return. Results using 20 wt.% ammonia – 80 wt.% DME and 40 wt.% ammonia – 60 wt.% DME show that ammonia causes longer ignition delays and limits the engine load conditions due to its high autoignition temperature and low flame speed. The inclusion of ammonia in the fuel mixture also decreases combustion temperature, resulting in higher CO and HC emissions; however, soot emissions remain extremely low. NOx emissions increase due to the formation of fuel NOx when ammonia is used. Exhaust ammonia emissions are on the order of a few hundred ppm under the conditions tested. However, it is shown that an increase of injection pressure by 30 bar can allow using mixtures with a higher ammonia content and lead to improved combustion and emissions. It is also found that double injection schemes do not extend the engine operating range and its effects on the exhaust emissions vary with operating conditions. It should be noted that the peak injection pressure in the current setup is 20 MPa. It is thought that using a higher injection pressure can further enhance fuel-air mixing to achieve better combustion and attain higher engine loads when even higher ammonia quantities are used.

It is important to discuss the present results in perspective in terms of the feasibility of using ammonia as a compression-ignition engine fuel. Note that the present test engine is a small utility engine that is rated at high speed (e.g., 3,480 rpm). Small engines also possess the disadvantage of high surface-to-volume ratio, causing more heat loss that deteriorates ammonia vaporization and combustion.

Consider the application of ammonia in a large diesel generator that has a high injection pressure and is rated at a moderate speed (e.g., 1,700 rpm). Under such operating conditions, combustion of ammonia is more feasible with the assistance in ignition from a secondary fuel such as DME or regular diesel fuel.

Modern compression-ignition engines typically have high injection pressures that can allow the use of higher ammonia concentrations in the fuel mixture. The fuel injection system can be modified to handle the issue with fuel return by eliminating the fuel return line or pressurizing and re-injecting ammonia into the fuel tank. It is noted that DME has been used in commercial diesel engines, which can serve as a good platform for future ammonia engine study. It is also of interest to note that mixture of 60%NH_3–40%DME is commercially available as a refrigerant. In the meantime, modern SCR technologies can also be employed to reduce exhaust ammonia and NOx emissions simultaneously. With the technological advancement in ammonia production from renewable resources, strategies in ammonia engine combustion, such as the one implemented in the present study, can help explore the potential use of ammonia as a carbon-free fuel. Nonetheless, technoeconomic study is also needed to help identify the feasibility of using ammonia as a fuel.

References

1. W.H. Avery, A role for ammonia in the hydrogen economy. Int. J. Hydrogen Energy 13 (12) (1988) 761–773.
2. T. Hejze, J.O. Besenhard, K. Kordesch, M. Cifrain, R.R. Aronsson, Current status of combined systems using alkaline fuel cells and ammonia as a hydrogen carrier. J. Power Sources 176 (2008) 490–493.
3. R. Michalsky, P.H. Pfromm, Chromium as reactant for solar thermochemical synthesis of ammonia from steam, nitrogen, and biomass at atmospheric pressure. Solar Energy 85 (2011) 2642–2654.
4. E. Koch, Ammonia – A Fuel for Motor Buses. J. Inst. Petroleum 31 (1945) 213–223.
5. E. S. Starkman, H.K. Newhall, R. Sutton, T. Maguire, L. Farbar, Ammonia as a Spark Ignition Engine Fuel: Theory and Application. SAE Technical Paper 660155, 1966.
6. T.J. Pearsall, C.G. Garabedian, Combustion of Anhydrous Ammonia in Diesel Engines. SAE Technical Paper 670947, 1967.
7. E. S. Starkman, G.E. James, H. K. Newhall, Ammonia as a Diesel Engine Fuel: Theory and Application. SAE Technical Paper 670946, 1967.
8. K. Bro, P. S. Pedersen, Alternative Diesel Engine Fuels: An Experimental Investigation of Methanol, Ehtanol, Methane and Ammonia in a D.I. Diesel Engine with Pilot Injection. SAE Technical Paper 770794, 1977.
9. R. Liu,, D. S.-K Ting, M. D. Checkel, Ammonia as a Fuel for SI Engine. SAE Technical Paper 2003-01-0395, 2003.

10. S. M. Grannell,, D.N. Assanis, S.V. Bohac, D.E. Gillespie, J Engng Gas Turbines Power 130 (2008).
11. J. J. MacKenzie, W. H. Avery, Ammonia Fuel: The Key to Hydrogen-Based Transportation. Proceedings of the Intersociety Energy Conversion Engineering Conference, Washington DC, USA. 3 (1996) 1761–1766.
12. M. Appl. Ammonia – Principles and Industrial Practice. Weinheim, New York, Chichester, Brisbane, Singapore, Toronto : WILEY-VCH, 1999.
13. W. A. Majewski and M. Khair**.** Diesel Emissions and Their control*.* Warrendale : SAE International, 2006.
14. G. L. Borman and W. K. Ragland. Combustion engineering. Boston : WCB/McGraw-Hill, 1998.
15. G. Billaud, A. Demortier, Dieelectric Constant of liquid Ammonia. The Journal of Physical Chemistry, Vol. 79, No. 26, 1975.
16. M. K. Veltman, S.-C. Kong, Well-to-Wheel Analysis of Ammonia and its Performance in Compression-Ignition Engines, Ames, IA (2011)
17. A. J. Reiter, S.-C. Kong. Demonstration of Compression-Ignition Engine Combustion Using Ammonia in Reducing Greenhouse Gas Emissions. Energy & Fuels 22 (2008) 2963–2971.
18. J.M. Modak (2002). Haber Process for Ammonia Synthesis. *Resonance*, *69-77*.
19. J.T. Gray, E. Dimitroff, N.T. Meckel, and R. D. J. Quillian (1966). Ammonia Fuel -- Engine Compatibility and Combustion. *SAE Technical Papers 660156*.
20. NIST WebBook. *National Institute of Standards and Technology Chemistry WebBook.* [Online] [Cited: August 10, 2010.] http://webbook.nist.gov/.

Table A-1 – Raw Data 100%DME

Mode	Main	Pilot	Pilot quantity	Engine Power	Engine Speed	Inlet Air Temperature	Exhaust Temperature	Oil Temperature	Cylinder Head Temp	Engine Power
	CAD BTDC	CAD BTDC	%	HP	rpm	deg C	deg C	deg C	deg C	kW
5	30	-	-	1.96	2554	30.0	563.0	72.0	50.3	1.44
	25	-	-	1.97	2560	30.0	561.0	64.0	48.8	1.45
	20	-	-	2	2553	30.0	608.0	75.0	46.6	1.47
7	25	-	-	1.14	2527	33.0	292.0	73.0	52.4	0.84
	20	-	-	1.17	2545	32.0	319.0	76.0	49.1	0.86
	15	-	-	1.13	2548	32.0	351.0	75.0	46.7	0.83
	10	-	-	1.18	2551	32.0	386.0	74.0	46.8	0.87
	5	-	-	1.15	2550	32.0	420.0	73.0	46.4	0.85
9	30	-	-	1.41	2899	30.0	378.0	77.0	46.0	1.04
	25	-	-	1.45	2902	30.0	416.0	77.0	46.7	1.07
	20	-	-	1.41	2899	30.0	492.0	77.0	48.2	1.04
	15	-	-	1.41	2901	30.0	538.0	77.0	48.3	1.04
11	30	-	-	1.56	3256	33.0	467.0	77.0	48.6	1.15
	25	-	-	1.46	3257	33.0	550.0	70.0	53.1	1.07
	20	-	-	1.31	3131	32.0	548.0	80.0	49.5	0.96
20	35	-	-	1.87	2197	34.0	493.0	71.0	50.9	1.38
	30	-	-	2.02	2203	35.0	485.0	71.0	46.0	1.49
	25	-	-	1.97	2206	35.0	484.0	64.0	45.6	1.45
	20	-	-	1.9	2209	33.0	517.0	64.0	45.0	1.40
21	30	-	-	1.04	2202	34.0	282.0	74.0	42.8	0.76
	25	-	-	1.04	2201	34.0	286.0	73.0	44.6	0.76
	20	-	-	1.02	2203	34.0	296.0	71.0	52.2	0.75
	15	-	-	0.96	2211	33.0	358.0	53.0	51.3	0.71
	10	-	-	1.05	2207	33.0	376.0	61.0	50.6	0.77
	5	-	-	1	2202	34.0	398.0	65.0	48.7	0.74
	0	-	-	0.98	2205	34.0	440.0	69.0	47.1	0.72

Table A-2 – Raw Data 100%DME

Mode	Main	Pilot	Pilot quantity	Air Consumption	Vol. Efficiency	Fuel Consumption Mix	Total Fuel Energy	Thermal Efficiency	BMEP
	CAD BTDC	CAD BTDC	%	kg/h	-	kg/h	MJ/h	-	bar
5	30	-	-	23.3	1.0	2.5	71.7	7.2	2.1161
	25	-	-	23.7	1.0	2.5	72.2	7.2	2.1219
7	20	-	-	23.6	1.0	2.6	74.5	7.1	2.1601
	25	-	-	25.0	0.8	1.3	38.1	7.9	1.2439
	20	-	-	24.9	0.8	1.4	39.8	7.8	1.2676
	15	-	-	25.1	0.8	1.5	42.4	7.1	1.2228
9	10	-	-	25.2	0.8	1.6	45.3	6.9	1.2755
	5	-	-	25.2	0.8	1.7	47.4	6.4	1.2435
	30	-	-	27.6	0.7	1.8	52.3	7.1	1.3411
	25	-	-	27.7	0.7	2.0	56.6	6.8	1.3777
11	20	-	-	27.6	0.8	2.3	65.6	5.7	1.3411
	15	-	-	27.6	0.8	2.4	69.5	5.4	1.3402
	30	-	-	29.6	0.7	2.4	67.6	6.1	1.3211
20	25	-	-	29.7	0.6	2.9	82.4	4.7	1.236
	20	-	-	29.0	0.6	2.8	79.0	4.4	1.1537
21	35	-	-	21.3	0.9	2.1	58.4	8.5	2.347
	30	-	-	21.6	0.9	2.0	55.5	9.6	2.5283
	25	-	-	22.0	0.9	2.0	56.4	9.3	2.4624
	20	-	-	22.1	0.9	2.1	59.6	8.4	2.3716
	30	-	-	22.4	0.9	1.2	34.9	7.9	1.3023
7	25	-	-	22.6	0.9	1.2	34.5	8.0	1.3029
	20	-	-	22.6	1.0	1.2	35.0	7.7	1.2767
9	15	-	-	22.8	0.9	1.5	41.5	6.1	1.1972
21	10	-	-	22.7	0.9	1.5	41.6	6.7	1.3118
	5	-	-	22.6	1.0	1.5	42.0	6.3	1.2522
	0	-	-	22.7	0.8	1.6	45.0	5.8	1.2255

Table A-3 – Raw Date 100%DME

Mode	Main	Pilot	Pilot quantity	FSN (ave)	Soot (ave)	Soot (ave)	NOx	NH3	Sum	CO
	CAD BTDC	CAD BTDC	%	-	mg/m³	g/kWh	ppm	ppm	ppm	ppm
5	30	-	-	0.084	1.125	0.048	261	NA	278	9720
	25	-	-	0.078	1.040	0.044	183	NA	199	9720
7	20	-	-	0.165	2.275	0.101	142	NA	155	9719
	25	-	-	0.006	0.075	0.004	231	NA	228	717
	20	-	-	0.009	0.115	0.006	138	NA	135	783
	15	-	-	0.004	0.045	0.003	84	NA	82	1311
9	10	-	-	0.004	0.055	0.003	62	NA	60	1741
	5	-	-	0.005	0.065	0.004	50	NA	48	1967
	30	-	-	0.007	0.095	0.005	283	NA	275	1357
	25	-	-	0.012	0.155	0.008	175	NA	175	2695
11	20	-	-	0.033	0.430	0.027	115	NA	119	6044
	15	-	-	0.073	0.970	0.064	71	NA	77	6058
	30	-	-	0.015	0.200	0.012	228	NA	229	4067
20	25	-	-	0.407	0.805	0.057	138	NA	148	9716
	20	-	-	0.113	1.540	0.118	108	NA	100	9718
21	35	-	-	0.018	0.240	0.009	528	NA	527	7094
	30	-	-	0.008	0.105	0.004	374	NA	371	4944
	25	-	-	0.007	0.095	0.003	255	NA	254	5308
	20	-	-	0.024	0.320	0.012	164	NA	174	6708
	30	-	-	0.002	0.025	0.001	457	NA	447	661
7	25	-	-	0.000	0.005	0.000	315	NA	306	663
	20	-	-	0.003	0.030	0.002	181	NA	176	729
9	15	-	-	0.003	0.035	0.002	100	NA	105	1451
21	10	-	-	0.004	0.045	0.003	72	NA	73	1493
	5	-	-	0.002	0.025	0.002	55	NA	55	1628
	0	-	-	0.004	0.055	0.004	44	NA	44	2287

Table A-4 – Raw Data 100%DME

Mode	Main	Pilot	Pilot quantity	CO2	THC (C3H8)	O2	Equivalence Ratio	Total PM	Total PM	BSPM
	CAD BTDC	CAD BTDC	%	%-v	ppm	%-v	-	g/h	g/kg-fuel	g/kWh
5	30	-	-	6.52	1772	10.76	0.972	0.069	0.027	0.048
	25	-	-	6.42	2028	11.02	0.961	0.064	0.025	0.044
7	20	-	-	6.85	1544	10.39	0.999	0.148	0.056	0.101
	25	-	-	3.6	151	16.12	0.482	0.003	0.002	0.004
	20	-	-	3.78	127	15.77	0.506	0.005	0.004	0.006
	15	-	-	3.94	190	15.52	0.533	0.002	0.001	0.003
9	10	-	-	4.18	227	15.17	0.567	0.003	0.002	0.003
	5	-	-	4.39	218	14.88	0.594	0.003	0.002	0.004
	30	-	-	4.5	197	14.72	0.599	0.005	0.003	0.005
	25	-	-	4.74	359	14.29	0.646	0.009	0.004	0.008
11	20	-	-	5.18	1062	13.33	0.753	0.028	0.012	0.027
	15	-	-	5.59	828	12.73	0.795	0.067	0.027	0.064
	30	-	-	5.21	640	13.52	0.722	0.013	0.006	0.012
20	25	-	-	5.64	2549	12.34	0.878	0.061	0.021	0.057
	20	-	-	5.65	1861	12.49	0.861	0.113	0.041	0.118
21	35	-	-	6.21	397	11.75	0.867	0.012	0.006	0.009
	30	-	-	5.96	409	12.37	0.811	0.005	0.003	0.004
	25	-	-	5.89	613	12.53	0.809	0.005	0.002	0.003
	20	-	-	6	991	12.04	0.853	0.017	0.008	0.012
	30	-	-	3.68	133	15.92	0.492	0.001	0.001	0.001
7	25	-	-	3.61	135	16.02	0.484	0.000	0.000	0.000
	20	-	-	3.65	135	15.98	0.489	0.001	0.001	0.002
9	15	-	-	4.27	213	14.96	0.576	0.002	0.001	0.002
21	10	-	-	4.27	195	14.86	0.579	0.002	0.001	0.003
	5	-	-	4.32	210	14.78	0.587	0.001	0.001	0.002
	0	-	-	4.6	256	14.41	0.627	0.003	0.002	0.004

Table A-5 – Raw Data 100%DME

Mode	Main	Pilot	Pilot quantity	NOx	NH3	THC (C3H8)	H2O	N2	CO	CO2	O2
	CAD BTDC	CAD BTDC	%	g/kg-fuel	g/kg-fuel	g/kg-fuel	g/kg-fuel	g/kg-fuel	g/kg-fuel	g/kg-fuel	g/kg-fuel
5	30	-	-	2.8	NA	27.5	168.4	7782.2	93.4	984.2	1181.3
	25	-	-	2.0	NA	31.7	166.1	7844.7	94.3	978.9	1222.0
7	20	-	-	1.5	NA	23.3	173.1	7582.3	90.9	1006.7	1110.5
	25	-	-	4.7	NA	4.5	166.3	14941.9	13.4	1058.3	3446.4
	20	-	-	2.7	NA	3.6	167.0	14278.7	14.0	1059.6	3215.0
	15	-	-	1.6	NA	5.1	167.3	13593.1	22.3	1051.1	3011.0
9	10	-	-	1.1	NA	5.8	168.5	12812.5	27.8	1050.4	2772.5
	5	-	-	0.8	NA	5.3	170.1	12261.8	30.1	1055.2	2601.2
	30	-	-	4.7	NA	4.8	170.7	12162.4	20.6	1072.0	2550.3
	25	-	-	2.7	NA	8.1	170.6	11317.9	38.0	1050.3	2302.8
11	20	-	-	1.5	NA	20.8	166.4	9810.3	73.8	993.9	1860.1
	15	-	-	0.9	NA	15.4	171.5	9328.2	70.2	1017.4	1685.1
	30	-	-	3.2	NA	13.0	170.9	10203.6	51.6	1039.7	1962.2
20	25	-	-	1.6	NA	43.3	156.9	8492.9	102.7	937.1	1491.2
	20	-	-	1.3	NA	32.2	164.4	8637.0	104.6	955.9	1536.8
21	35	-	-	6.2	NA	6.8	180.3	8612.5	75.7	1041.6	1433.3
	30	-	-	4.7	NA	7.5	178.3	9151.4	56.1	1063.4	1605.2
	25	-	-	3.2	NA	11.2	176.4	9161.7	60.4	1053.7	1630.2
	20	-	-	2.0	NA	17.3	172.5	8747.9	72.7	1022.2	1491.8
	30	-	-	9.1	NA	3.9	166.6	14663.7	12.1	1060.6	3336.9
7	25	-	-	6.4	NA	4.0	166.0	14901.3	12.4	1057.3	3412.2
	20	-	-	3.6	NA	4.0	166.3	14739.6	13.4	1057.2	3366.1
9	15	-	-	1.7	NA	5.4	168.5	12638.2	22.8	1056.6	2692.2
21	10	-	-	1.2	NA	4.9	168.1	12599.8	23.4	1052.0	2662.6
	5	-	-	0.9	NA	5.2	168.2	12439.0	25.2	1050.6	2614.0
	0	-	-	0.7	NA	5.9	170.0	11675.1	33.2	1050.0	2392.2

Table A-6 – Raw Data 100%DME

Mode	Main	Pilot	Pilot quantity	BSNOx	BSNH3	BSHC (C3H8)	BSH2O	BSN2	BSCO	BSCO2	BSO2
	CAD BTDC	CAD BTDC	%	g/kWh	g/kWh	g/kWh	g/kWh	g/kWh	g/kWh	g/kWh	g/kWh
5	30	-	-	4.83	NA	48.14	295.03	13634.35	163.59	1724.38	2069.64
	25	-	-	3.43	NA	55.68	291.41	13759.03	165.42	1716.90	2143.33
7	20	-	-	2.61	NA	41.64	308.68	13523.17	162.12	1795.51	1980.66
	25	-	-	7.51	NA	7.20	266.13	23917.23	21.47	1693.98	5516.54
	20	-	-	4.36	NA	5.89	272.25	23272.27	22.76	1726.98	5239.93
	15	-	-	2.79	NA	9.24	300.47	24410.46	39.97	1887.48	5407.24
9	10	-	-	1.98	NA	10.65	309.60	23536.87	51.15	1929.64	5093.10
	5	-	-	1.64	NA	10.51	335.53	24180.12	59.33	2080.82	5129.45
	30	-	-	8.30	NA	8.48	303.00	21592.35	36.52	1903.15	4527.58
	25	-	-	5.03	NA	15.14	318.77	21149.16	71.01	1962.64	4303.19
11	20	-	-	3.42	NA	46.37	370.84	21860.54	164.44	2214.69	4144.86
	15	-	-	2.13	NA	36.37	404.48	22005.18	165.52	2400.11	3975.07
	30	-	-	6.58	NA	27.07	354.80	21186.09	107.23	2158.71	4074.09
20	25	-	-	4.32	NA	117.06	423.91	22943.89	277.54	2531.73	4028.57
	20	-	-	3.68	NA	93.12	474.98	24952.70	302.27	2761.60	4439.89
21	35	-	-	9.26	NA	10.21	269.43	12872.18	113.17	1556.73	2142.18
	30	-	-	6.14	NA	9.84	234.77	12049.24	73.91	1400.16	2113.48
	25	-	-	4.36	NA	15.38	241.70	12550.05	82.78	1443.38	2233.13
	20	-	-	2.93	NA	25.99	259.07	13140.28	109.24	1535.45	2240.83
	30	-	-	14.64	NA	6.25	267.74	23569.19	19.49	1704.74	5363.53
7	25	-	-	10.14	NA	6.37	263.91	23686.72	19.64	1680.59	5423.92
	20	-	-	5.96	NA	6.51	273.26	24217.26	22.08	1736.92	5530.45
9	15	-	-	3.55	NA	11.09	348.60	26150.58	47.28	2186.29	5570.69
21	10	-	-	2.33	NA	9.26	318.50	23877.77	44.36	1993.66	5045.92
	5	-	-	1.87	NA	10.45	338.38	25023.30	50.68	2113.39	5258.58
	0	-	-	1.53	NA	13.08	373.92	25674.19	73.05	2309.00	5260.49

Table A-7 – Raw Data 20%NH3-80%DME

Mode	Main	Pilot	Pilot quantity	Engine Power	Engine Speed	Inlet Air Temperature	Exhaust Temperature	Oil Temperature	Cylinder Head Temp	Engine Power
	CAD BTDC	CAD BTDC	%	HP	rpm	deg C	deg C	deg C	deg C	kW
5	15	-	-	1.92	2558	33.5	592.2	73.4	59.1	1.4
	20	-	-	1.95	2543	34.1	553.8	78.0	61.4	1.4
7	10	-	-	1.15	2558	26.0	479.2	72.1	48.2	0.8
	15	-	-	1.06	2551	26.2	389.6	73.1	47.2	0.8
	20	-	-	1.12	2542	26.5	364.5	74.6	47.6	0.8
	25	-	-	1.15	2545	26.9	339.4	76.1	48.7	0.8
9	15	-	-	1.34	2896	34.5	534.2	79.2	58.2	1.0
	20	-	-	1.34	2896	34.5	513.2	80.3	59.1	1.0
	25	-	-	1.34	2892	34.7	444.0	83.0	60.0	1.0
	30	-	-	1.43	2894	34.9	430.3	84.9	60.6	1.1
11	25	-	-	1.57	3250	37.4	612.2	77.6	57.4	1.2
	30	-	-	1.52	3251	37.6	515.8	83.9	57.7	1.1
	35	-	-	1.52	3250	37.5	476.4	88.1	57.7	1.1
20	30	-	-	1.63	2203	29.1	488.9	71.6	54.3	1.2
	35	-	-	1.62	2201	29.2	491.1	74.7	57.4	1.2
21	5	-	-	0.93	2208	31.6	435.0	67.7	48.7	0.7
	10	-	-	0.99	2205	30.4	364.4	65.0	47.7	0.7
	15	-	-	1.03	2213	30.4	339.5	61.5	47.2	0.8
	20	-	-	1.01	2217	30.4	310.9	55.1	47.1	0.7
	25	-	-	0.97	2203	31.4	306.0	69.3	48.9	0.7
7	10	25	30	1.11	2552	47.9	607.8	632.3	55.1	0.8
	10	30	30	0.96	2552	47.4	585.1	78.8	55.6	0.7
9	10	28	30	1.17	2896	46.4	620.2	81.4	54.4	0.9
21	10	30	30	1.05	2203	55.8	361.0	80.1	58.9	0.8
	10	35	30	1.01	2210	54.5	364.2	77.9	58.8	0.7
	10	40	30	1.02	2201	55.4	387.9	72.6	58.1	0.8
	10	45	30	0.99	2200	55.2	368.2	80.9	59.8	0.7
7	10	30	50	1.17	2551	53.2	414.9	74.2	57.8	0.9
	10	35	50	1.13	2602	53.6	428.5	77.1	58.6	0.8
	10	40	50	1.05	2566	52.4	418.3	79.5	60.3	0.8
	10	45	50	1.06	2641	50.7	445.9	75.0	60.7	0.8
9	10	30	50	1.33	2928	51.0	575.7	70.3	59.1	1.0
	10	35	50	1.34	2931	52.3	575.6	76.2	62.2	1.0
	10	40	50	1.44	2976	53.0	557.1	81.3	64.3	1.1
	10	45	50	1.43	2969	53.0	559.5	80.5	64.0	1.1
11	10	40	50	1.36	3182	52.4	566.8	70.8	56.6	1.0
21	10	30	50	0.98	2203	56.1	491.9	78.7	68.0	0.7
	10	35	50	0.98	2221	55.9	488.7	86.8	72.1	0.7
	10	40	50	0.98	2200	57.7	492.6	92.9	76.1	0.7
	10	45	50	0.86	2163	58.4	496.7	99.1	80.4	0.6

Table A-8 – Raw Data 20%NH3-80%DME

Mode	Main	Pilot	Pilot quantity	Air Consumption	Vol. Efficiency	Fuel Consumption Mix	Total Fuel Energy	Thermal Efficiency	BMEP
	CAD BTDC	CAD BTDC	%	kg/h	-	kg/h	MJ/h	-	bar
5	15	-	-	23.3	0.8	2.5	65.5	7.8	2.1
	20	-	-	22.9	0.8	2.4	62.6	8.2	2.1
7	10	-	-	24.1	0.8	1.8	48.9	6.2	1.2
	15	-	-	24.0	0.8	1.5	39.9	7.0	1.1
	20	-	-	23.9	0.8	1.4	37.2	7.9	1.2
	25	-	-	23.7	0.8	1.3	34.6	8.8	1.2
9	15	-	-	26.8	0.8	2.3	62.2	5.7	1.3
	20	-	-	26.8	0.8	2.2	58.9	6.0	1.3
	25	-	-	26.8	0.8	2.0	54.3	6.5	1.3
	30	-	-	26.7	0.8	2.0	53.6	7.1	1.4
11	25	-	-	28.3	0.8	3.1	82.6	5.0	1.3
	30	-	-	28.4	0.8	2.6	68.4	5.9	1.3
	35	-	-	28.3	0.8	2.3	60.5	6.6	1.3
20	30	-	-	20.6	0.8	2.1	54.7	7.9	2.0
	35	-	-	20.3	0.8	2.0	52.3	8.2	2.0
21	5	-	-	21.7	0.9	1.4	37.8	6.5	1.2
	10	-	-	21.9	0.9	1.2	32.9	8.0	1.2
	15	-	-	22.1	0.9	1.2	31.3	8.7	1.3
	20	-	-	22.7	0.9	1.1	29.7	9.0	1.3
	25	-	-	21.5	0.8	1.0	27.4	9.4	1.2
7	10	25	30	19.0	0.7	1.9	51.2	5.7	1.2
	10	30	30	19.0	0.7	1.8	48.9	5.2	1.0
9	10	28	30	21.7	0.7	2.1	56.2	5.5	1.1
21	10	30	30	19.0	0.8	1.3	33.4	8.3	1.3
	10	35	30	19.0	8.1	1.3	33.7	7.9	1.3
	10	40	30	18.9	0.8	1.4	36.7	7.4	1.3
	10	45	30	19.1	0.8	1.3	34.5	7.6	1.2
7	10	30	50	20.5	0.7	1.6	42.5	7.3	1.3
	10	35	50	20.8	0.7	1.7	45.5	6.6	1.2
	10	40	50	20.1	0.7	1.7	45.8	6.1	1.1
	10	45	50	20.4	0.7	1.9	49.8	5.6	1.1
9	10	30	50	19.9	0.6	2.0	54.2	6.5	1.2
	10	35	50	19.2	0.6	1.9	51.3	6.9	1.3
	10	40	50	19.6	0.6	1.9	51.6	7.4	1.3
	10	45	50	19.8	0.6	1.9	51.0	7.4	1.3
11	10	40	50	21.0	0.6	2.4	64.2	5.6	1.2
21	10	30	50	17.2	0.7	1.6	43.3	6.0	1.2
	10	35	50	17.2	0.7	1.7	43.7	5.9	1.2
	10	40	50	16.6	0.7	1.6	42.8	6.1	1.2
	10	45	50	15.8	0.7	1.6	43.1	5.3	1.1

Table A-9 – Raw Data 20%NH3-80%DME

Mode	Main	Pilot	Pilot quantity	FSN (ave)	Soot (ave)	Soot (ave)	NOx	NH3	Sum	CO
	CAD BTDC	CAD BTDC	%	-	mg/m³	g/kWh	ppm	ppm	ppm	ppm
5	15	-	-	0.014	0.187	0.008	373	510	883	7749
	20	-	-	0.010	0.130	0.005	352	404	756	6627
7	10	-	-	0.008	0.105	0.007	615	135	750	3448
	15	-	-	0.002	0.020	0.001	531	169	700	1931
	20	-	-	0.003	0.040	0.002	513	118	631	1408
	25	-	-	0.003	0.035	0.002	484	99	583	1331
9	15	-	-	0.003	0.045	0.003	395	381	776	4335
	20	-	-	0.005	0.075	0.005	350	419	769	3977
	25	-	-	0.003	0.035	0.002	320	397	717	2905
	30	-	-	0.003	0.035	0.002	326	370	696	2515
11	25	-	-	0.025	0.325	0.022	400	770	1170	9624
	30	-	-	0.012	0.155	0.010	382	733	1115	6090
	35	-	-	0.007	0.090	0.005	380	666	1046	3639
20	30	-	-	0.012	0.160	0.007	464	366	830	9213
	35	-	-	0.013	0.175	0.007	562	253	815	7886
21	5	-	-	0.004	0.040	0.003	533	71	604	2344
	10	-	-	0.003	0.030	0.002	458	53	511	1231
	15	-	-	0.007	0.090	0.005	419	62	481	1265
	20	-	-	0.013	0.170	0.009	427	63	490	1138
	25	-	-	0.002	0.035	0.002	463	77	540	1078
7	10	25	30	0.009	0.110	0.007	301	644	945	9587
	10	30	30	0.007	0.095	0.007	435	721	1156	9586
9	10	28	30	0.010	0.130	0.009	311	750	1061	9585
21	10	30	30	0.004	0.045	0.002	437	317	754	1300
	10	35	30	0.002	0.015	0.001	536	431	967	1332
	10	40	30	0.006	0.065	0.003	623	481	1104	2552
	10	45	30	0.002	0.025	0.001	597	423	1020	1722
7	10	30	50	0.007	0.090	0.005	355	205	560	2940
	10	35	50	0.005	0.065	0.003	470	275	745	3670
	10	40	50	0.007	0.090	0.005	580	361	941	4816
	10	45	50	0.008	0.105	0.006	606	318	924	6138
9	10	30	50	0.007	0.090	0.005	365	338	703	8060
	10	35	50	0.006	0.080	0.004	398	379	777	8135
	10	40	50	0.006	0.085	0.004	467	342	809	7655
	10	45	50	0.007	0.080	0.004	625	299	924	6363
11	10	40	50	0.009	0.110	0.006	348	553	901	9627
21	10	30	50	0.008	0.100	0.006	348	338	686	6864
	10	35	50	0.008	0.105	0.006	450	366	816	7275
	10	40	50	0.004	0.055	0.003	500	378	878	8299
	10	45	50	0.006	0.080	0.005	501	431	932	9531

Table A-10 – Raw Data 20%NH3-80%DME

Mode	Main	Pilot	Pilot quantity	CO2	THC (C3H8)	O2	Equivalence Ratio	Total PM	Total PM	BSPM
	CAD BTDC	CAD BTDC	%	%-v	ppm	%-v	-	g/h	g/kg-fuel	g/kWh
5	15	-	-	6.15	851	10.620	0.943	0.012	0.005	0.008
	20	-	-	5.96	1071	10.870	0.915	0.008	0.003	0.005
7	10	-	-	4.71	499	13.080	0.705	0.006	0.003	0.007
	15	-	-	4.07	287	14.280	0.596	0.001	0.001	0.001
	20	-	-	3.99	224	14.520	0.575	0.002	0.001	0.002
	25	-	-	3.86	202	14.740	0.557	0.002	0.001	0.002
9	15	-	-	5.24	642	12.470	0.777	0.003	0.001	0.003
	20	-	-	4.94	713	12.980	0.736	0.005	0.002	0.005
	25	-	-	4.67	480	13.600	0.680	0.002	0.001	0.002
	30	-	-	4.68	407	13.620	0.675	0.002	0.001	0.002
11	25	-	-	6.05	2080	10.670	0.978	0.026	0.008	0.022
	30	-	-	5.12	1355	12.260	0.808	0.011	0.004	0.010
	35	-	-	4.99	673	12.830	0.740	0.006	0.003	0.005
20	30	-	-	5.39	1308	11.400	0.890	0.008	0.004	0.007
	35	-	-	5.58	856	11.030	0.894	0.008	0.004	0.007
21	5	-	-	4.28	329	14.100	0.624	0.002	0.001	0.003
	10	-	-	3.88	188	14.800	0.556	0.001	0.001	0.002
	15	-	-	3.76	194	15.040	0.539	0.004	0.003	0.005
	20	-	-	3.57	169	15.270	0.514	0.007	0.006	0.009
	25	-	-	3.59	163	15.260	0.516	0.001	0.001	0.002
7	10	25	30	6.45	3393	8.690	1.120	0.006	0.003	0.007
	10	30	30	6.11	4056	9.010	1.101	0.005	0.003	0.007
9	10	28	30	6.31	4312	8.560	1.141	0.008	0.004	0.009
21	10	30	30	4.12	227	14.400	0.589	0.002	0.001	0.002
	10	35	30	4.16	250	14.400	0.593	0.001	0.000	0.001
	10	40	30	4.46	456	13.780	0.653	0.002	0.002	0.003
	10	45	30	4.25	323	14.400	0.606	0.001	0.001	0.001
7	10	30	50	4.71	334	13.150	0.695	0.004	0.002	0.005
	10	35	50	5.03	689	13.060	0.736	0.003	0.002	0.003
	10	40	50	5.03	962	12.740	0.763	0.004	0.002	0.005
	10	45	50	5.19	1408	12.180	0.816	0.005	0.003	0.006
9	10	30	50	5.77	1414	11.140	0.914	0.005	0.002	0.005
	10	35	50	5.40	2117	11.410	0.895	0.004	0.002	0.004
	10	40	50	5.38	1987	11.520	0.882	0.004	0.002	0.004
	10	45	50	5.37	1921	11.550	0.865	0.004	0.002	0.004
11	10	40	50	5.65	4264	10.210	1.023	0.006	0.003	0.006
21	10	30	50	5.61	747	11.360	0.871	0.004	0.002	0.006
	10	35	50	5.83	942	10.920	0.909	0.004	0.003	0.006
	10	40	50	6.02	1549	10.590	0.956	0.002	0.001	0.003
	10	45	50	6.13	2782	9.710	1.039	0.003	0.002	0.005

Table A-11 – Raw Data 20%NH3-80%DME

Mode	Main	Pilot	Pilot quantity	NOx	NH3	THC (C3H8)	H2O	N2	CO	CO2	O2
	CAD BTDC	CAD BTDC	%	g/kg-fuel	g/kg-fuel	g/kg-fuel	g/kg-fuel	g/kg-fuel	g/kg-fuel	g/kg-fuel	g/kg-fuel
5	15	-	-	4.0	3.3	13.5	163.4	8019.0	76.0	948.2	1190.8
	20	-	-	3.9	2.7	17.4	159.0	8256.1	66.9	945.1	1253.6
7	10	-	-	8.9	1.2	10.6	161.0	10834.3	45.9	986.1	1991.6
	15	-	-	9.3	1.8	7.4	164.5	13060.1	31.1	1031.3	2631.7
	20	-	-	9.6	1.3	6.1	170.1	13899.6	24.2	1077.1	2850.7
	25	-	-	9.6	1.2	5.9	174.7	14759.5	24.3	1107.3	3075.3
9	15	-	-	5.1	2.9	12.1	159.6	9555.7	51.0	968.4	1676.1
	20	-	-	4.7	3.4	14.1	157.0	10042.3	49.3	961.3	1837.1
	25	-	-	4.7	3.5	10.2	158.1	10792.1	38.8	978.9	2073.4
	30	-	-	4.8	3.3	8.8	158.8	10874.5	33.8	988.3	2091.7
11	25	-	-	4.2	4.8	31.8	153.8	7736.3	91.4	903.4	1158.7
	30	-	-	4.7	5.5	24.7	151.3	9232.8	69.2	914.0	1591.7
	35	-	-	5.3	5.6	13.7	162.0	10321.2	46.3	997.0	1864.4
20	30	-	-	5.3	2.5	21.8	154.0	8472.2	95.7	879.7	1353.1
	35	-	-	6.6	1.8	14.7	162.3	8736.5	84.1	935.0	1344.1
21	5	-	-	8.9	0.7	8.1	166.6	12470.3	36.1	1036.5	2483.4
	10	-	-	8.8	0.6	5.3	170.5	14346.2	21.9	1082.7	3003.4
	15	-	-	8.6	0.8	5.8	175.1	15181.0	23.8	1111.7	3234.2
	20	-	-	9.4	0.8	5.5	178.7	16360.8	23.1	1137.8	3539.4
	25	-	-	10.5	1.0	5.4	184.1	16777.2	22.4	1173.5	3627.7
7	10	25	30	3.4	4.3	55.9	168.2	8472.0	97.9	1035.2	1014.4
	10	30	30	5.1	5.1	69.5	162.2	8831.3	102.1	1023.0	1097.1
9	10	28	30	3.6	5.2	73.3	164.6	8777.2	101.2	1047.0	1032.9
21	10	30	30	7.3	3.2	5.5	156.1	12379.4	19.9	991.0	2519.0
	10	35	30	8.9	4.3	6.1	156.6	12286.4	20.3	994.2	2502.9
	10	40	30	9.4	4.4	10.1	156.2	11233.5	35.4	973.1	2186.5
	10	45	30	9.7	4.1	7.7	157.5	12002.8	25.6	994.2	2449.9
7	10	30	50	5.1	1.8	7.0	157.5	10641.9	38.5	968.1	1965.8
	10	35	50	6.4	2.2	13.7	158.9	10018.1	45.4	978.2	1847.1
	10	40	50	7.6	2.8	18.5	155.4	9706.8	57.6	946.2	1742.9
	10	45	50	7.5	2.3	25.4	151.5	9142.7	69.0	917.1	1565.3
9	10	30	50	4.0	2.2	23.0	156.1	8247.1	81.5	916.7	1287.2
	10	35	50	4.5	2.6	35.1	145.9	8429.0	84.0	876.4	1346.8
	10	40	50	5.4	2.4	33.4	146.9	8543.7	80.2	885.4	1378.8
	10	45	50	7.3	2.1	32.9	146.2	8712.0	67.9	900.0	1407.8
11	10	40	50	3.5	3.3	62.6	127.6	7521.3	88.1	812.5	1067.8
21	10	30	50	4.2	2.4	13.1	164.8	8916.9	74.9	962.0	1416.8
	10	35	50	5.3	2.6	16.4	169.1	8836.6	78.6	989.3	1347.6
	10	40	50	5.8	2.6	26.5	170.4	8676.1	88.0	1003.6	1283.9
	10	45	50	5.6	2.9	45.3	161.6	8326.2	96.4	974.4	1122.5

Table A-12 – Raw Data 20%NH3-80%DME

Mode	Main	Pilot	Pilot quantity	BSNOx	BSNH3	BSHC (C3H8)	BSH2O	BSN2	BSCO	BSCO2	BSO2
	CAD BTDC	CAD BTDC	%	g/kWh	g/kWh	g/kWh	g/kWh	g/kWh	g/kWh	g/kWh	g/kWh
5	15	-	-	7.0	5.8	23.6	286.0	14038.8	133.1	1660.0	2084.7
	20	-	-	6.4	4.4	28.7	262.5	13634.7	110.4	1560.8	2070.3
7	10	-	-	19.5	2.6	23.2	350.5	23594.2	100.0	2147.4	4337.1
	15	-	-	18.0	3.4	14.3	318.6	25291.8	60.3	1997.2	5096.4
	20	-	-	16.4	2.3	10.5	291.3	23800.6	41.4	1844.4	4881.3
	25	-	-	14.9	1.8	9.1	270.7	22869.1	37.6	1715.8	4765.0
9	15	-	-	12.1	7.0	28.9	380.9	22801.2	121.7	2310.8	3999.4
	20	-	-	10.6	7.6	31.8	353.1	22581.1	110.7	2161.7	4130.8
	25	-	-	9.7	7.2	21.3	328.7	22435.1	80.6	2035.1	4310.2
	30	-	-	9.2	6.3	16.9	306.2	20965.3	65.2	1905.3	4032.7
11	25	-	-	11.3	13.0	85.9	414.8	20865.0	246.6	2436.4	3125.0
	30	-	-	10.9	12.6	56.9	348.8	21287.4	159.5	2107.4	3670.0
	35	-	-	10.8	11.4	28.1	331.7	21129.8	94.7	2041.1	3816.8
20	30	-	-	9.1	4.3	37.5	264.7	14565.4	164.5	1512.3	2326.2
	35	-	-	10.9	2.9	24.3	268.9	14471.0	139.3	1548.7	2226.4
21	5	-	-	18.7	1.5	17.0	348.8	26104.0	75.6	2169.8	5198.6
	10	-	-	15.0	1.0	9.0	289.7	24376.4	37.1	1839.6	5103.3
	15	-	-	13.3	1.2	9.1	272.6	23630.4	37.0	1730.5	5034.2
	20	-	-	14.2	1.3	8.2	269.0	24625.3	34.7	1712.5	5327.2
	25	-	-	15.2	1.5	7.9	267.6	24390.1	32.6	1706.0	5273.8
7	10	25	30	8.0	10.3	132.2	398.1	20053.2	231.8	2450.4	2401.0
	10	30	30	13.2	13.2	181.1	422.6	23008.2	266.1	2665.2	2858.3
9	10	28	30	8.9	12.9	181.1	406.8	21688.2	250.1	2587.0	2552.3
21	10	30	30	11.9	5.2	9.1	255.8	20283.7	32.6	1623.7	4127.4
	10	35	30	15.2	7.3	10.4	268.5	21068.4	34.7	1704.9	4291.9
	10	40	30	17.4	8.1	18.7	288.4	20750.5	65.4	1797.4	4038.9
	10	45	30	17.3	7.4	13.7	281.4	21443.6	45.8	1776.2	4376.9
7	10	30	50	9.5	3.3	13.0	293.9	19852.5	71.7	1806.1	3667.2
	10	35	50	13.1	4.6	28.2	328.0	20675.5	93.7	2018.8	3812.1
	10	40	50	16.9	6.3	41.2	346.8	21661.4	128.6	2111.5	3889.4
	10	45	50	18.1	5.7	61.5	367.1	22148.0	167.2	2221.6	3791.8
9	10	30	50	8.5	4.7	48.3	327.9	17319.0	171.1	1925.1	2703.2
	10	35	50	8.8	5.1	69.0	286.8	16573.4	165.2	1723.2	2648.0
	10	40	50	9.9	4.3	61.5	270.3	15721.2	147.5	1629.2	2537.1
	10	45	50	13.4	3.8	60.2	267.7	15955.2	124.3	1648.3	2578.3
11	10	40	50	8.4	8.0	151.7	309.0	18210.4	213.3	1967.1	2585.3
21	10	30	50	9.4	5.5	29.7	372.8	20172.3	169.5	2176.3	3205.1
	10	35	50	12.3	6.0	37.7	389.0	20328.8	180.7	2275.9	3100.3
	10	40	50	13.0	5.9	59.3	381.8	19433.3	197.2	2247.8	2875.8
	10	45	50	14.3	7.4	116.2	414.4	21353.8	247.3	2499.0	2878.8

Table A-13 – Raw Data 40%NH3-60%DME

Mode	Main	Pilot	Pilot quantity	Engine Power	Engine Speed	Inlet Air Temperature	Exhaust Temperature	Oil Temperature	Cylinder Head Temp	Engine Power
	CAD BTDC	CAD BTDC	%	HP	rpm	deg C	deg C	deg C	deg C	kW
3	35	-	-	2.33	3016	82.78	427.86	87.77	58.78	1.71
5	20	-	-	1.95	2649	75.56	436.42	80.06	57.89	1.43
	25	-	-	1.94	2614	73.89	383.62	80.83	58.33	1.43
	30	-	-	1.90	2618	77.78	374.34	81.38	58.53	1.40
	35	-	-	1.86	2642	76.11	369.77	82.51	59.49	1.37
7	15	-	-	1.12	2551	73.89	538.04	73.82	59.26	0.83
	20	-	-	1.25	2620	72.78	368.80	77.77	56.73	0.92
	25	-	-	1.21	2637	75.00	320.06	78.76	55.37	0.89
	30	-	-	1.15	2602	77.22	315.15	78.25	55.51	0.84
	35	-	-	1.06	2601	76.11	296.51	79.50	56.03	0.78
9	20	-	-	1.36	2975	76.67	414.77	84.34	57.31	1.00
	25	-	-	1.35	2981	75.56	409.62	70.59	54.44	0.99
	30	-	-	1.36	2927	73.89	382.09	75.96	55.74	1.00
	35	-	-	1.39	2985	75.00	383.97	80.07	57.07	1.02
	40	-	-	1.40	2912	78.89	360.74	83.20	58.17	1.03
11	25	-	-	1.43	3333	77.78	516.36	85.42	55.23	1.05
	30	-	-	1.45	3306	76.67	382.45	85.77	55.39	1.07
	35	-	-	1.45	3300	76.11	369.55	86.66	55.45	1.07
	40	-	-	1.47	3302	78.33	377.24	88.22	56.27	1.08
20	20	-	-	1.74	2270	90.56	531.79	83.85	68.43	1.28
	25	-	-	1.80	2279	88.33	489.57	85.43	69.69	1.32
	30	-	-	1.93	2267	87.78	461.72	87.17	70.78	1.42
	35	-	-	1.95	2265	86.11	420.83	89.33	72.11	1.43
21	20	-	-	1.00	2280	90.00	448.55	61.06	56.25	0.74
	25	-	-	1.05	2257	91.11	405.83	69.11	58.56	0.77
	30	-	-	0.95	2262	89.44	461.56	65.50	58.36	0.70
	35	-	-	0.93	2235	87.22	451.02	76.67	62.46	0.68
	40	-	-	1.00	2256	85.00	445.47	76.19	67.03	0.73

Table A-14 – Raw Data 40%NH3-60%DME

Mode	Main	Pilot	Pilot quantity	Air Consumption	Vol. Efficiency	Fuel Consumption Mix	Total Fuel Energy	Thermal Efficiency	BMEP
	CAD BTDC	CAD BTDC	%	kg/h	-	kg/h	MJ/h	-	bar
3	35	-	-	18.76	0.63	1.55	38.09	16.17	2.13
5	20	-	-	16.75	0.63	1.31	32.25	16.00	2.03
	25	-	-	16.82	0.64	1.19	29.26	17.55	2.05
	30	-	-	16.48	0.63	1.11	27.15	18.51	2.00
	35	-	-	16.86	0.64	1.08	26.50	18.58	1.94
7	15	-	-	16.26	0.63	1.42	34.88	8.52	1.21
	20	-	-	17.05	0.64	1.12	27.44	12.06	1.32
	25	-	-	17.23	0.65	1.03	25.35	12.59	1.26
	30	-	-	16.68	0.64	1.01	24.78	12.23	1.21
	35	-	-	16.85	0.65	0.98	23.95	11.75	1.13
9	20	-	-	19.30	0.65	1.24	30.57	11.75	1.26
	25	-	-	18.51	0.62	1.31	32.15	11.13	1.25
	30	-	-	18.91	0.64	1.24	30.52	11.76	1.28
	35	-	-	17.71	0.59	1.15	28.25	13.04	1.28
	40	-	-	17.81	0.61	1.07	26.32	14.06	1.32
11	25	-	-	21.05	0.63	1.45	35.65	10.63	1.18
	30	-	-	20.85	0.63	1.75	42.90	8.94	1.21
	35	-	-	20.82	0.63	1.37	33.61	11.44	1.21
	40	-	-	20.42	0.62	1.38	33.96	11.47	1.23
20	20	-	-	13.77	0.63	1.50	36.81	12.53	2.12
	25	-	-	13.85	0.63	1.37	33.57	14.16	2.17
	30	-	-	13.69	0.62	1.35	33.21	15.39	2.35
	35	-	-	13.74	0.62	1.23	30.24	17.07	2.37
21	20	-	-	14.96	0.68	1.18	28.87	9.18	1.21
	25	-	-	14.57	0.67	1.03	25.32	10.98	1.28
	30	-	-	14.20	0.65	1.25	30.65	8.20	1.16
	35	-	-	13.06	0.60	1.10	26.91	9.16	1.15
	40	-	-	13.63	0.62	1.04	25.51	10.37	1.22

Table A-15 – Raw Data 40%NH3-60%DME

Mode	Main	Pilot	Pilot quantity	FSN (ave)	Soot (ave)	Soot (ave)	NOx	NH3	Sum	CO
	CAD BTDC	CAD BTDC	%	-	mg/m³	g/kWh	ppm	ppm	ppm	ppm
3	35	-	-	0.002	0.020	0.000	529	412	941	2366
5	20	-	-	0.005	0.055	0.001	406	922	1328	2696
	25	-	-	0.005	0.055	0.001	415	590	1005	1883
	30	-	-	0.002	0.025	0.001	445	571	1016	1734
	35	-	-	0.005	0.060	0.001	590	1000	1590	1840
7	15	-	-	0.014	0.175	0.009	347	1204	1551	7402
	20	-	-	0.006	0.075	0.003	396	1145	1541	1803
	25	-	-	0.002	0.025	0.001	455	824	1279	1541
	30	-	-	0.003	0.040	0.001	495	575	1070	1527
	35	-	-	0.002	0.020	0.001	668	648	1316	1307
9	20	-	-	0.004	0.040	0.002	458	968	1426	2840
	25	-	-	0.004	0.040	0.002	472	540	1012	2323
	30	-	-	0.003	0.035	0.001	498	525	1023	1875
	35	-	-	0.005	0.065	0.002	560	390	950	1943
	40	-	-	0.003	0.045	0.001	711	505	1216	1637
11	25	-	-	0.005	0.060	0.003	775	720	1495	1567
	30	-	-	0.005	0.045	0.002	515	1361	1876	3854
	35	-	-	0.002	0.030	0.001	571	1346	1917	1663
	40	-	-	0.006	0.080	0.003	600	833	1433	1535
20	20	-	-	0.010	0.125	0.003	397	403	800	7821
	25	-	-	0.003	0.030	0.001	326	896	1222	7854
	30	-	-	0.005	0.060	0.001	324	1626	1950	7048
	35	-	-	0.005	0.060	0.001	466	511	977	4486
21	20	-	-	0.008	0.095	0.004	311	297	608	3372
	25	-	-	0.002	0.060	0.002	316	312	628	3244
	30	-	-	0.008	0.100	0.005	313	455	768	6606
	35	-	-	0.007	0.085	0.004	379	350	729	4840
	40	-	-	0.005	0.070	0.003	535	242	777	3387

Table A-16 – Raw Data 40%NH3-60%DME

Mode	Main	Pilot	Pilot quantity	CO2	THC (C3H8)	O2	Equivalence Ratio	Total PM	Total PM	BSPM
	CAD BTDC	CAD BTDC	%	%-v	ppm	%-v	-	g/h	g/kg-fuel	g/kWh
3	35	-	-	4.36	219	11.95	0.722	0.001	0.001	0.000
5	20	-	-	4.09	374	12.55	0.685	0.002	0.002	0.001
	25	-	-	3.94	209	13.07	0.640	0.002	0.002	0.001
	30	-	-	3.86	192	13.19	0.627	0.001	0.001	0.001
	35	-	-	3.8	200	13.35	0.617	0.002	0.002	0.001
7	15	-	-	4.56	1568	10.96	0.869	0.007	0.005	0.009
	20	-	-	3.51	249	13.93	0.573	0.002	0.002	0.003
	25	-	-	3.27	170	14.66	0.524	0.001	0.001	0.001
	30	-	-	3.27	171	14.45	0.529	0.001	0.001	0.001
	35	-	-	3.15	173	14.73	0.506	0.001	0.001	0.001
9	20	-	-	3.41	690	13.97	0.583	0.002	0.001	0.002
	25	-	-	3.96	261	12.7	0.660	0.002	0.001	0.002
	30	-	-	3.86	208	13.03	0.634	0.001	0.001	0.001
	35	-	-	3.93	205	12.88	0.646	0.002	0.002	0.002
	40	-	-	3.78	203	13.21	0.616	0.002	0.001	0.001
11	25	-	-	3.7	198	13.37	0.603	0.003	0.002	0.003
	30	-	-	4.1	990	12	0.732	0.002	0.001	0.002
	35	-	-	3.5	203	13.72	0.574	0.001	0.001	0.001
	40	-	-	3.64	198	13.54	0.592	0.003	0.002	0.003
20	20	-	-	5.35	1724	10.55	0.951	0.004	0.003	0.003
	25	-	-	4.7	1713	10.86	0.892	0.001	0.001	0.001
	30	-	-	4.67	1157	10.99	0.863	0.002	0.001	0.001
	35	-	-	4.76	432	11.32	0.810	0.002	0.001	0.001
21	20	-	-	4.66	488	12.88	0.734	0.003	0.003	0.004
	25	-	-	4.25	424	13.32	0.682	0.002	0.002	0.002
	30	-	-	4.92	774	10.86	0.874	0.003	0.003	0.005
	35	-	-	5.1	449	10.86	0.859	0.002	0.002	0.004
	40	-	-	5.16	197	11.84	0.804	0.002	0.002	0.003

Table A-17 – Raw Data 40%NH3-60%DME

Mode	Main	Pilot	Pilot quantity	NOx	NH3	THC (C3H8)	H2O	N2	CO	CO2	O2
	CAD BTDC	CAD BTDC	%	g/kg-fuel	g/kg-fuel	g/kg-fuel	g/kg-fuel	g/kg-fuel	g/kg-fuel	g/kg-fuel	g/kg-fuel
3	35	-	-	7.2	3.4	4.4	137.8	10355.1	29.5	855.2	1704.8
5	20	-	-	5.8	7.9	7.8	136.0	10837.7	35.4	844.2	1883.9
	25	-	-	6.5	5.6	4.8	142.1	11879.2	27.2	893.5	2155.7
	30	-	-	7.4	5.7	4.7	146.0	12502.6	26.3	921.5	2290.2
	35	-	-	10.2	10.4	5.1	150.7	13044.9	29.2	949.2	2425.2
7	15	-	-	4.5	9.4	29.8	144.2	9836.1	87.8	849.6	1485.2
	20	-	-	6.7	11.6	6.2	135.5	12734.4	28.1	858.6	2478.3
	25	-	-	8.4	9.1	4.6	136.7	13794.4	26.1	870.7	2838.8
	30	-	-	9.0	6.3	4.6	135.4	13713.1	25.6	862.8	2772.9
	35	-	-	12.7	7.4	4.8	135.0	14281.5	22.9	867.5	2950.3
9	20	-	-	7.9	10.0	17.4	134.2	12918.2	44.9	846.8	2523.1
	25	-	-	7.4	5.1	6.0	144.3	11946.7	33.6	899.9	2098.9
	30	-	-	8.4	5.3	5.1	149.3	12774.3	29.1	939.9	2307.5
	35	-	-	9.5	4.0	5.1	154.0	12925.9	30.4	967.3	2305.7
	40	-	-	13.0	5.5	5.5	157.9	13867.3	27.6	1000.5	2542.9
11	25	-	-	12.5	7.0	4.7	135.8	12189.3	23.2	862.1	2265.7
	30	-	-	6.9	11.0	19.5	128.1	10232.9	47.6	796.6	1695.6
	35	-	-	9.6	13.6	5.0	134.7	12736.3	25.8	854.6	2436.3
	40	-	-	9.8	8.2	4.8	135.7	12387.3	23.2	862.9	2334.4
20	20	-	-	4.2	2.6	26.7	137.3	7969.5	75.5	811.1	1163.2
	25	-	-	3.8	6.2	29.1	133.1	8778.9	83.2	782.0	1314.2
	30	-	-	3.8	11.3	19.6	133.1	8775.3	74.7	777.8	1331.1
	35	-	-	5.9	3.9	8.0	144.5	9585.2	51.9	864.8	1495.7
21	20	-	-	4.4	2.5	10.2	155.5	10637.3	43.9	954.4	1918.5
	25	-	-	5.0	2.9	9.8	156.7	11759.5	46.7	962.1	2192.9
	30	-	-	4.0	3.5	14.6	156.2	9756.3	77.7	909.0	1459.2
	35	-	-	5.1	2.8	8.8	165.0	10175.6	59.3	982.3	1521.3
	40	-	-	7.8	2.1	4.2	178.9	10990.6	45.3	1085.2	1811.0

Table A-18 – Raw Data 40%NH3-60%DME

Mode	Main	Pilot	Pilot quantity	BSNOx	BSNH3	BSHC (C3H8)	BSH2O	BSN2	BSCO	BSCO2	BSO2
	CAD BTDC	CAD BTDC	%	g/kWh	g/kWh	g/kWh	g/kWh	g/kWh	g/kWh	g/kWh	g/kWh
3	35	-	-	6.5	3.0	4.0	124.9	9386.2	26.8	775.2	1545.3
5	20	-	-	5.3	7.2	7.2	124.6	9931.0	32.4	773.6	1726.3
	25	-	-	5.4	4.6	4.0	118.7	9922.7	22.7	746.4	1800.7
	30	-	-	5.8	4.5	3.7	115.6	9899.0	20.9	729.6	1813.3
	35	-	-	8.0	8.2	4.0	118.9	10290.5	23.1	748.8	1913.1
7	15	-	-	7.7	16.1	51.2	248.0	16916.0	150.9	1461.2	2554.2
	20	-	-	8.1	14.1	7.5	164.7	15478.5	34.1	1043.7	3012.3
	25	-	-	9.7	10.6	5.3	159.1	16059.2	30.4	1013.6	3304.9
	30	-	-	10.8	7.5	5.5	162.3	16436.3	30.7	1034.2	3323.6
	35	-	-	15.8	9.2	6.0	168.4	17818.9	28.6	1082.4	3681.1
9	20	-	-	9.8	12.4	21.7	167.5	16115.1	56.0	1056.4	3147.5
	25	-	-	9.8	6.7	7.9	190.1	15731.8	44.2	1185.0	2763.9
	30	-	-	10.5	6.6	6.4	186.1	15922.3	36.2	1171.6	2876.2
	35	-	-	10.7	4.5	5.8	173.2	14534.7	34.2	1087.7	2592.7
	40	-	-	13.6	5.8	5.7	164.6	14454.8	28.7	1042.9	2650.7
11	25	-	-	17.2	9.6	6.5	187.3	16815.0	32.1	1189.3	3125.5
	30	-	-	11.4	18.0	32.0	210.1	16776.2	78.1	1305.9	2779.8
	35	-	-	12.3	17.5	6.4	172.5	16312.2	33.1	1094.5	3120.3
	40	-	-	12.6	10.5	6.1	173.5	15836.7	29.6	1103.2	2984.4
20	20	-	-	4.9	3.0	31.3	160.7	9326.0	88.3	949.1	1361.2
	25	-	-	3.9	6.4	30.1	137.7	9086.9	86.1	809.5	1360.3
	30	-	-	3.6	10.8	18.7	126.8	8360.6	71.2	741.0	1268.2
	35	-	-	5.1	3.3	6.9	124.1	8231.3	44.5	742.6	1284.5
21	20	-	-	7.1	4.0	16.3	248.3	16989.7	70.2	1524.3	3064.1
	25	-	-	6.6	3.9	13.0	209.2	15703.7	62.4	1284.8	2928.5
	30	-	-	7.2	6.3	26.1	279.1	17431.1	138.8	1624.0	2607.1
	35	-	-	8.1	4.5	14.1	264.2	16291.5	95.0	1572.8	2435.7
	40	-	-	11.1	3.0	6.0	253.0	15542.7	64.1	1534.7	2561.0

Appendix B Additional Plots

B.1 Single Injection

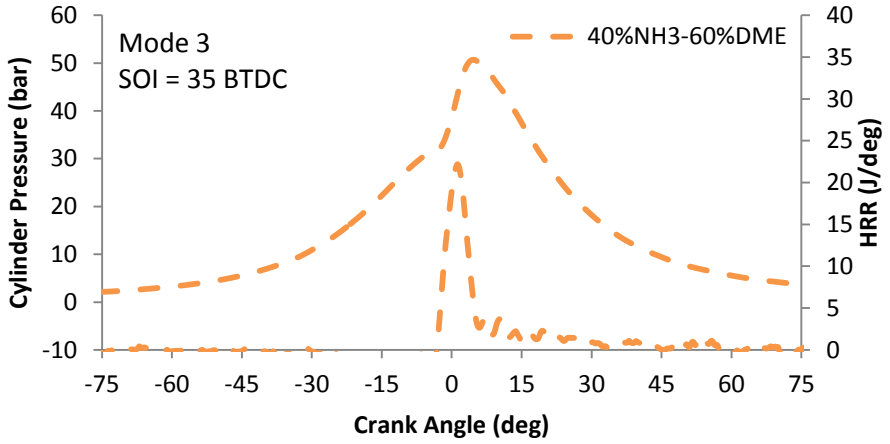

Figure B.1 – Cylinder pressure and heat release rate for Mode 3 using single injection

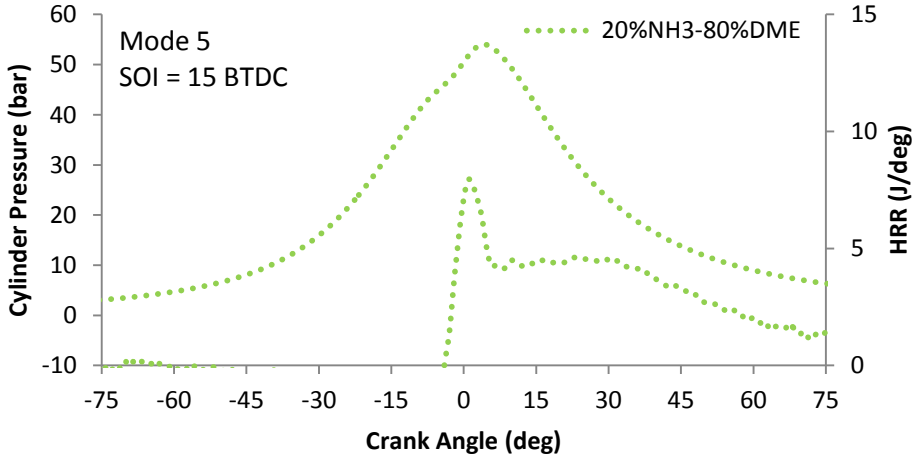

Figure B.2 – Cylinder pressure and heat release rate for Mode 5 using single injection

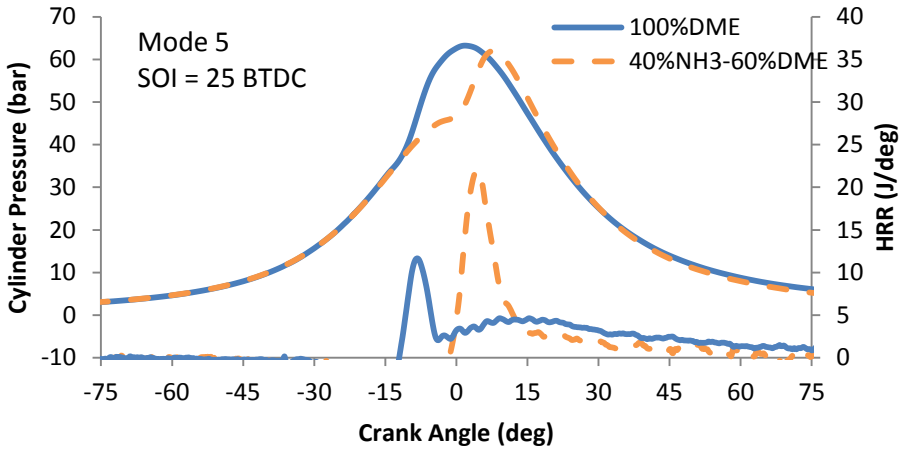

Figure B.3 – Cylinder pressure and heat release rate for Mode 5 using single injection

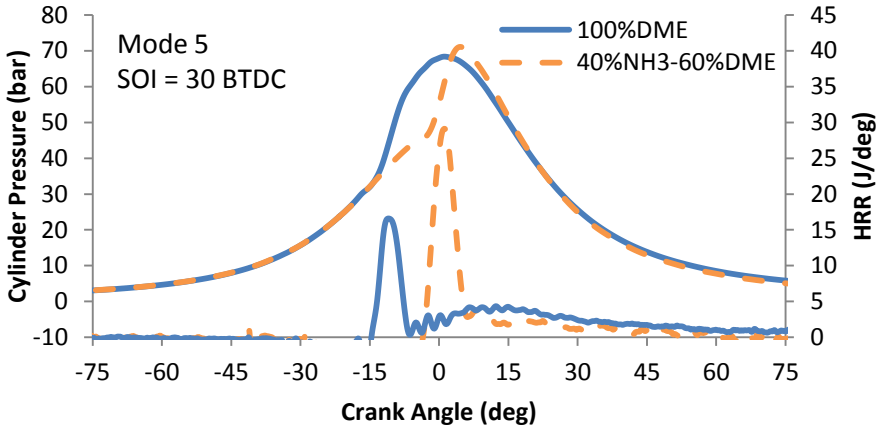

Figure B.4 – Cylinder pressure and heat release rate for Mode 5 using single injection

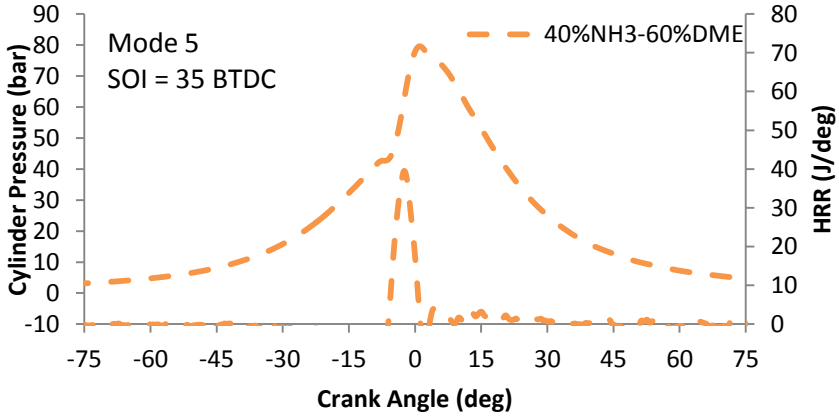

Figure B.5 – Cylinder pressure and heat release rate for Mode 5 using single injection

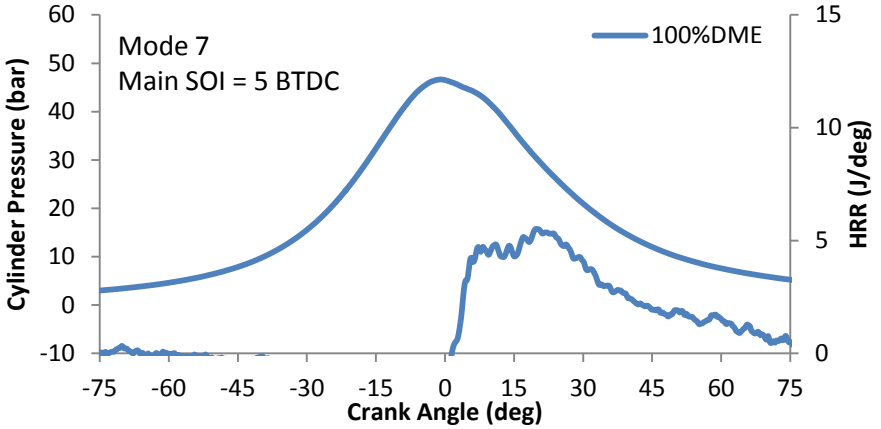

Figure B.6 – Cylinder pressure and heat release rate for Mode 7 using single injection

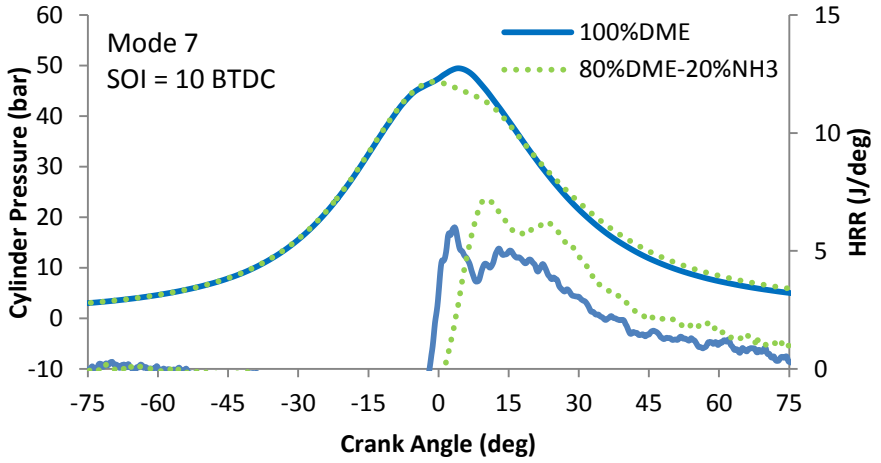

Figure B.7 – Cylinder pressure and heat release rate for Mode 7 using single injection

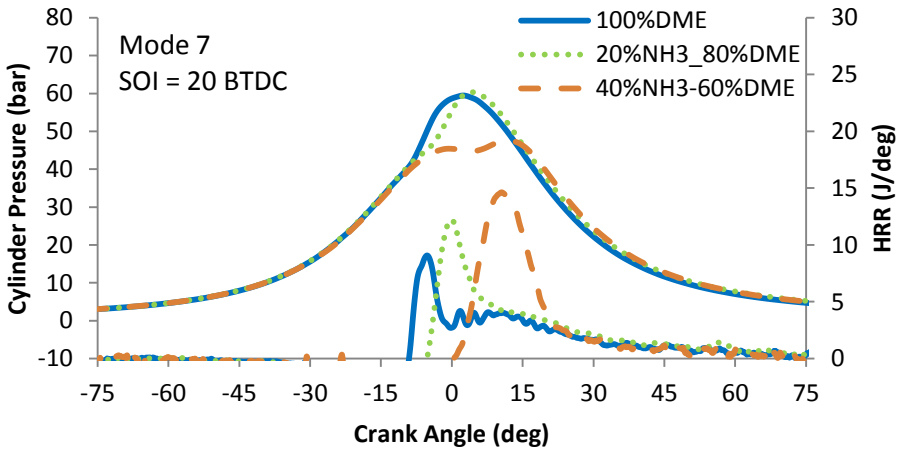

Figure B.8 – Cylinder pressure and heat release rate for Mode 7 using single injection

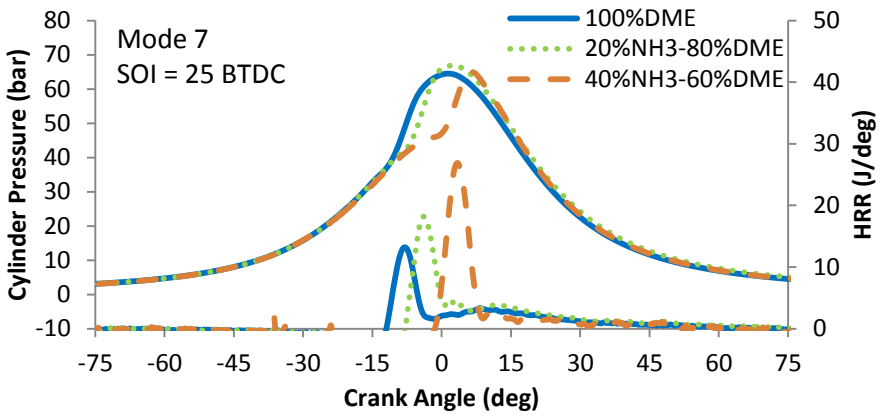

Figure B.9 – Cylinder pressure and heat release rate for Mode 7 using single injection

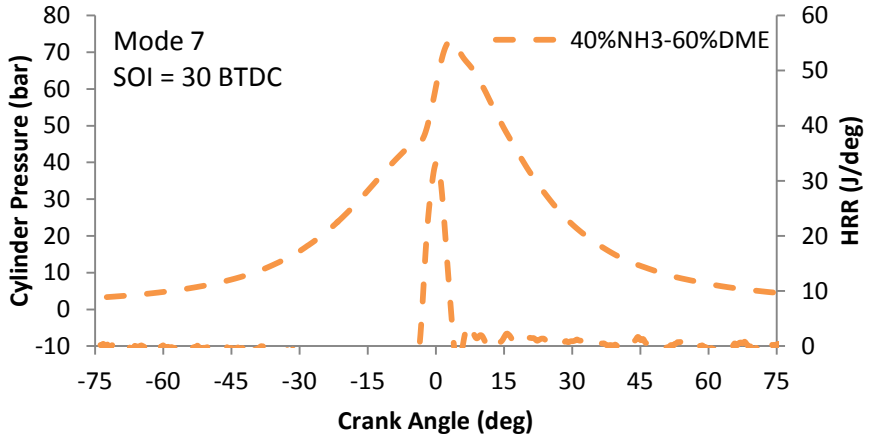

Figure B.10 – Cylinder pressure and heat release rate for Mode 7 using single injection

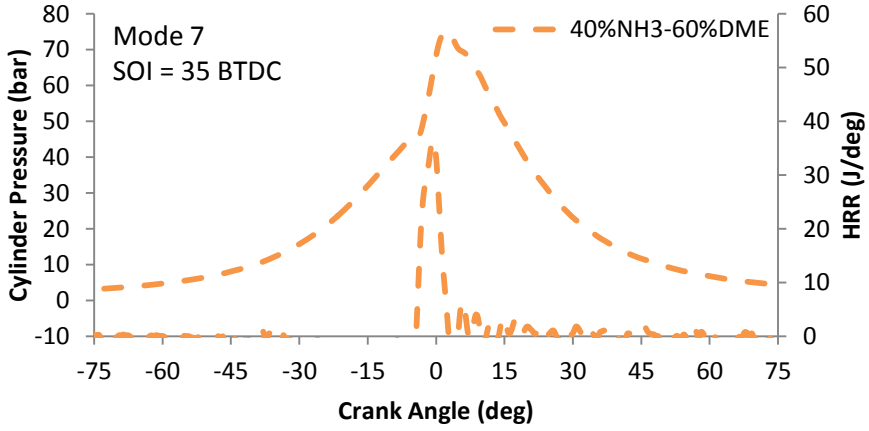

Figure B.11 – Cylinder pressure and heat release rate for Mode 7 using single injection

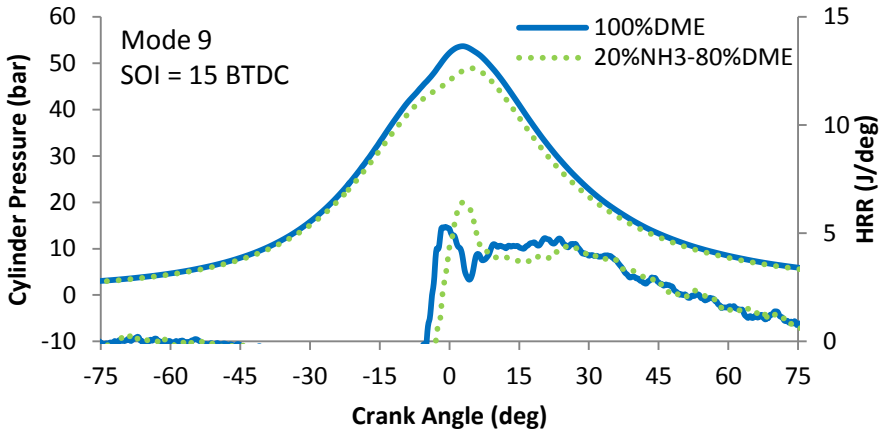

Figure B.12 – Cylinder pressure and heat release rate for Mode 9 using single injection

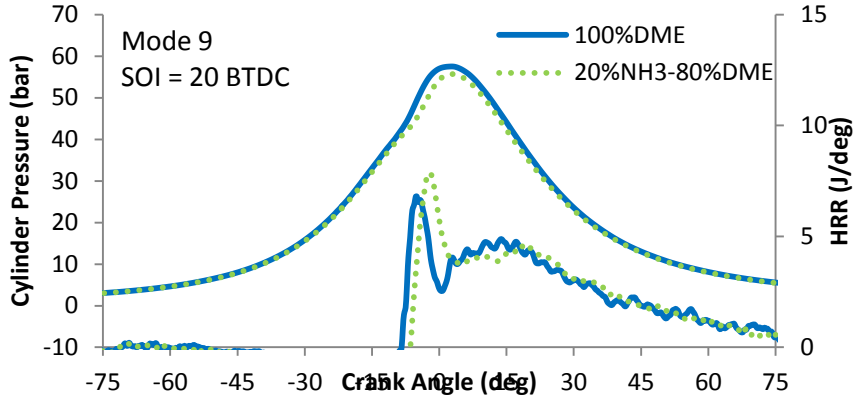

Figure B.13 – Cylinder pressure and heat release rate for Mode 9 using single injection

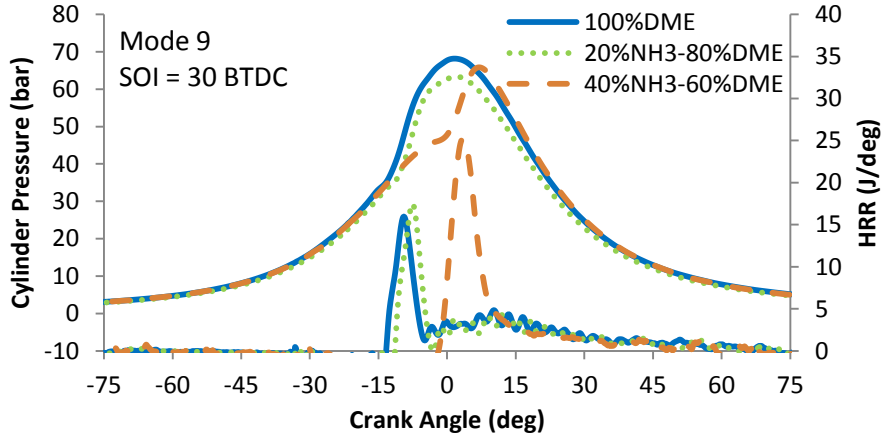

Figure B.14 – Cylinder pressure and heat release rate for Mode 9 using single injection

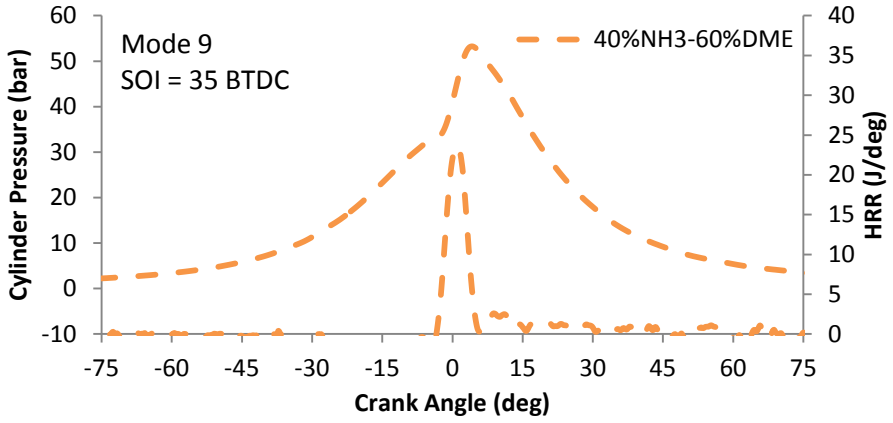

Figure B.15 – Cylinder pressure and heat release rate for Mode 9 using single injection

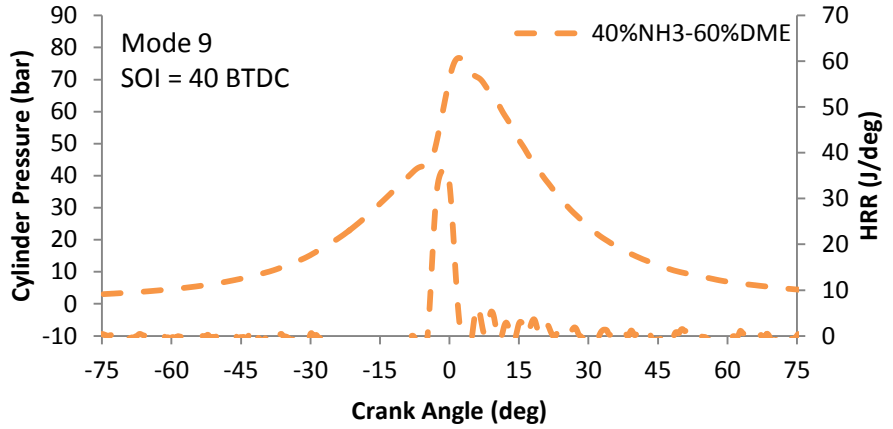

Figure B.16 – Cylinder pressure and heat release rate for Mode 9 using single injection

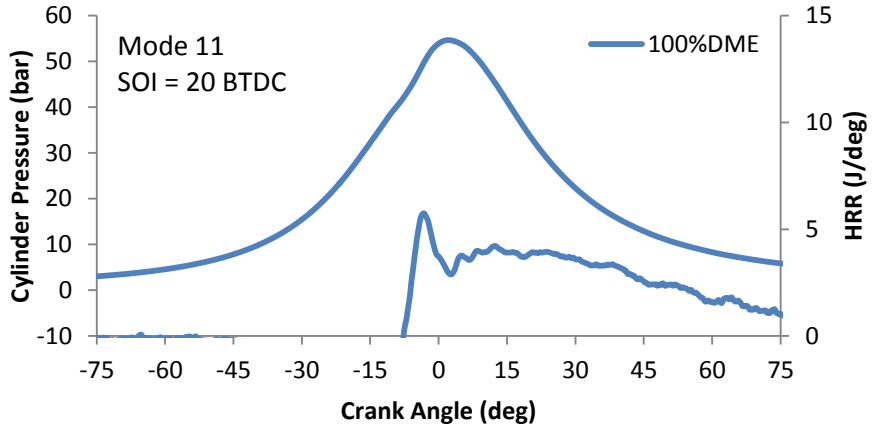

Figure B.17 – Cylinder pressure and heat release rate for Mode 11 using single injection

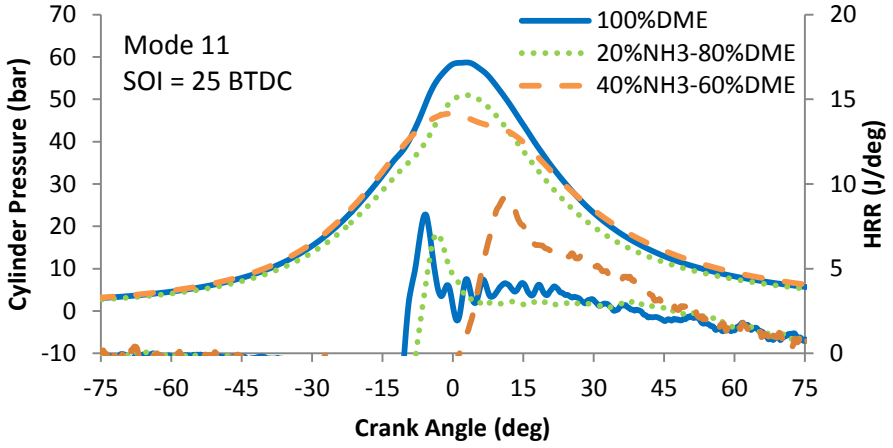

Figure B.18 – Cylinder pressure and heat release rate for Mode 11 using single injection

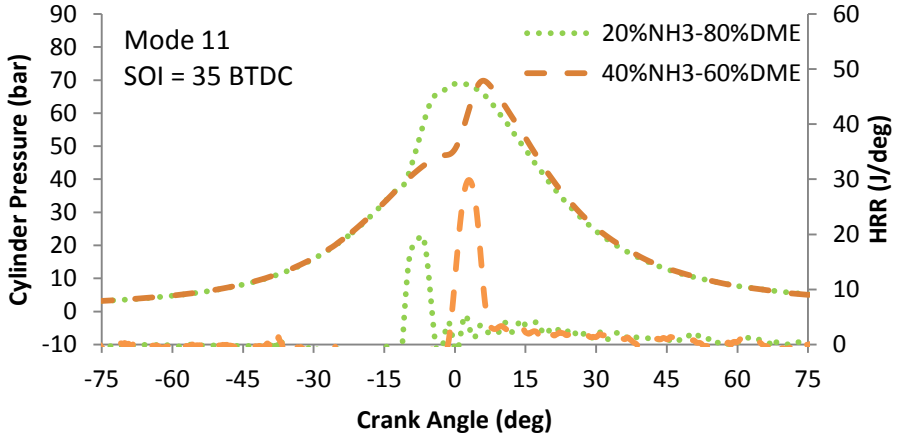

Figure B.19 – Cylinder pressure and heat release rate for Mode 11 using single injection

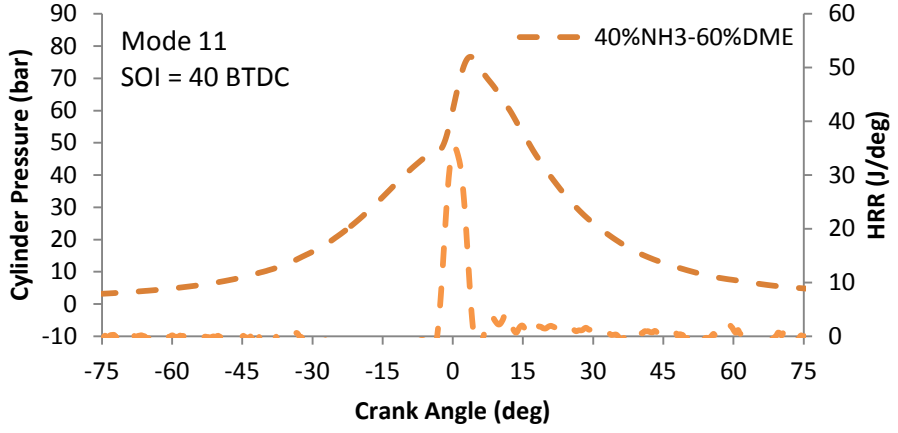

Figure B.20 – Cylinder pressure and heat release rate for Mode 11 using single injection

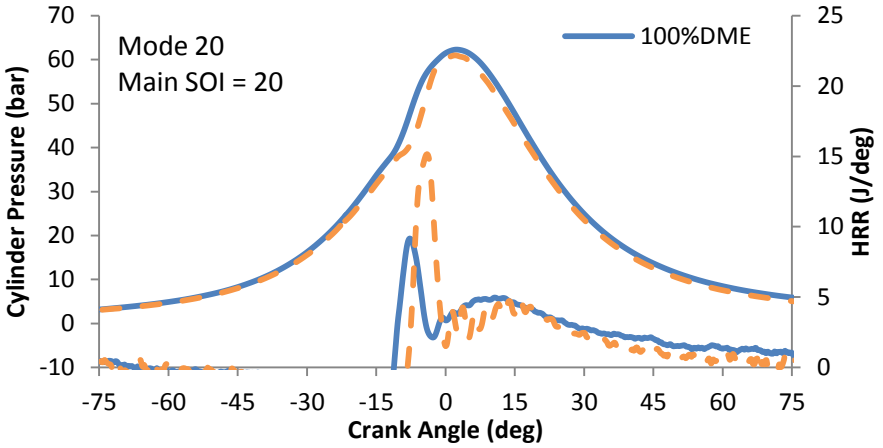

Figure B.21 – Cylinder pressure and heat release rate for Mode 20 using single injection

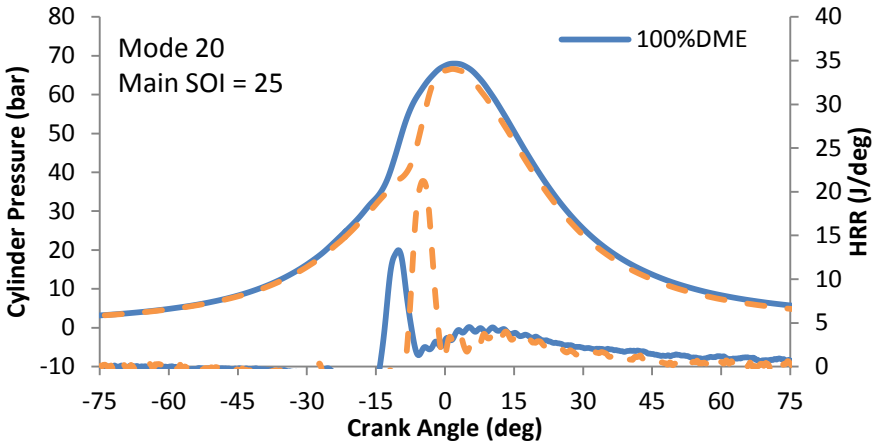

Figure B.22 – Cylinder pressure and heat release rate for Mode 20 using single injection

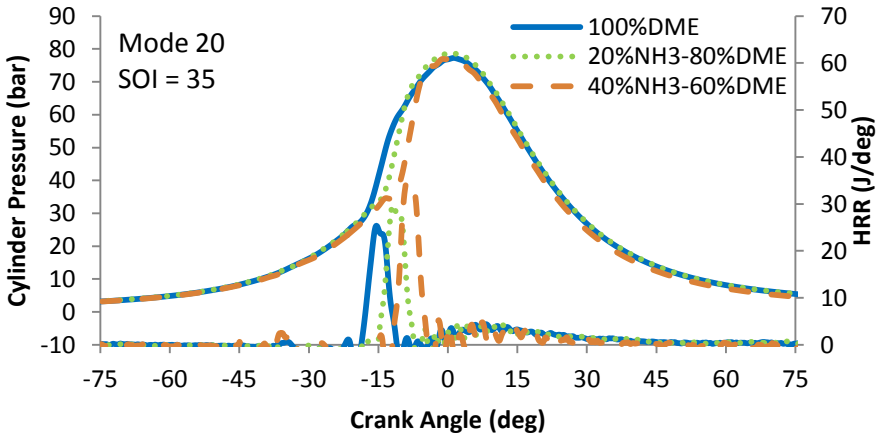

Figure B.23 – Cylinder pressure and heat release rate for Mode 20 using single injection

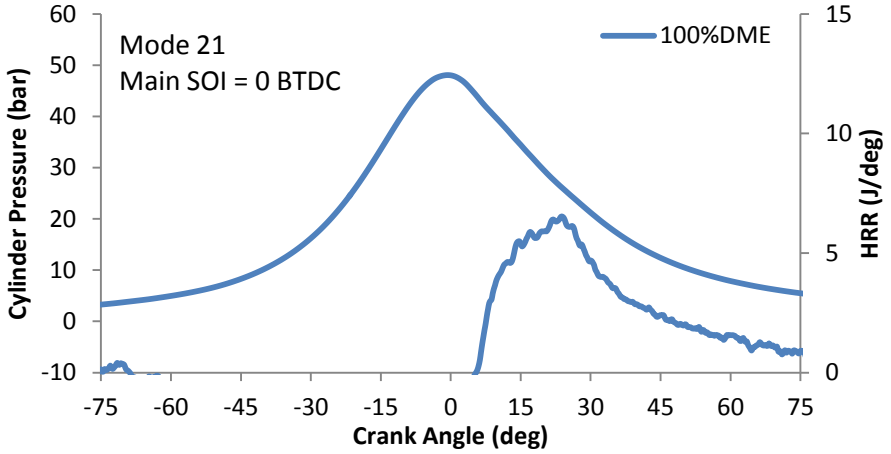

Figure B.24 – Cylinder pressure and heat release rate for Mode 21 using single injection

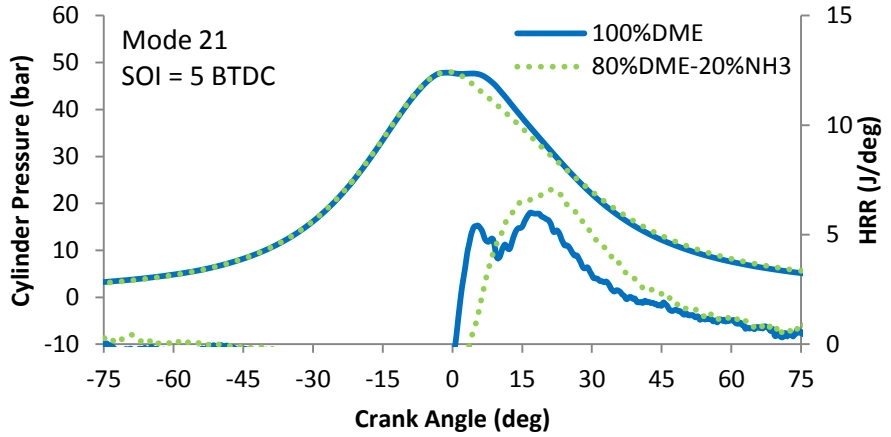

Figure B.25 – Cylinder pressure and heat release rate for Mode 21 using single injection

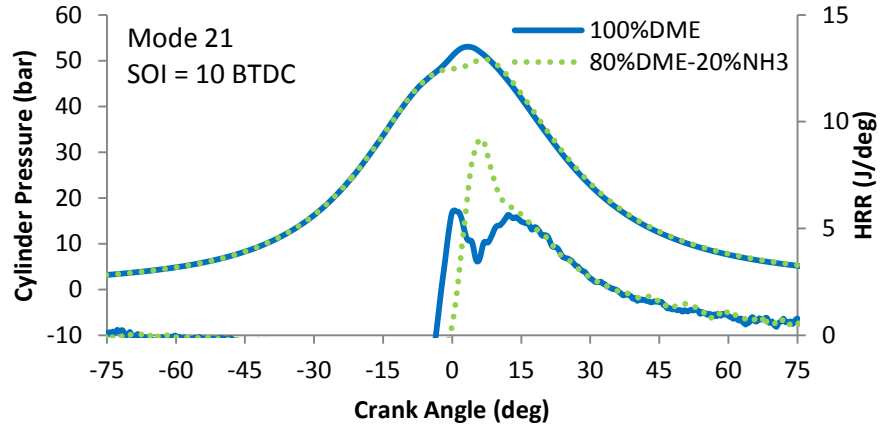

Figure B.26 – Cylinder pressure and heat release rate for Mode 21 using single injection

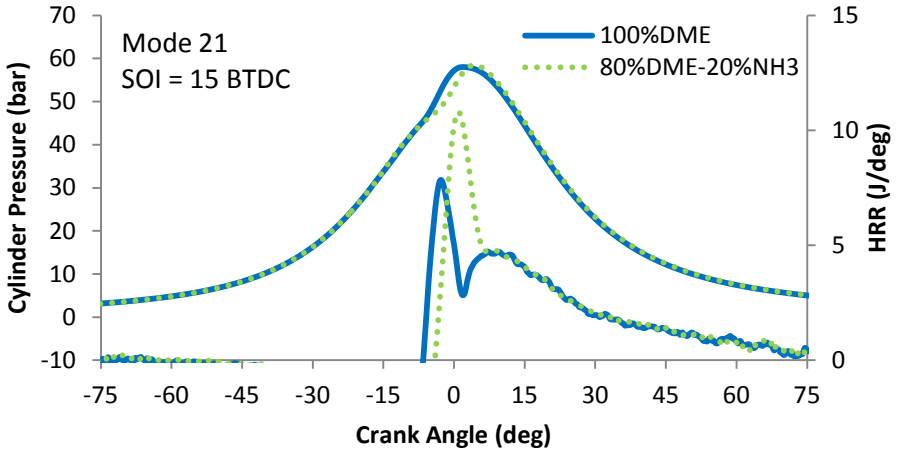

Figure B.27 – Cylinder pressure and heat release rate for Mode 21 using single injection

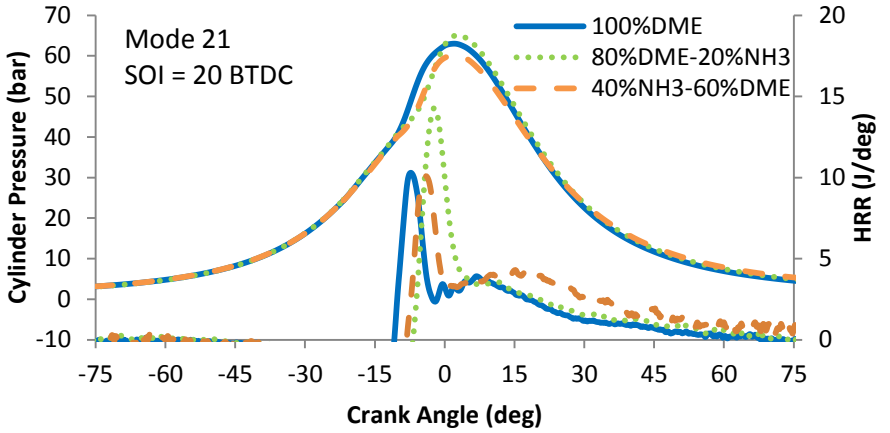

Figure B.28 – Cylinder pressure and heat release rate for Mode 21 using single injection

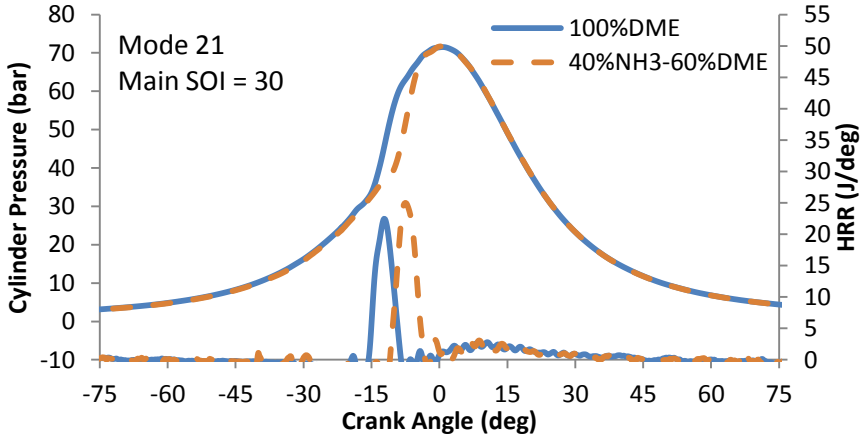

Figure B.29 – Cylinder pressure and heat release rate for Mode 21 using single injection

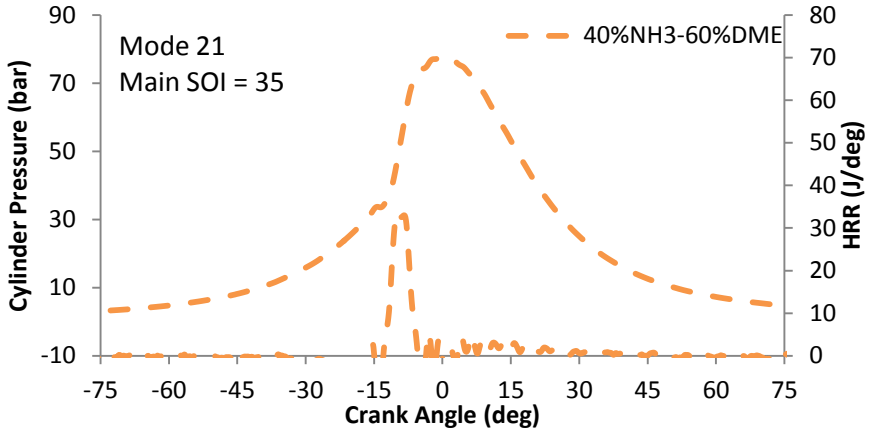

Figure B.30 – Cylinder pressure and heat release rate for Mode 21 using single injection

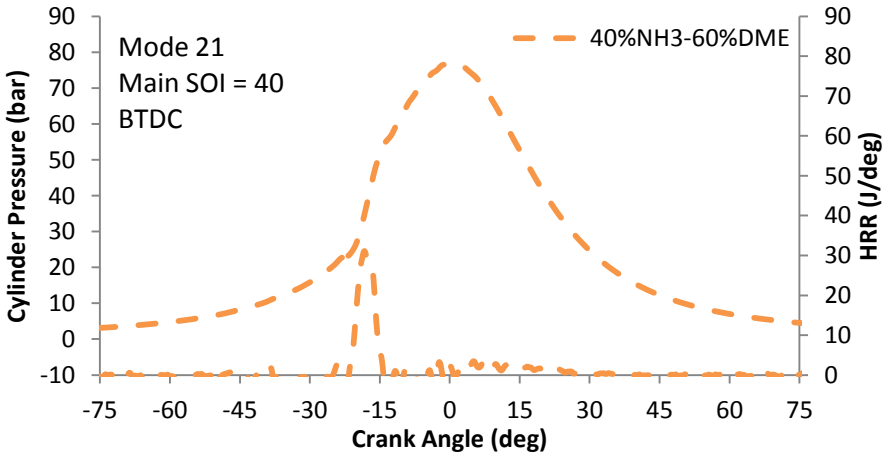

Figure B.31 – Cylinder pressure and heat release rate for Mode 21 using single injection

B.2 Double injections

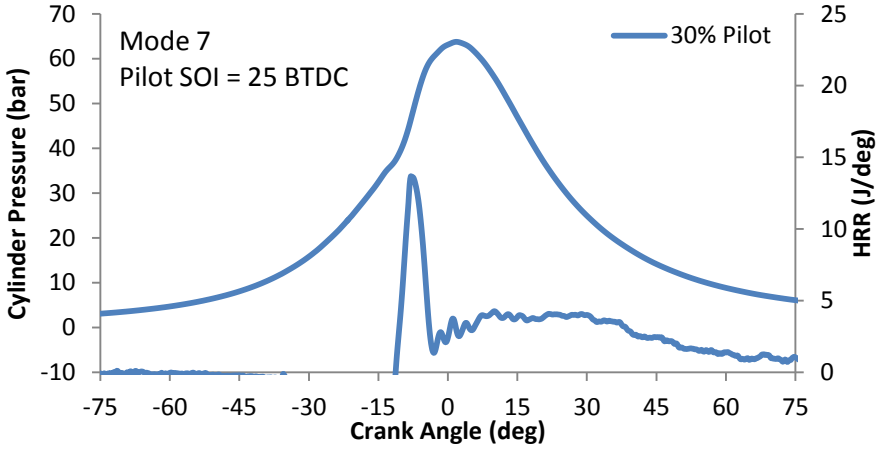

Figure B.32 – Cylinder pressure and heat release rate for Mode 7 using double injections

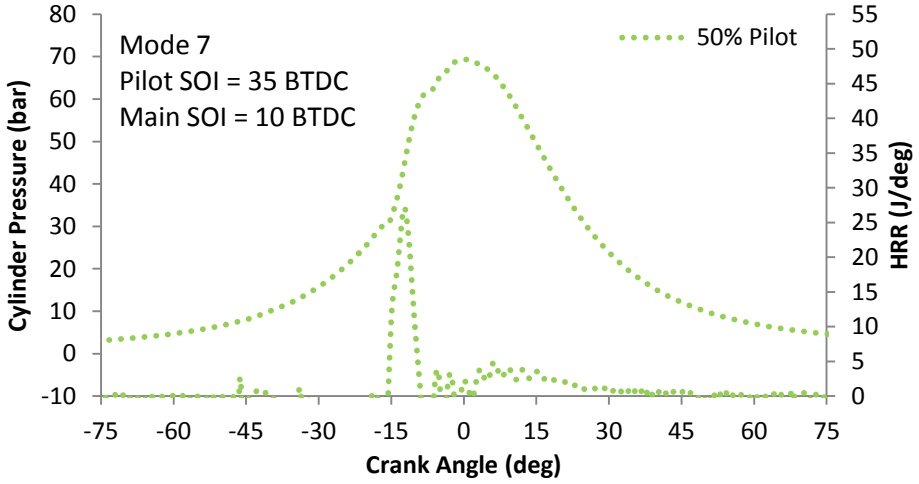

Figure B.33 – Cylinder pressure and heat release rate for Mode 7 using double injections

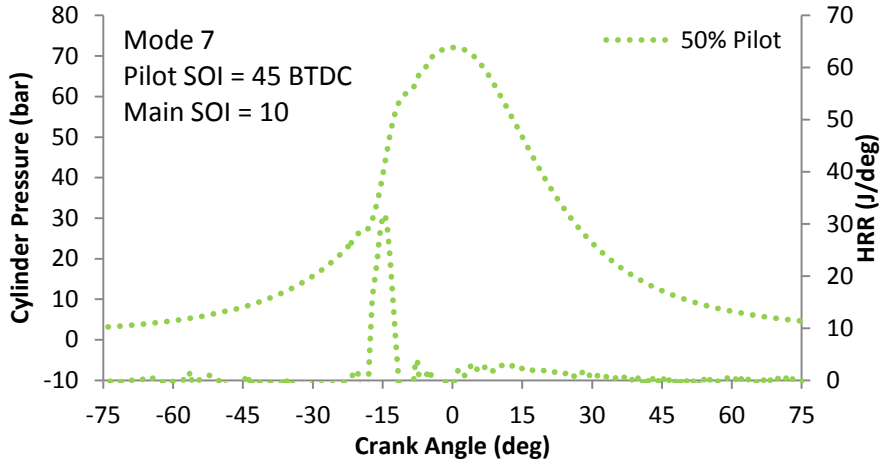

Figure B.34 – Cylinder pressure and heat release rate for Mode 7 using double injections

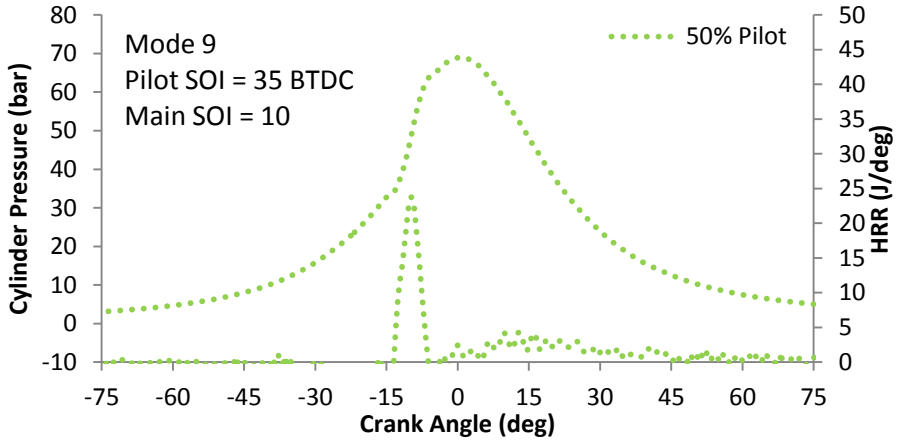

Figure B.35 – Cylinder pressure and heat release rate for Mode 7 using double injections

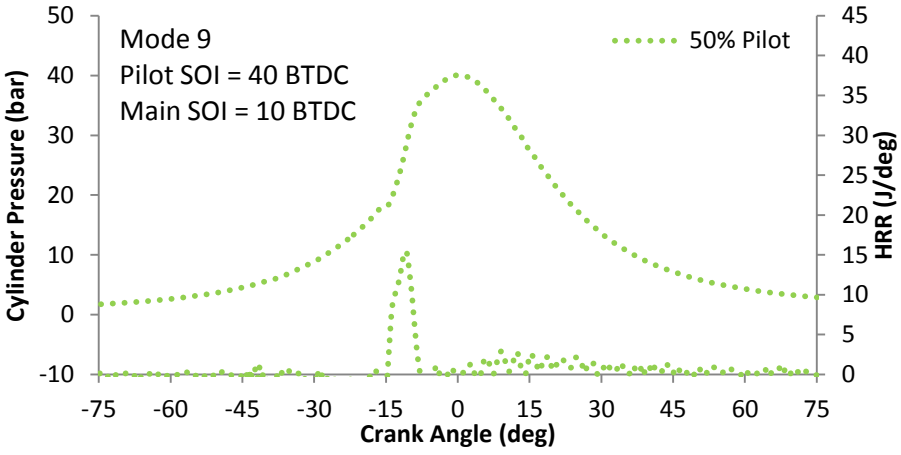

Figure B.36 – Cylinder pressure and heat release rate for Mode 7 using double injections

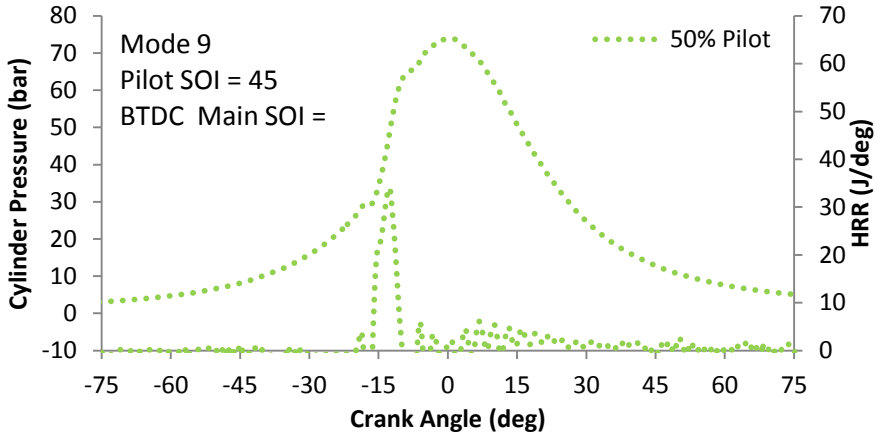

Figure B.37 – Cylinder pressure and heat release rate for Mode 7 using double injections

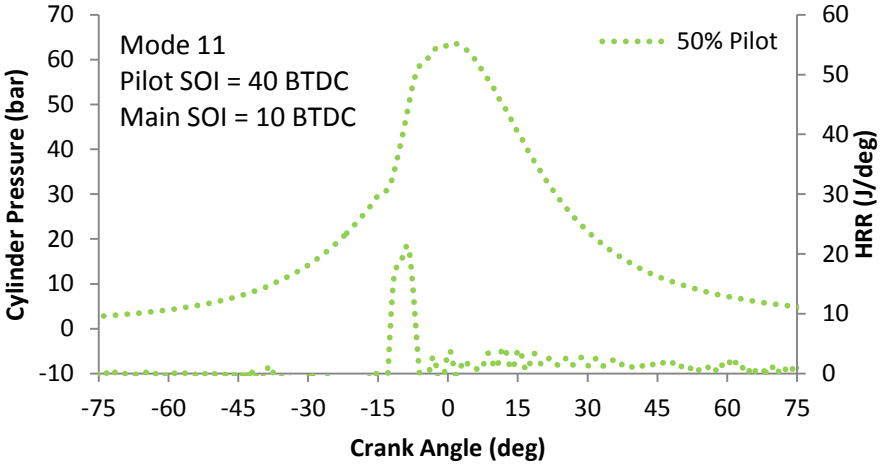

Figure B.38 – Cylinder pressure and heat release rate for Mode 7 using double injections

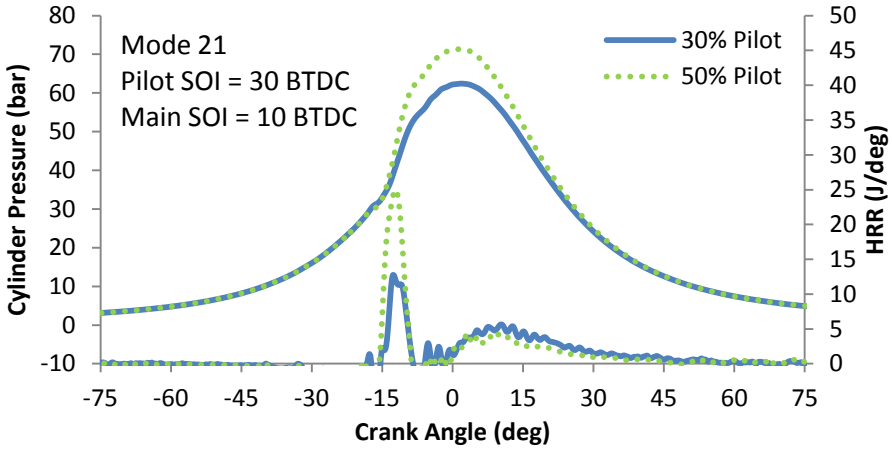

Figure B.39 – Cylinder pressure and heat release rate for Mode 7 using double injections

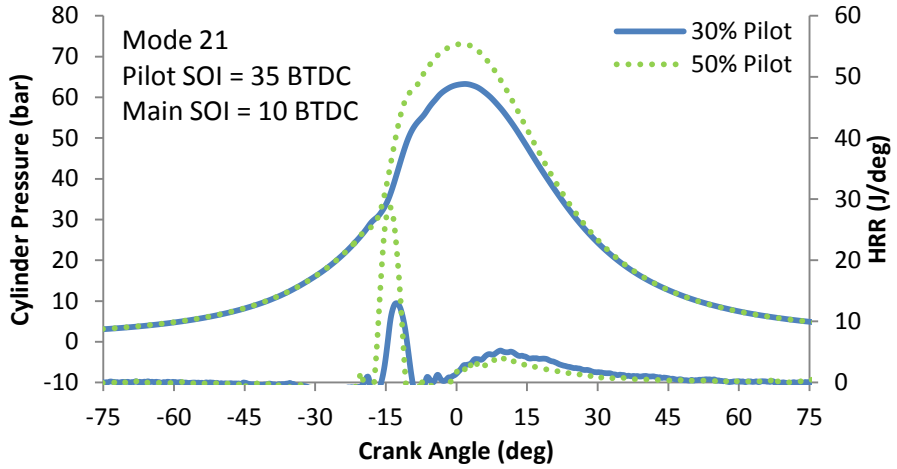

Figure B.40 – Cylinder pressure and heat release rate for Mode 7 using double injections

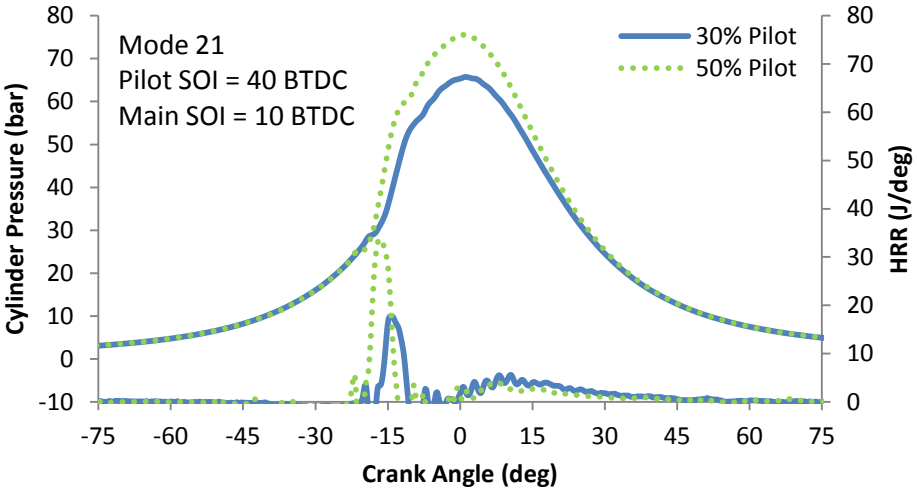

Figure B.41 – Cylinder pressure and heat release rate for Mode 7 using double injections